Rare B Decays in Belle, Belle II and LHCb

Slavomira Stefkova

APS-DPF, Sacramento, USA

April 6th, 2024

Karlsruhe Institute of Technology

Institute of Experimental Particle Physics

slavomira.stefkova@kit.edu

B-physics

B-hadrons decays:

- Light enough to be produced abundantly,
  but heavy enough to have many decays
- Predictions for SM observables are well-known

One of the main missions of B-factories is to perform searches for new physics (*NP*) in rare B decays

Rare B decay: branching fraction $\mathscr{B}(B \to \text{decay products}) < 5 \times 10^{-5}$

→ only less then 5 in 100000 B-hadron decays in this way

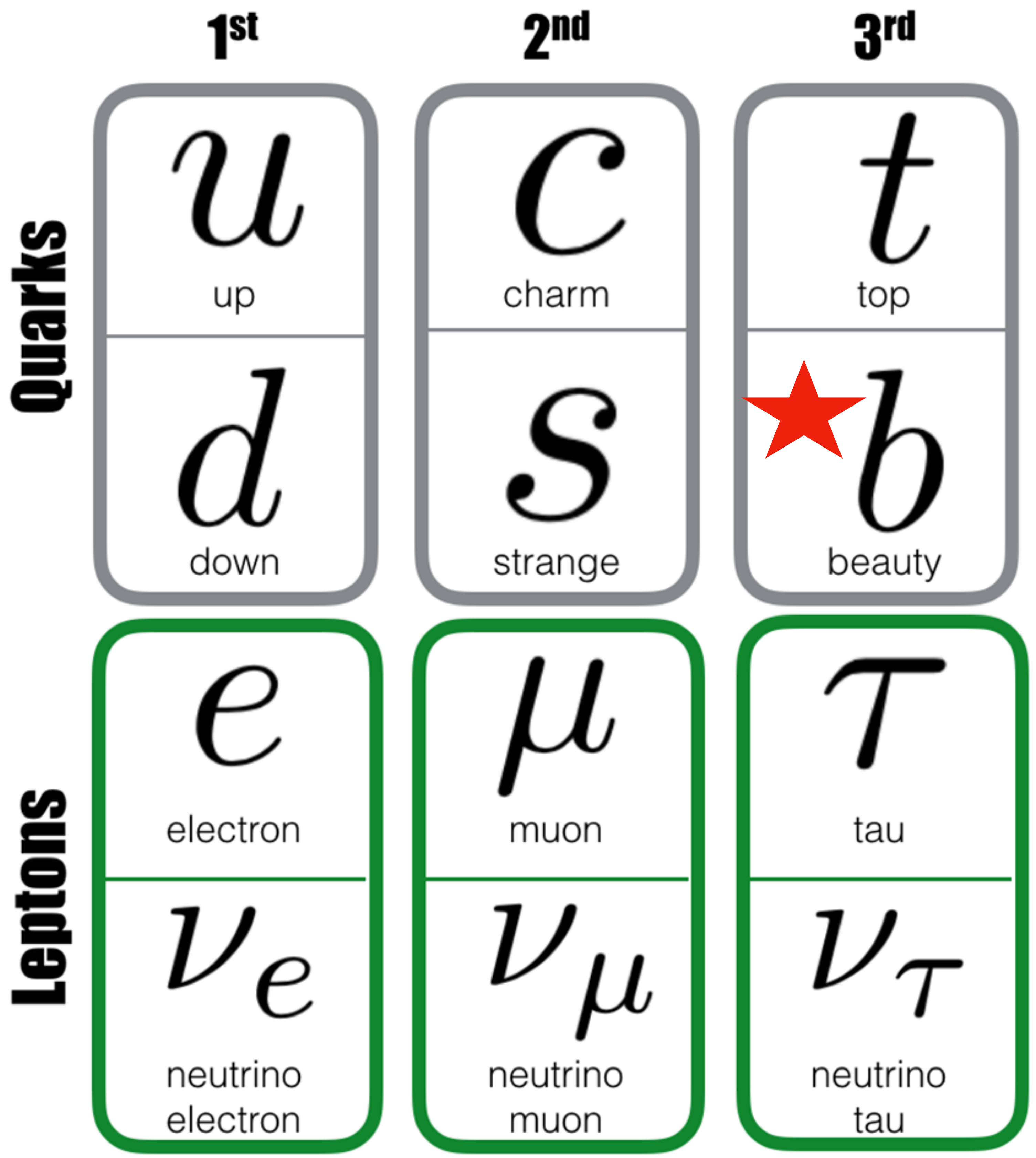

Rare B Decays

Rare B decays:

- GIM suppressed flavour changing neutral currents (FCNC)
  $\rightarrow \quad b \rightarrow s/d(\gamma)$
  - forbidden at tree level, allowed at loop level
  - electroweak decays, radiative electroweak decays
  - m_ν^2/M_W^2 suppressed lepton flavour violating decays
- Helicity suppressed purely leptonic decays

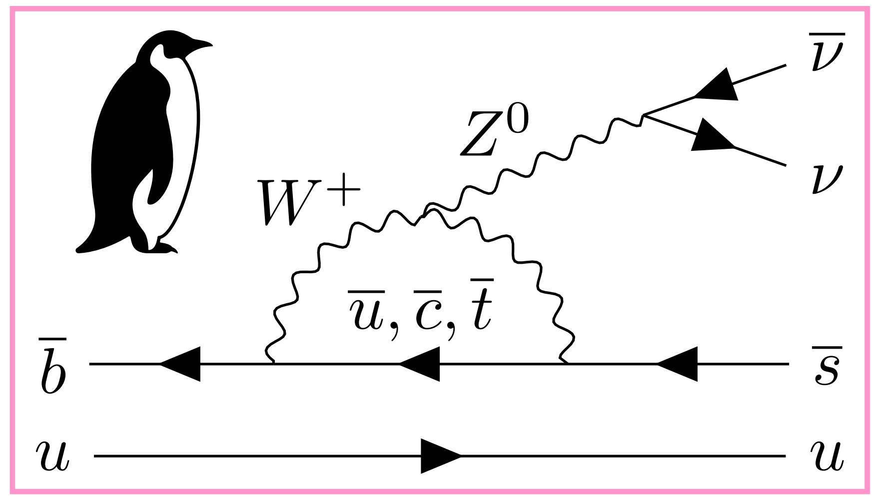

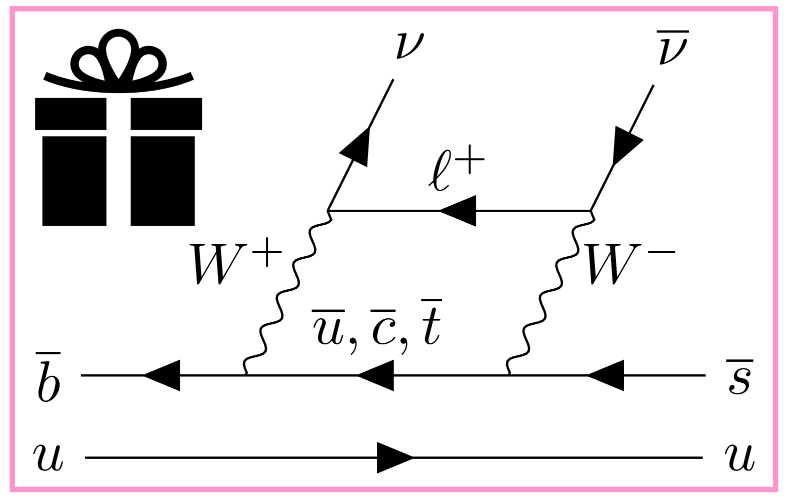

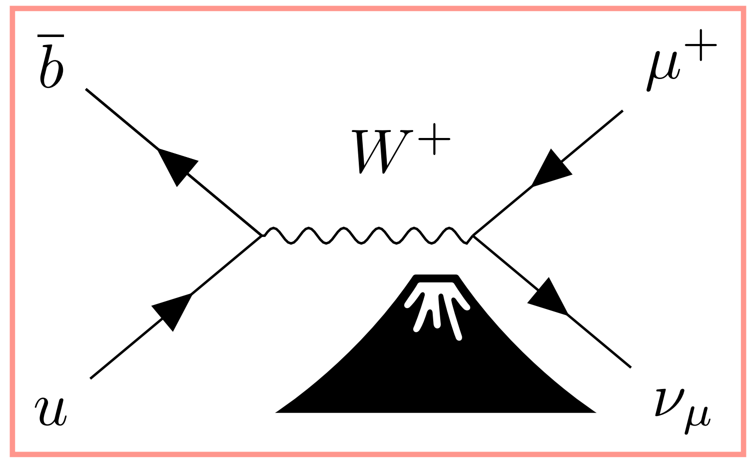

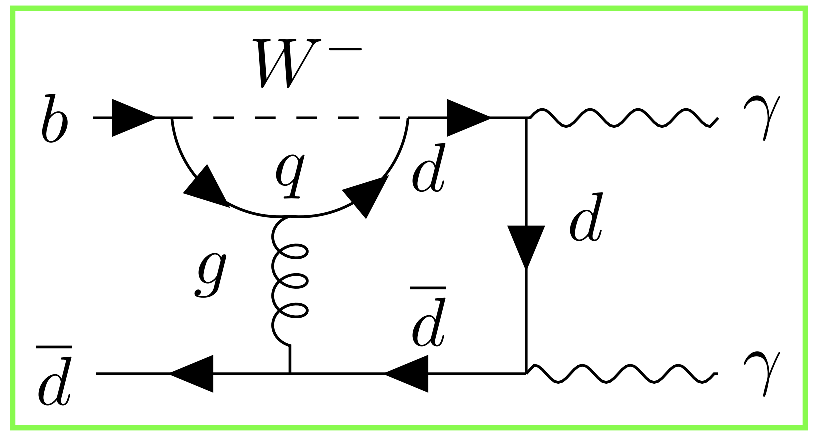

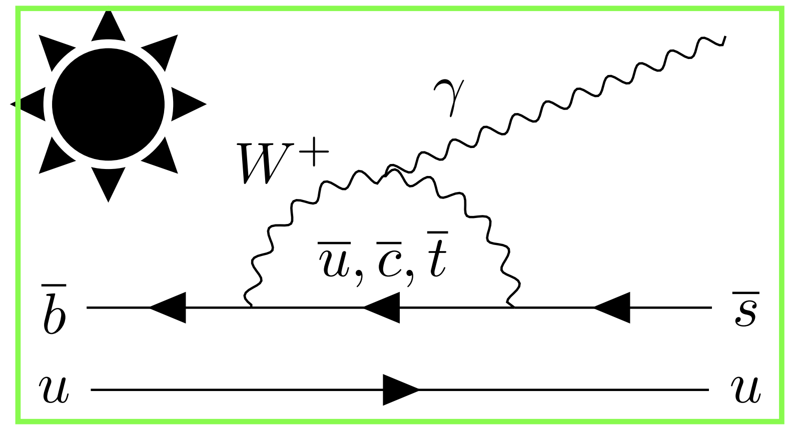

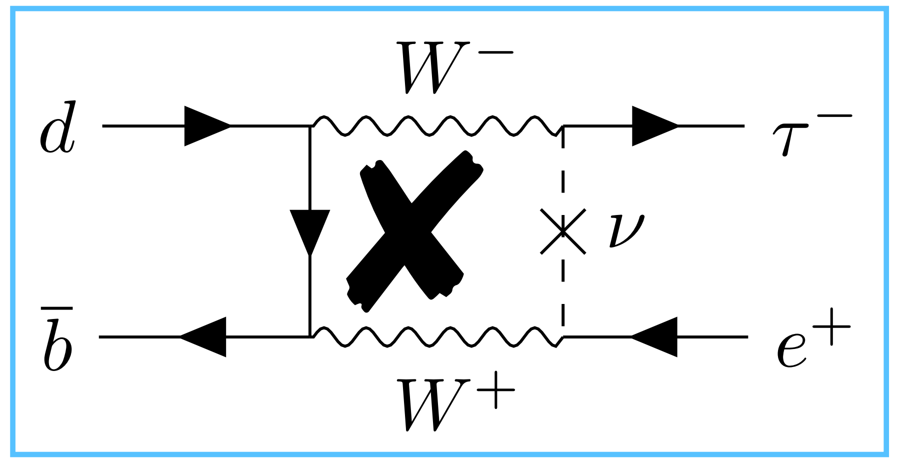

Rare B Decays

Rare B decays:

- GIM suppressed flavour changing neutral currents (FCNC)
  $\rightarrow \quad b \rightarrow s/d(\gamma)$
  - forbidden at tree level, allowed at loop level
  - electroweak decays, radiative electroweak decays
  - m_ν^2/M_W^2 suppressed lepton flavour violating decays
- Helicity suppressed purely leptonic decays

Very sensitive to NP since SM contribution small!

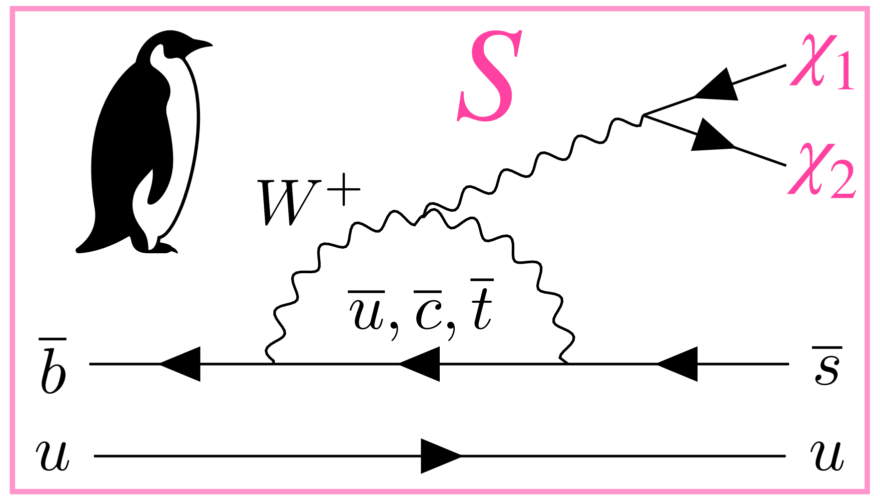

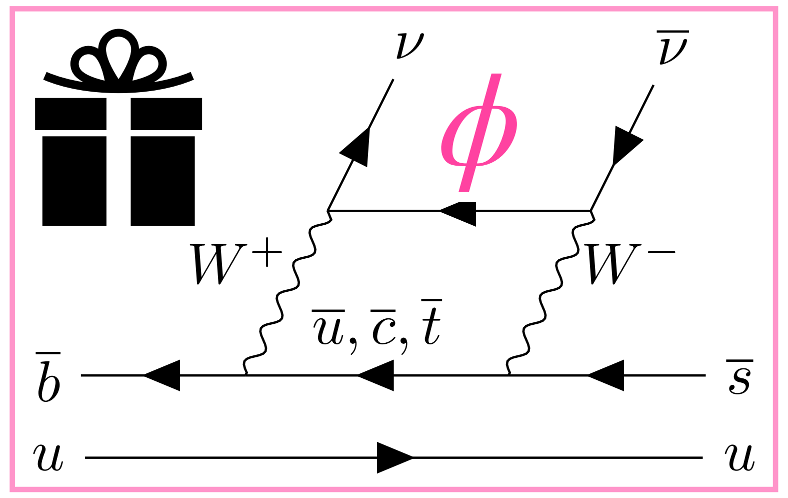

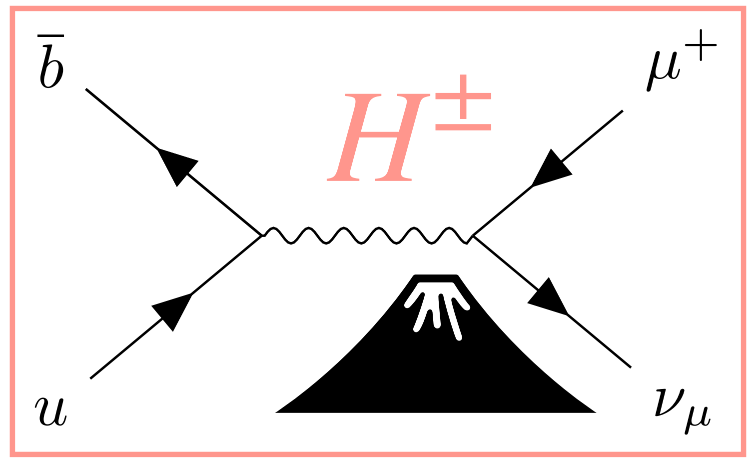

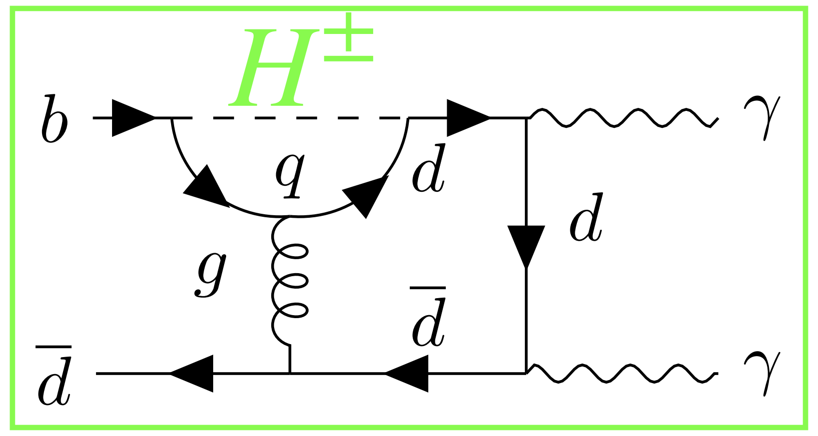

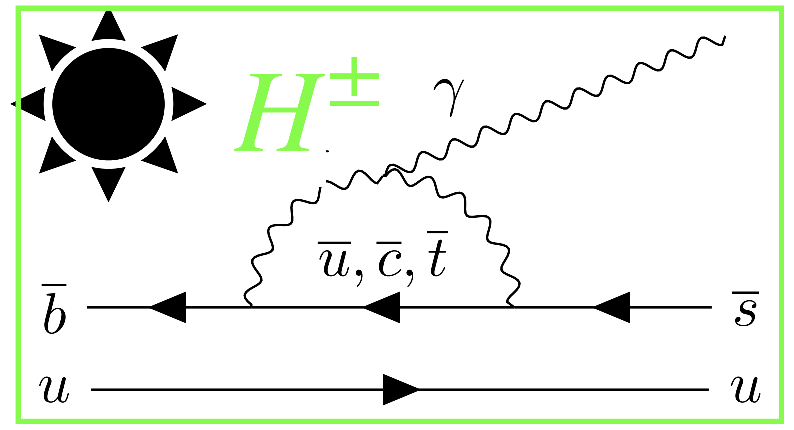

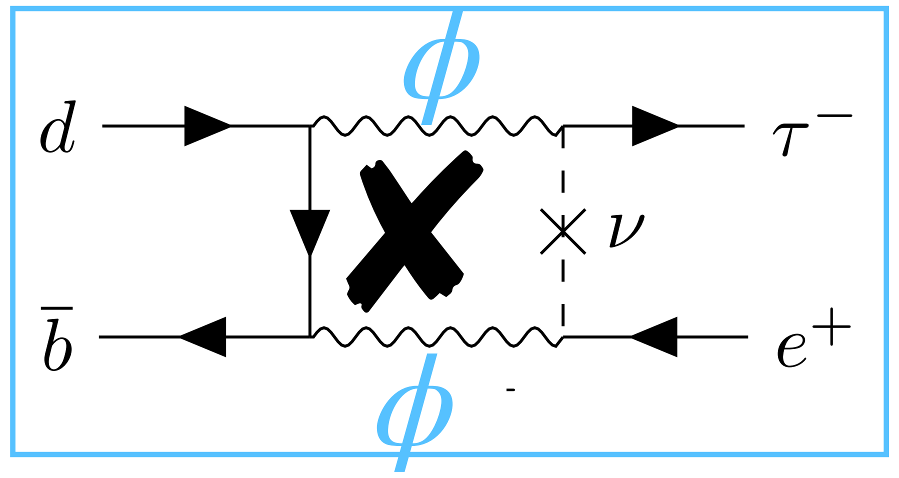

Rare B Decays

Rare B decays:

- GIM suppressed flavour changing neutral currents (FCNC)
  $\rightarrow \quad b \rightarrow s/d(\gamma)$
  - forbidden at tree level, allowed at loop level
  - electroweak decays, radiative electroweak decays
  - m_ν^2/M_W^2 suppressed lepton flavour violating decays
- Helicity suppressed purely leptonic decays

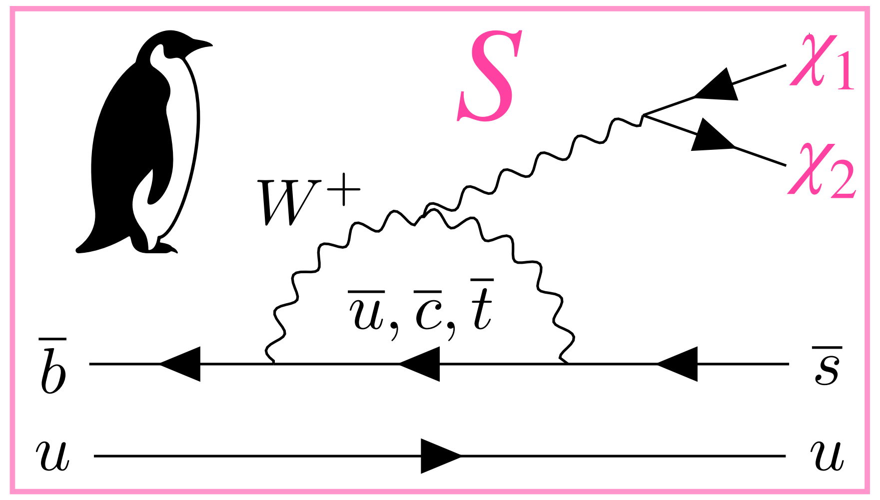

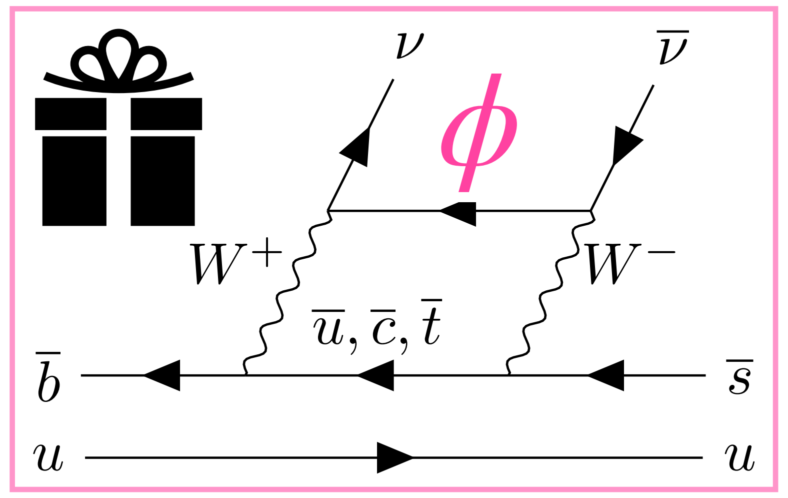

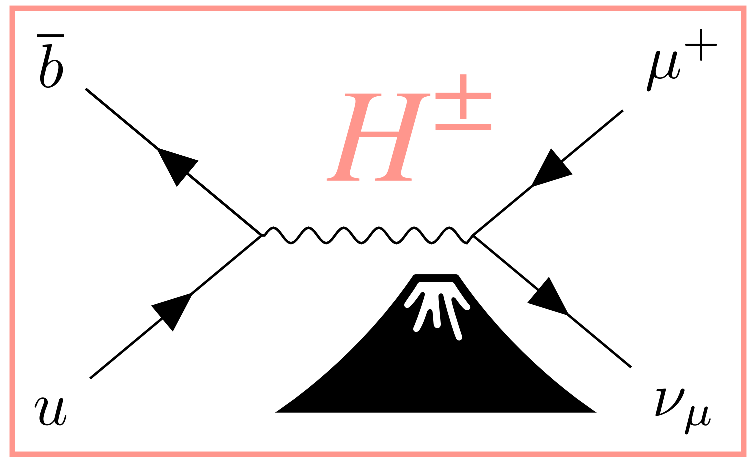

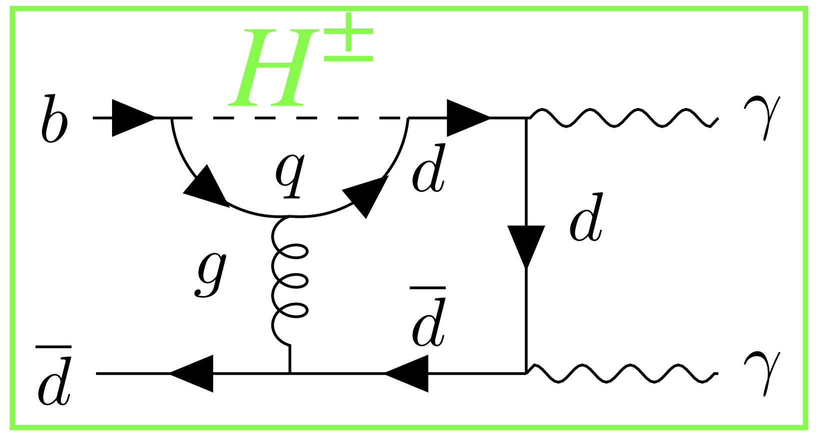

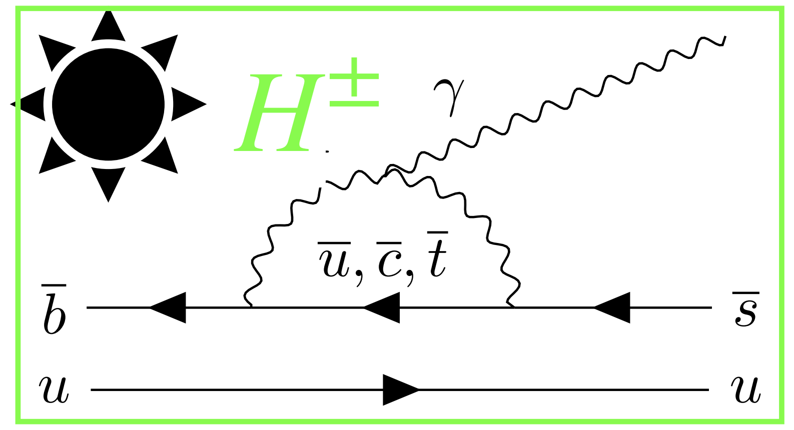

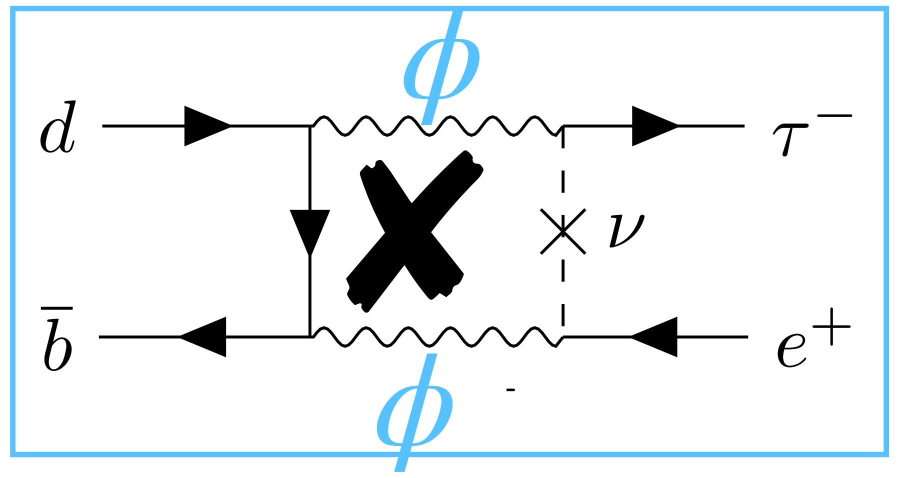

Very sensitive to NP since SM contribution small!

Limit

Angular Observables, Asymmetries

Ratios , Amplitude Analyses

CP observables

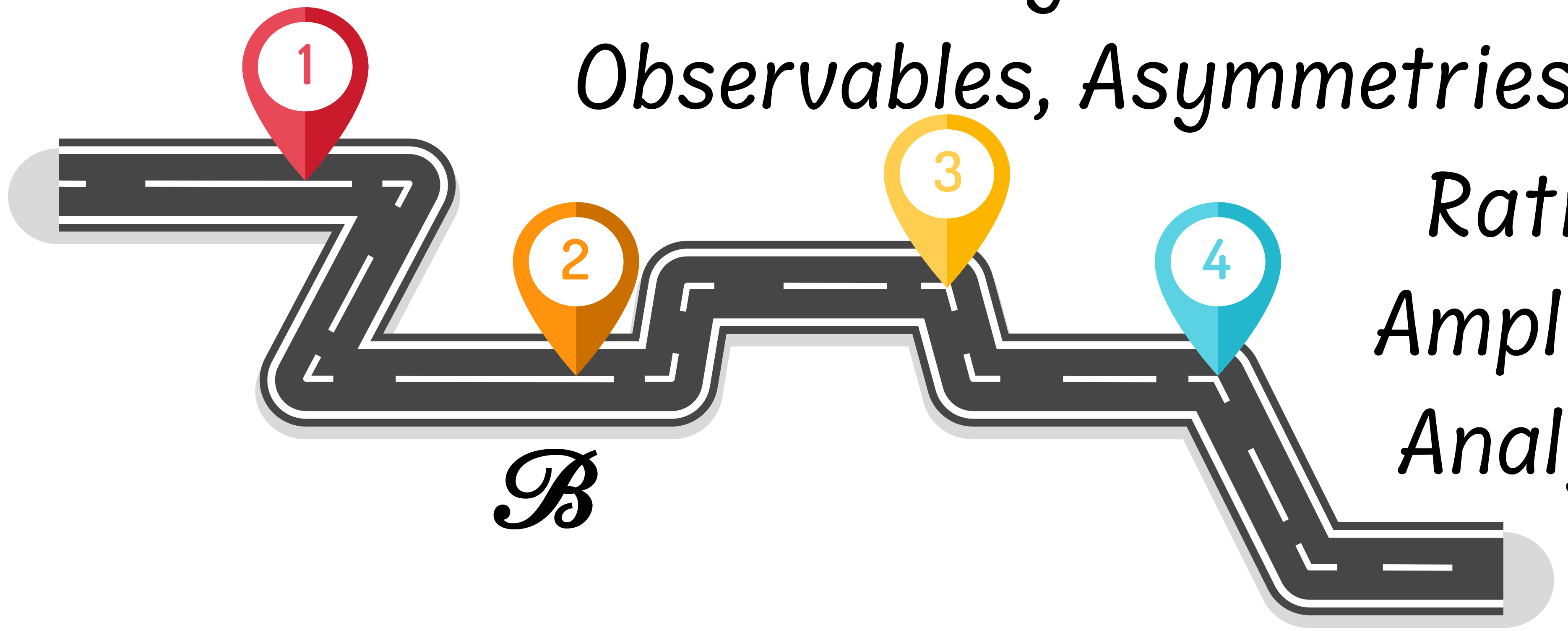

Accelerators

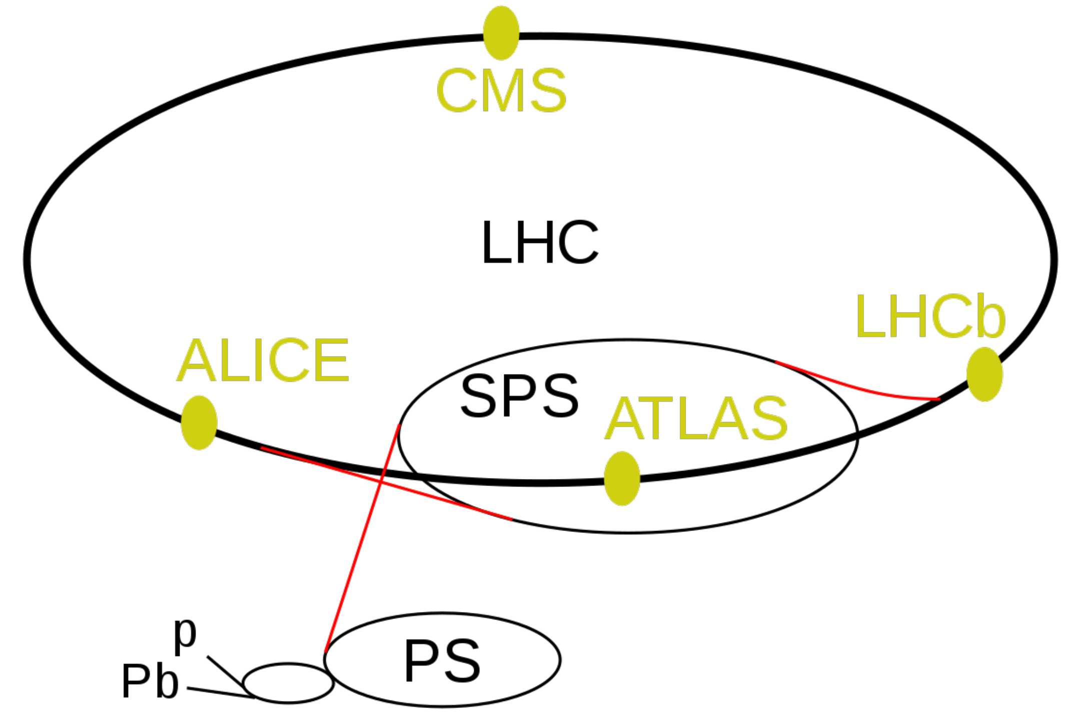

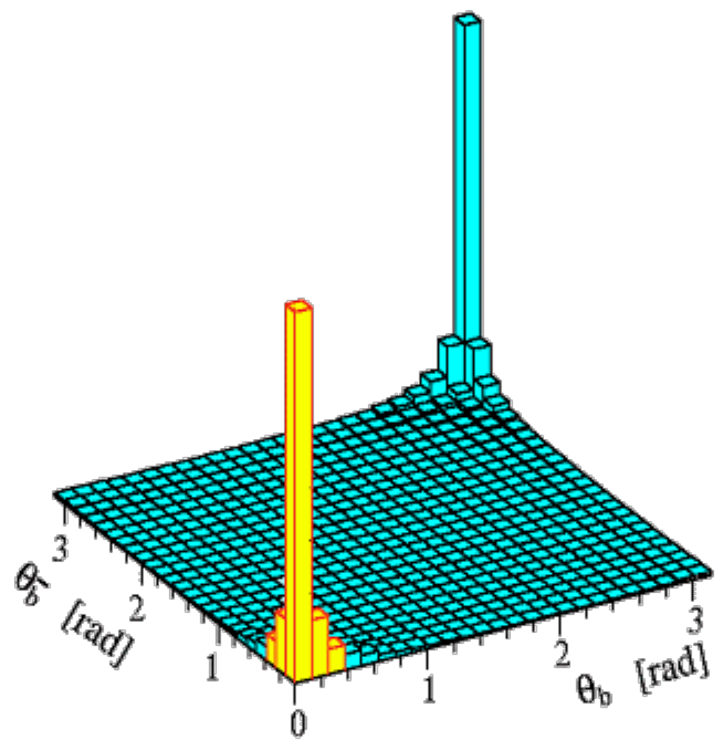

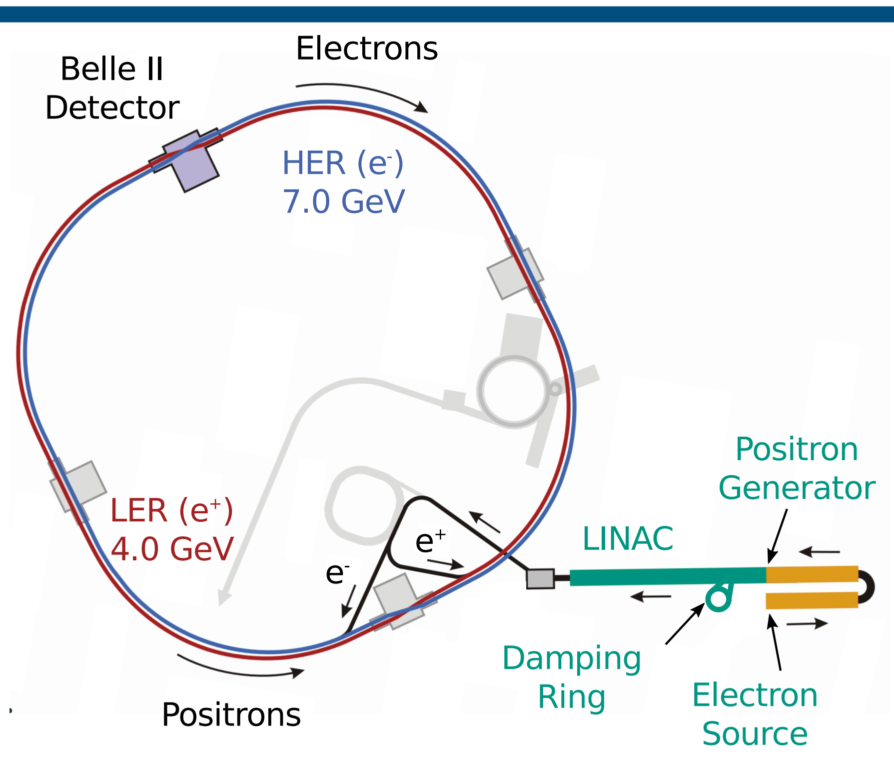

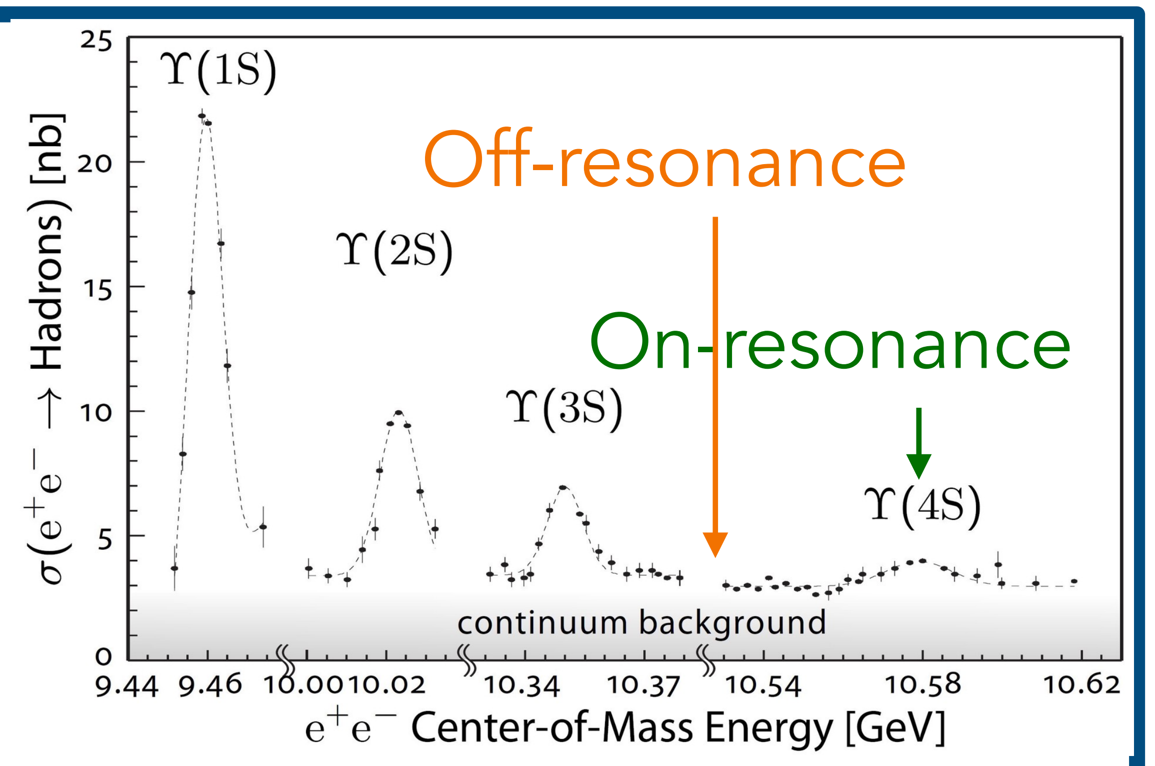

LHC

- pp collisions at 7,8,13 TeV
- b-quarks produced by gluon fusion
- All b-hadron species (b-baryons)
- Highly boosted topology
- $\sigma_{bb} = 100\ \mu\text{b}$
- Noise/Signal=1000

SuperKEKB

- e^+e^- energy-asymmetric collisions at $\sqrt{s} = 10.58$ GeV (on-resonance data)
- 60 MeV below to constrain $e^+e^- \to q\bar{q}$ (continuum) bkgs (off-resonance data)
- $B\bar{B}$ produced via $\Upsilon(4(S))$
- Exclusive $B\bar{B}$ production
- Asymmetric beam energy → boost
- $\sigma_{bb} = 1.1$ nb
- Noise/Signal=4

Accelerators

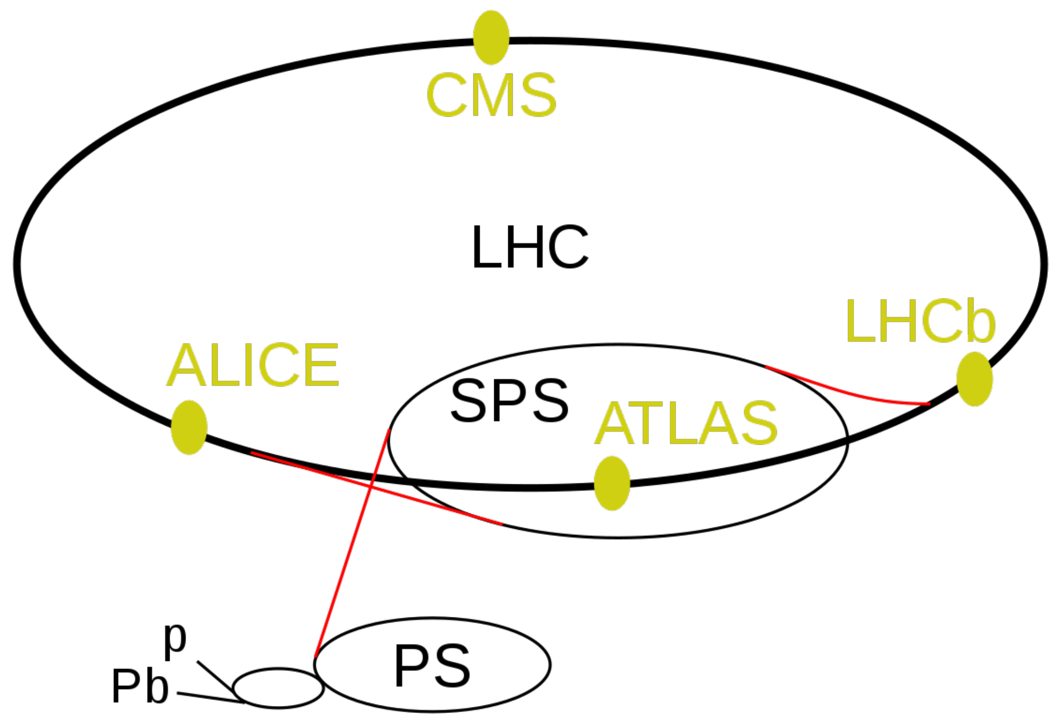

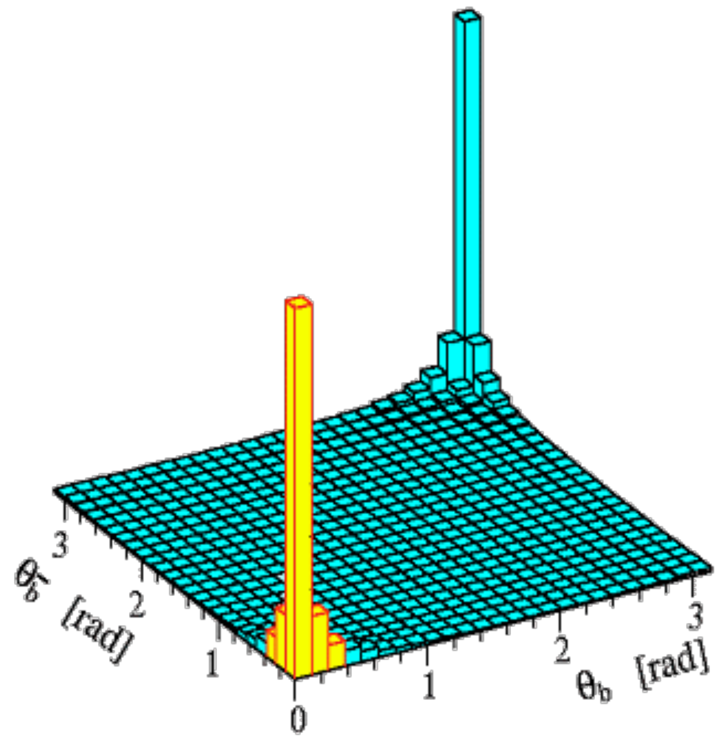

LHC

- pp collisions at 7,8,13 TeV
- b-quarks produced by gluon fusion
- all b-hadron species (b-baryons)
- Highly boosted topology
- $\sigma_{bb} = 100 \mu b$
- Different backgrounds (Noise/Signal=1000)

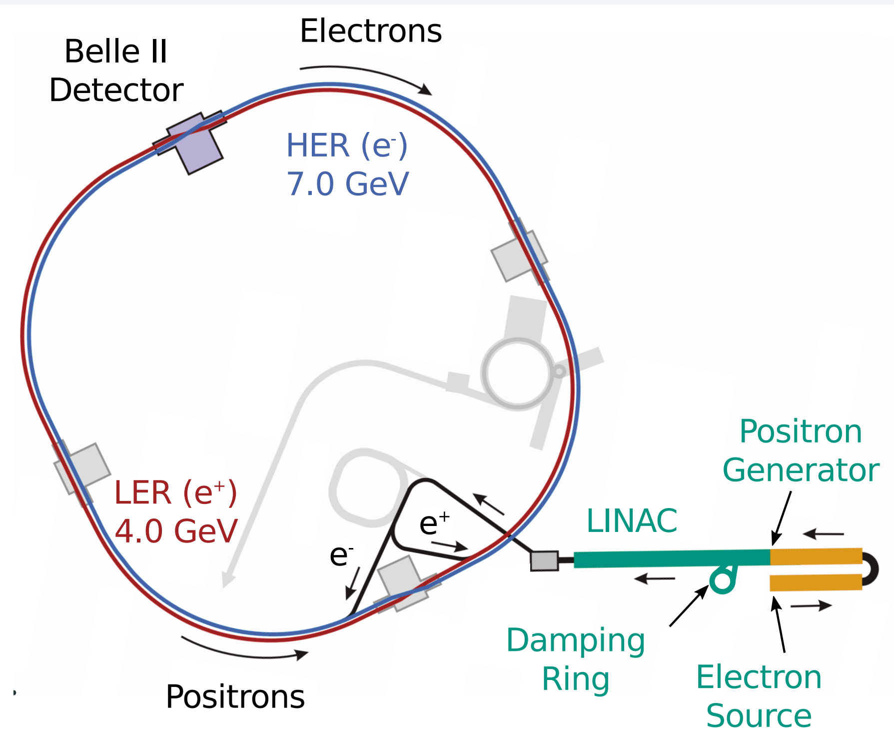

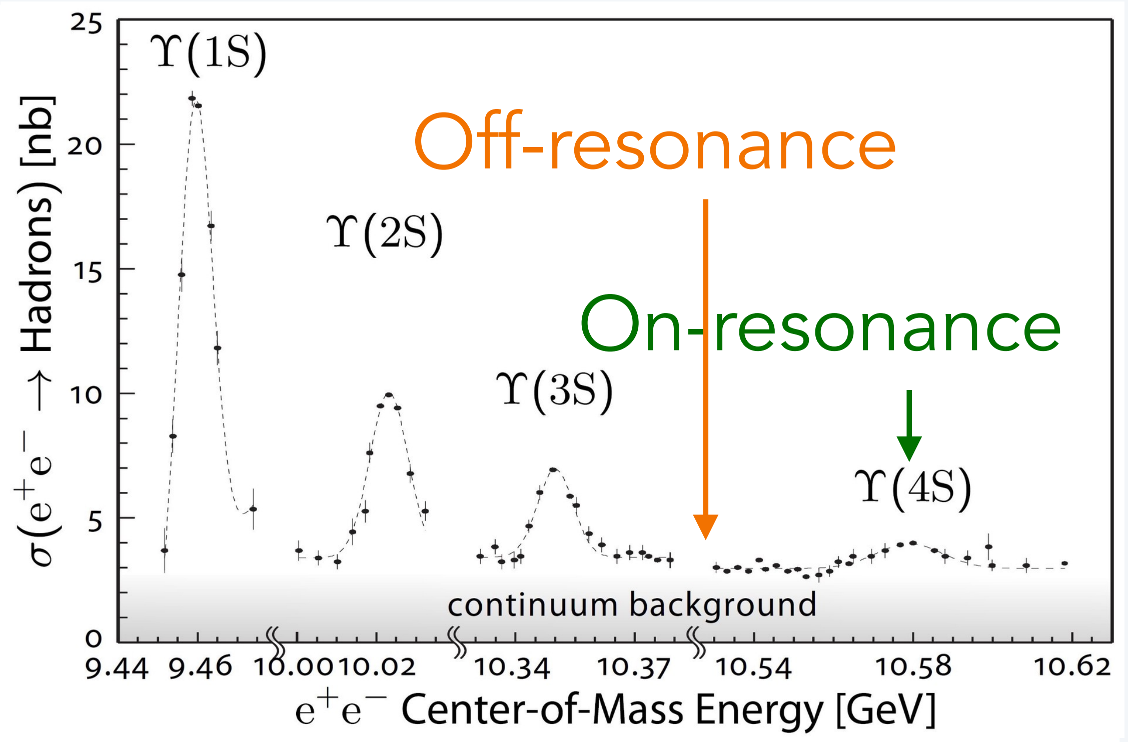

SuperKEKB

- e^+e^- energy-asymmetric collisions at $\sqrt{s} = 10.58$ GeV (on-resonance data)
- 60 MeV below to constrain $e^+e^- \rightarrow q\bar{q}$ (continuum) bkgs (off-resonance data)
- $B\bar{B}$ produced via $\Upsilon(4(S))$
- Exclusive $B\bar{B}$ production
- Asymmetric beam energy → boost
- $\sigma_{bb} = 1.1$ nb
- Different backgrounds (Noise/Signal=4)

Approximate rule:

1 fb^{-1} = 1 ab^{-1}

The Three Beasts

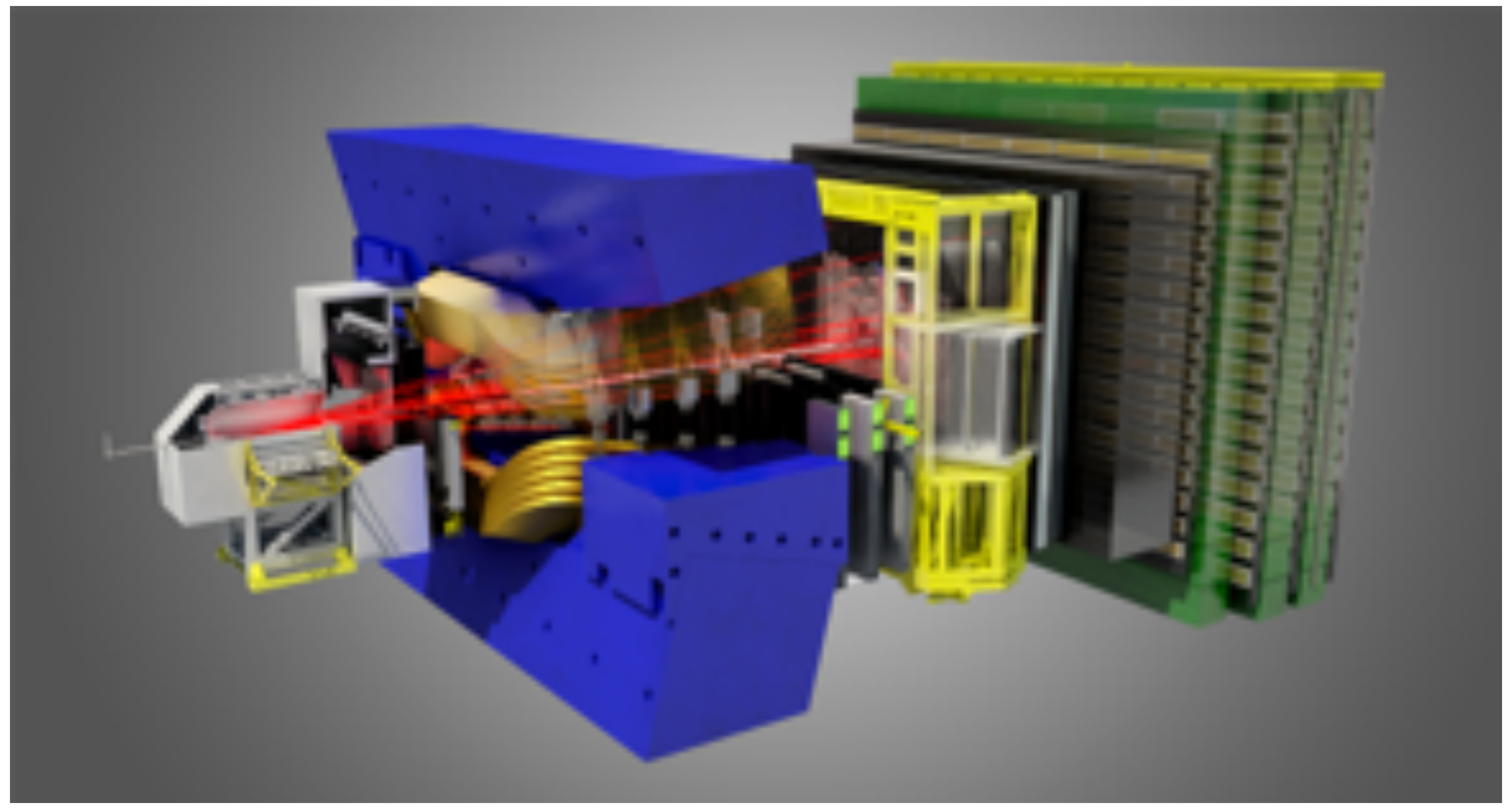

LHCb

- LHC (pp collisions at 7,8,13 TeV)
- Forward-looking spectrometer
- Taking data since 2011
- Collected **9 $\mathbf{fb^{-1}}$ data so far**
  - **4x10^{12} $b\bar{b}$ pairs**
  - B_u (40%), B_d(40%), B_s(10%), B_c and b-baryons (10%)

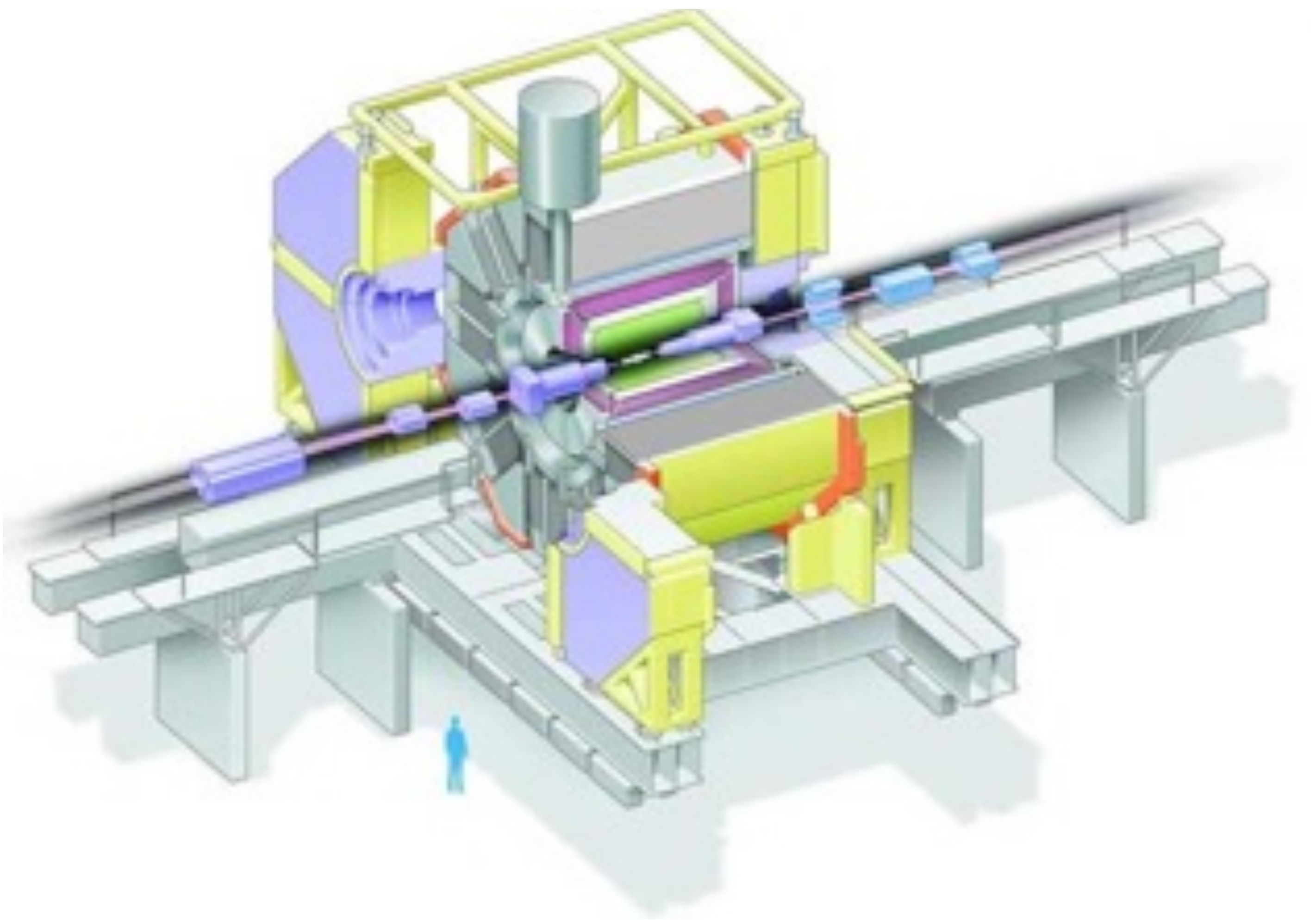

Belle

- KEKB (8 GeV e^-/ 3.5 GeV e^+)
- General purpose detector
- Took data from 1999-2010
- Collected **711 $\mathbf{fb^{-1}}$** data
  - **770 mil. $B\bar{B}$ pairs**

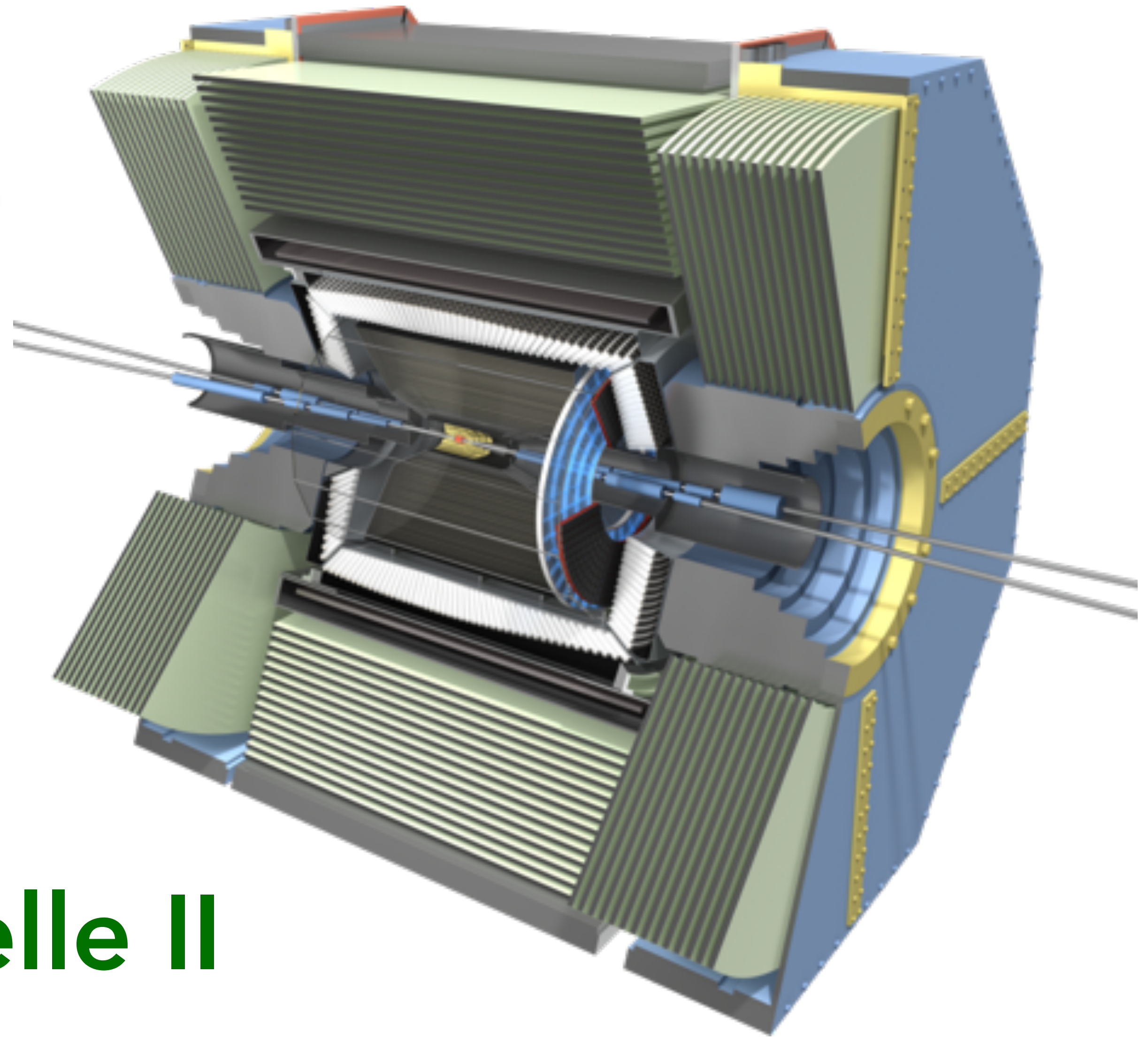

Belle II

- SuperKEKB (7 GeV e^-/4 GeV e^+)
- General purpose detector
- Taking data since 2019
- Collected **362 $\mathbf{fb^{-1}}$ data in Run 1**
  - **370 mil. $B\bar{B}$ pairs**
- Resumed data-taking this year after ~ 1.5y long shut-down

The Three Beasts

Increasing instantaneous luminosity is the key!

LHCb

- LHC (pp collisions at 7,8,13 TeV)
- Forward-looking spectrometer
- Taking data since 2011
- Collected **9 $\mathbf{fb^{-1}}$ data so far**
  - **4x10[12] $b\bar{b}$ pairs**
  - B_u (40%), B_d(40%), B_s(10%), B_c and b-baryons (10%)
- **Plan: 300 $\mathbf{fb^{-1}}$**

Belle

- KEKB (8 GeV e^-/ 3.5 GeV e^+)
- General purpose detector
- Took data from 1999-2010
- Collected **711 $\mathbf{fb^{-1}}$** data
  - **770 mil. $B\bar{B}$ pairs**

Belle II

- SuperKEKB (7 GeV e^-/4 GeV e^+)
- General purpose detector
- Taking data since 2019
- Collected **362 $\mathbf{fb^{-1}}$ data in Run 1**
  - **370 mil. $B\bar{B}$ pairs**
- Resumed data-taking this year after ~ 1.5y long shut-down
- **Plan: 50 $\mathbf{ab^{-1}}$**

Typical Event

LHCb

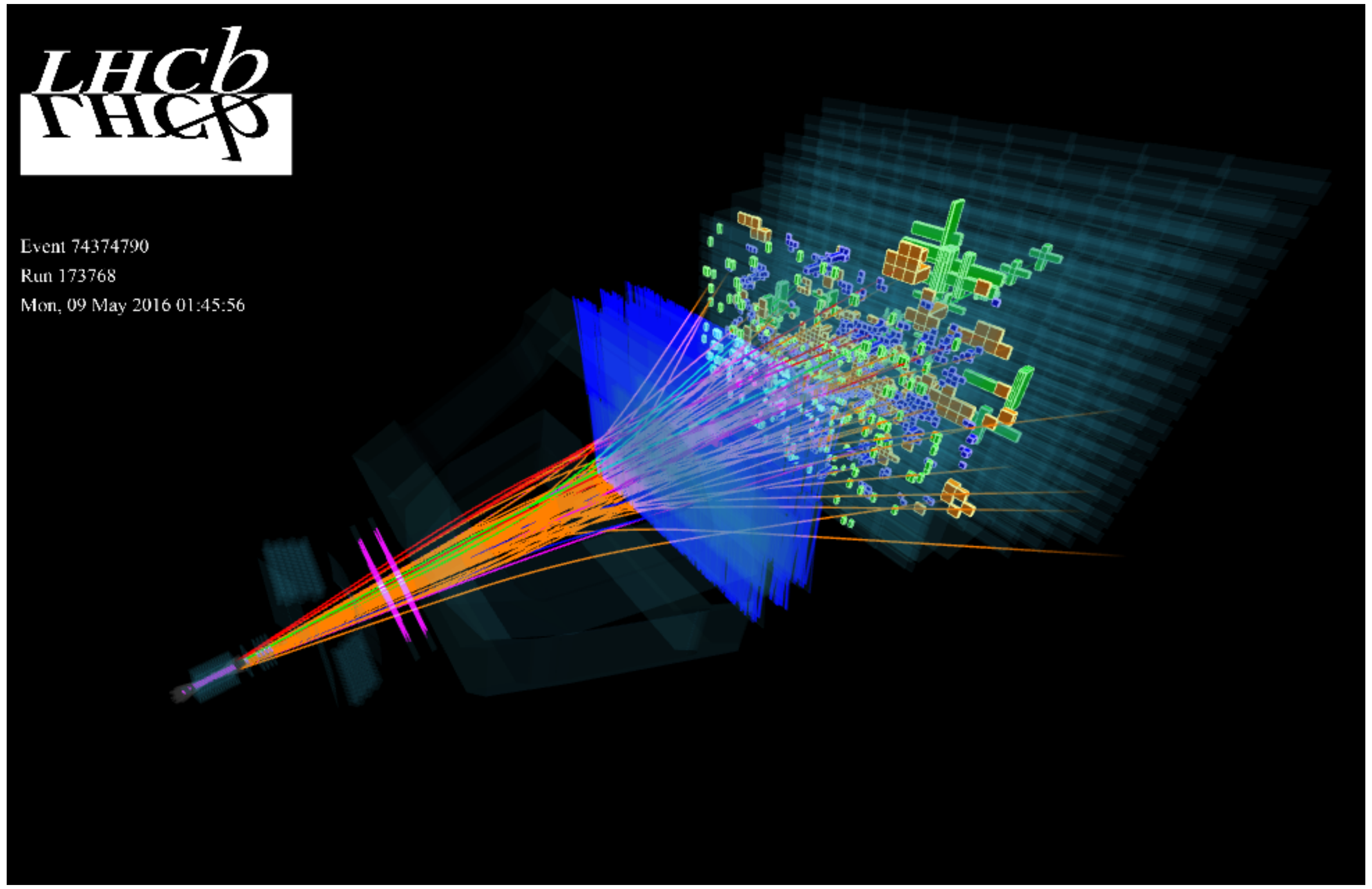

- Rather busy environment
- On average 100 tracks
- Longitudinal momentum of the B not known
- Lower trigger efficiency in general

Belle II

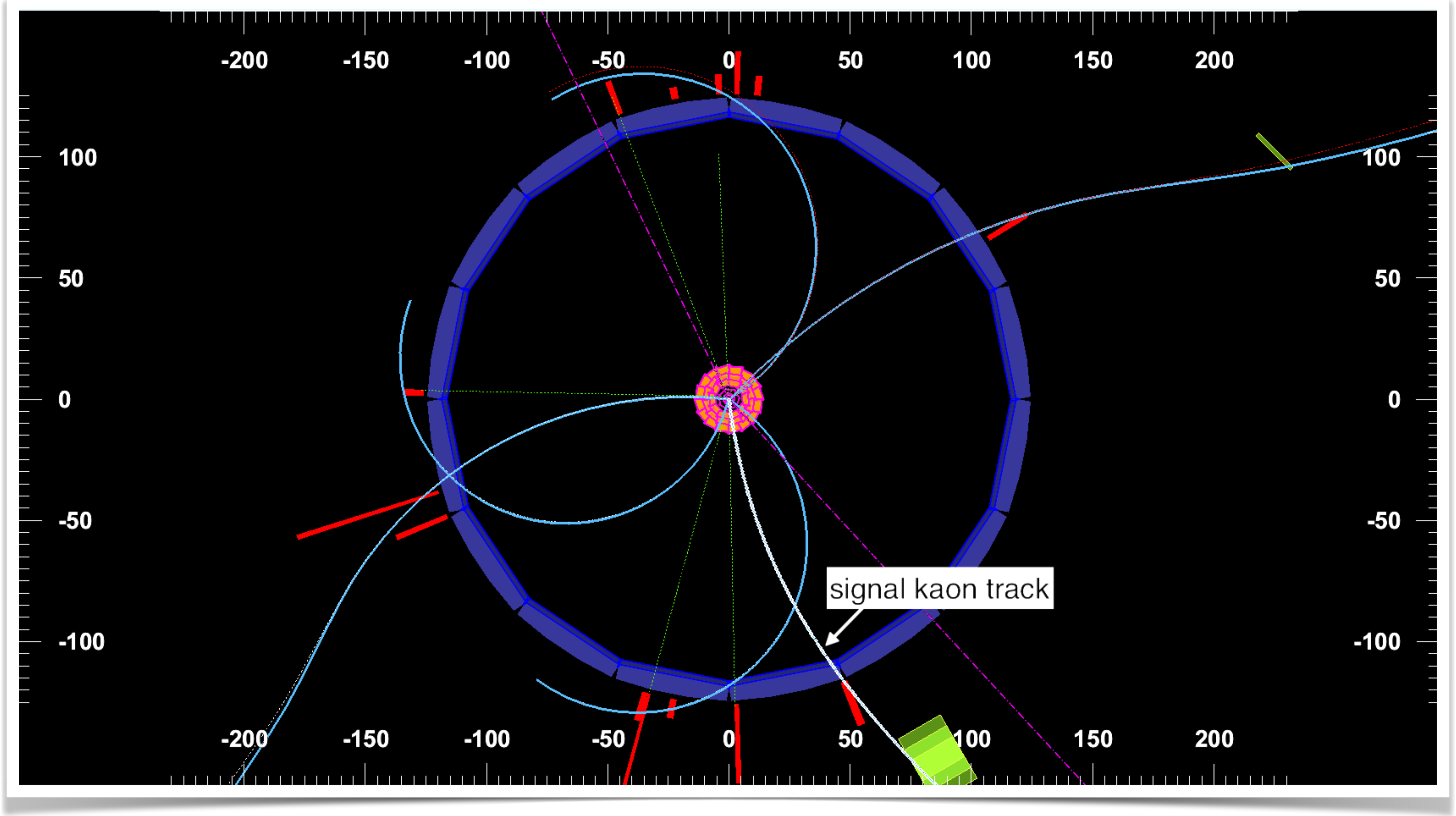

- Very clean environment
- On average: 11 tracks
- Known initial state kinematics
- Near 100% efficiency for B decays
- Sensitive to lower energy deposits

Neutral Performance

	Belle II	LHCb
γ detection efficiency	99.9%	95 %
$\sigma(E)/E$	$\frac{2.2\,\%}{\sqrt{E}} \oplus 1\,\%$	$\frac{10\,\%}{\sqrt{E}} \oplus 1\,\%$
π^0 reconstruction	Better mass resolution	Worse mass resolution

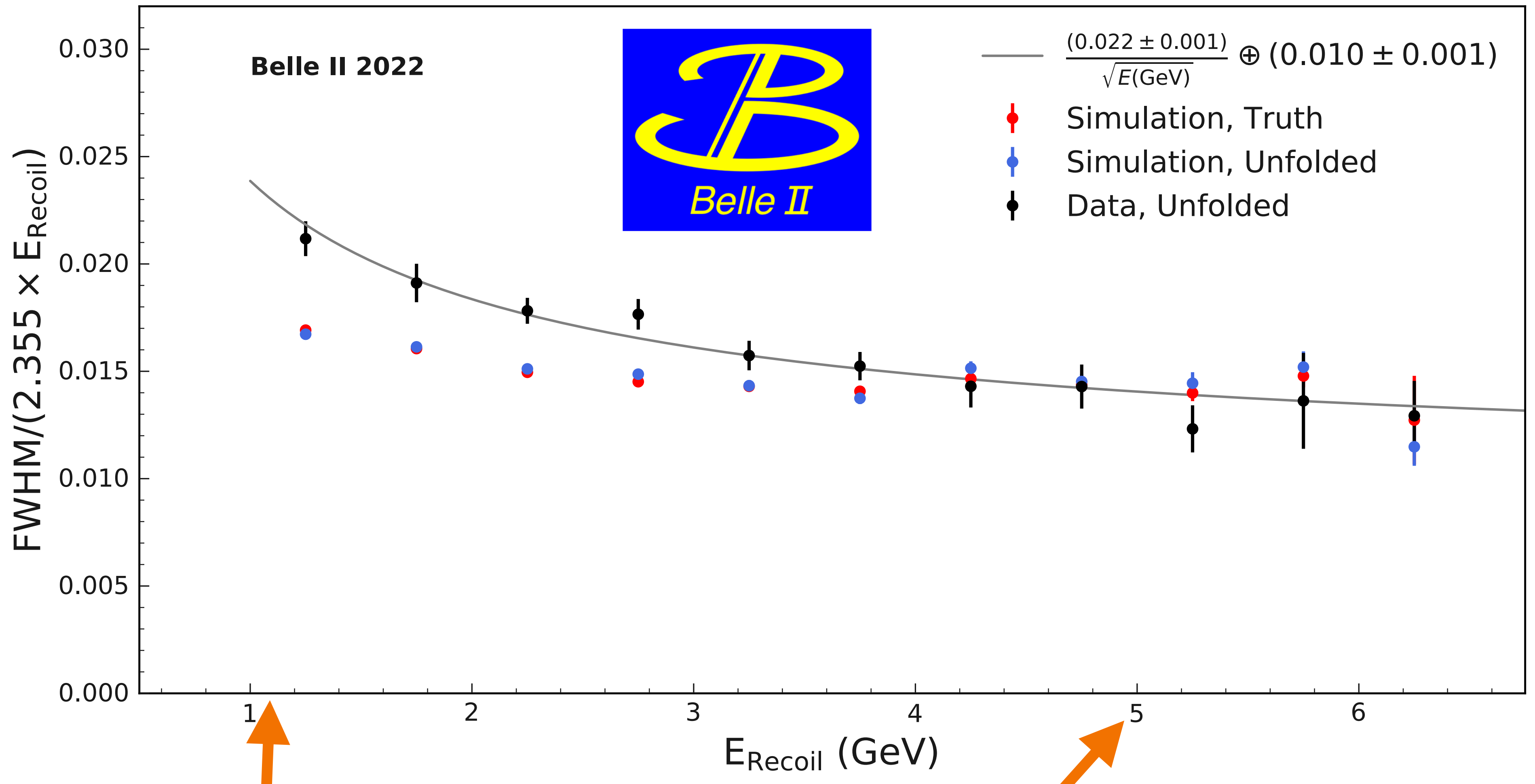

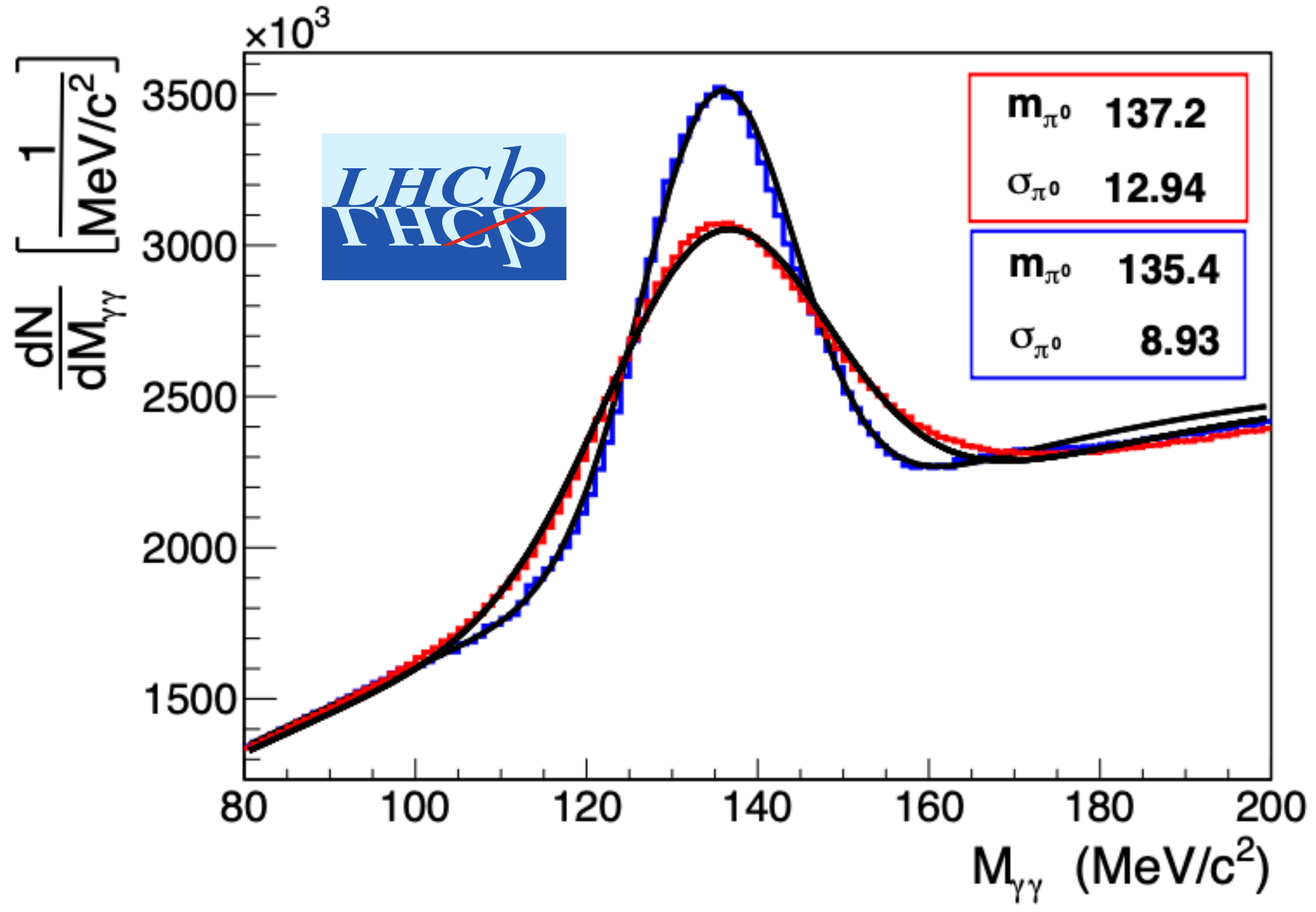

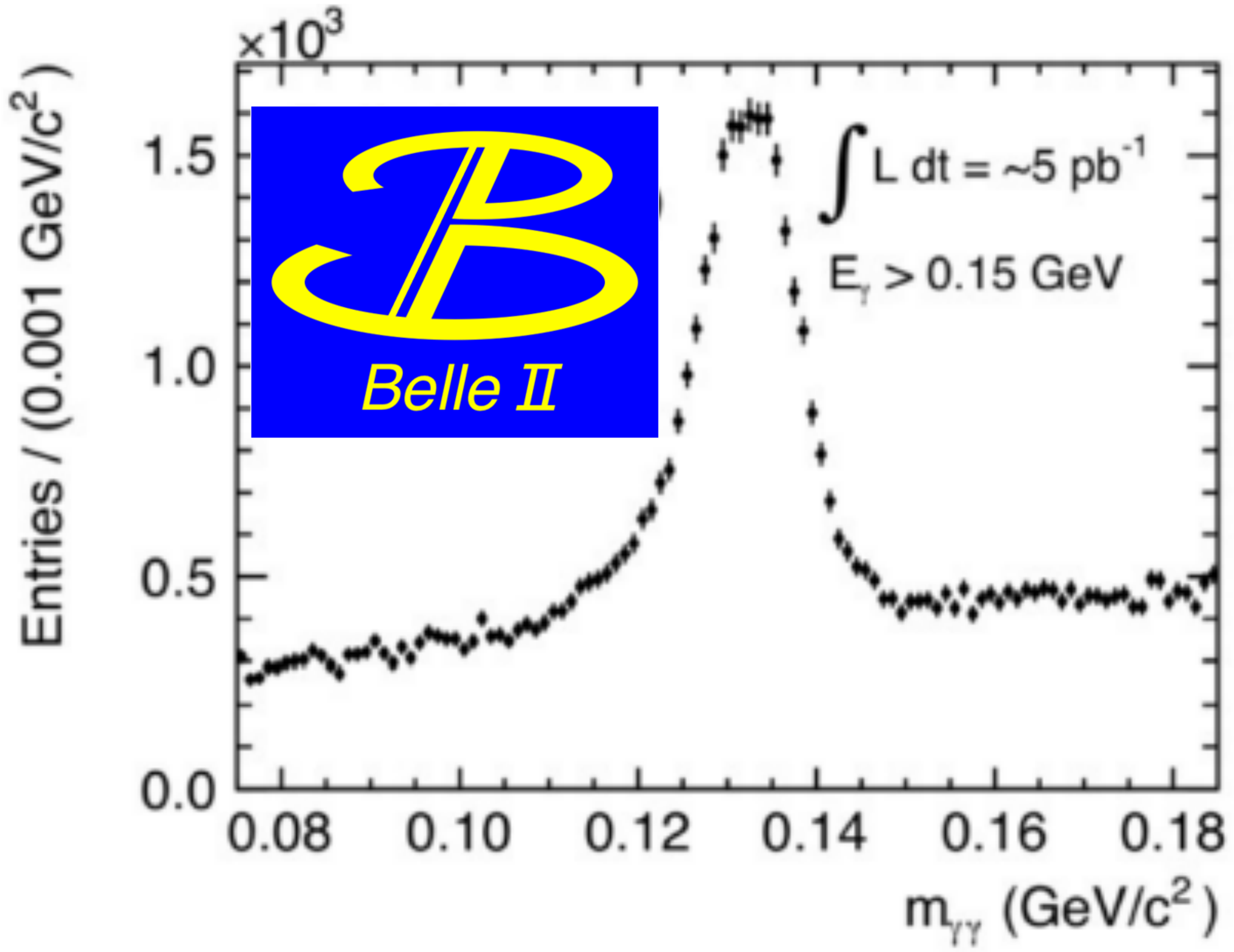

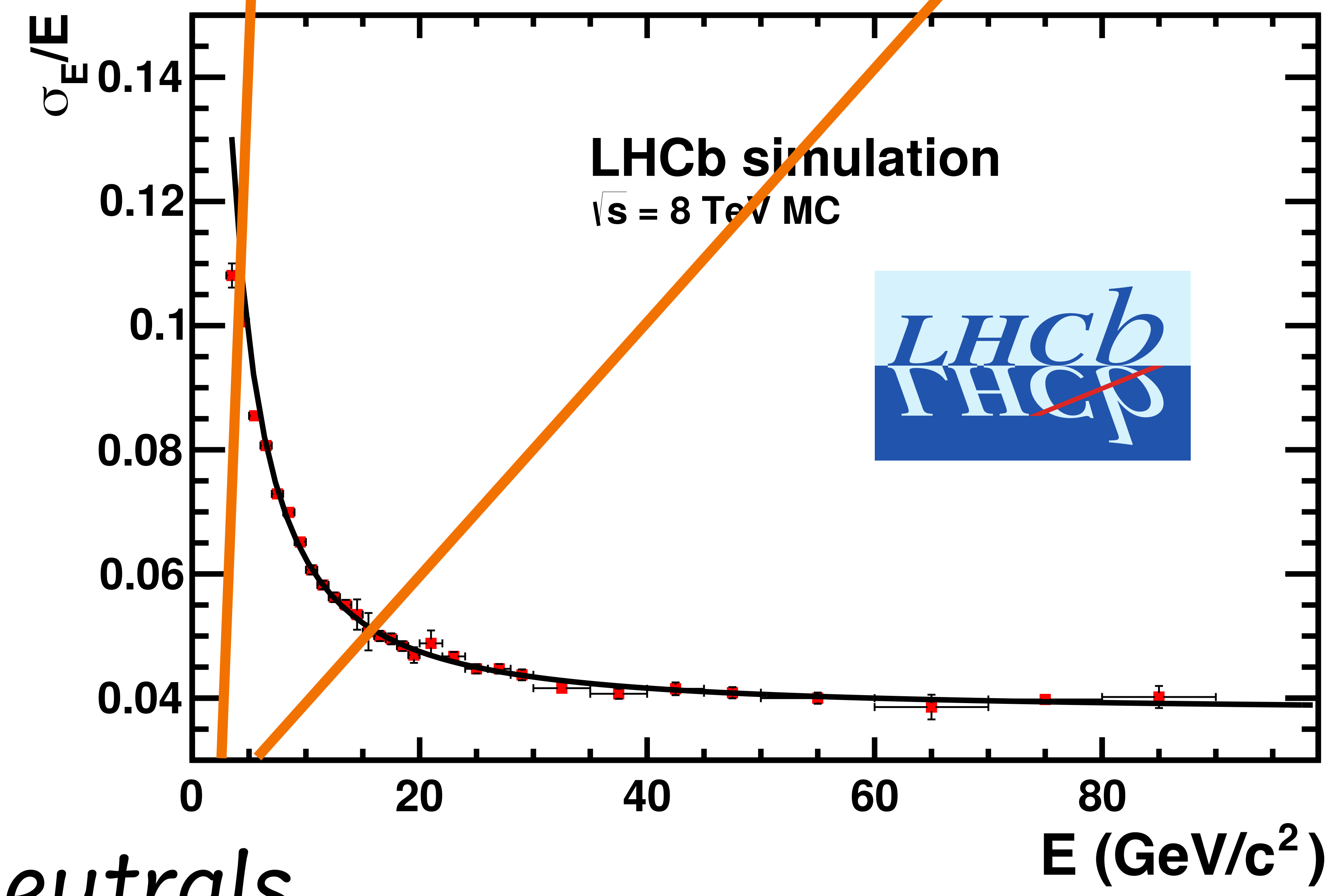

Belle II is generally better with neutrals

Charged Track Performance

	Belle II	LHCb
Muon trigger efficiency	100 %	90 %
Muon ID efficiency	95 %	97 %
$\pi \rightarrow \mu$ misID	7 %	1-3%

	Belle II	LHCb
Kaon ID efficiency	90 %	95 %
$K \rightarrow \pi$ misID	5 %	5 %

	Belle II	LHCb
Total $B^+ \rightarrow K^+\mu^+\mu^-$ efficiency	30 %	5 %
Total $B^+ \rightarrow K^+e^+e^-$ efficiency	30 %	<5 %

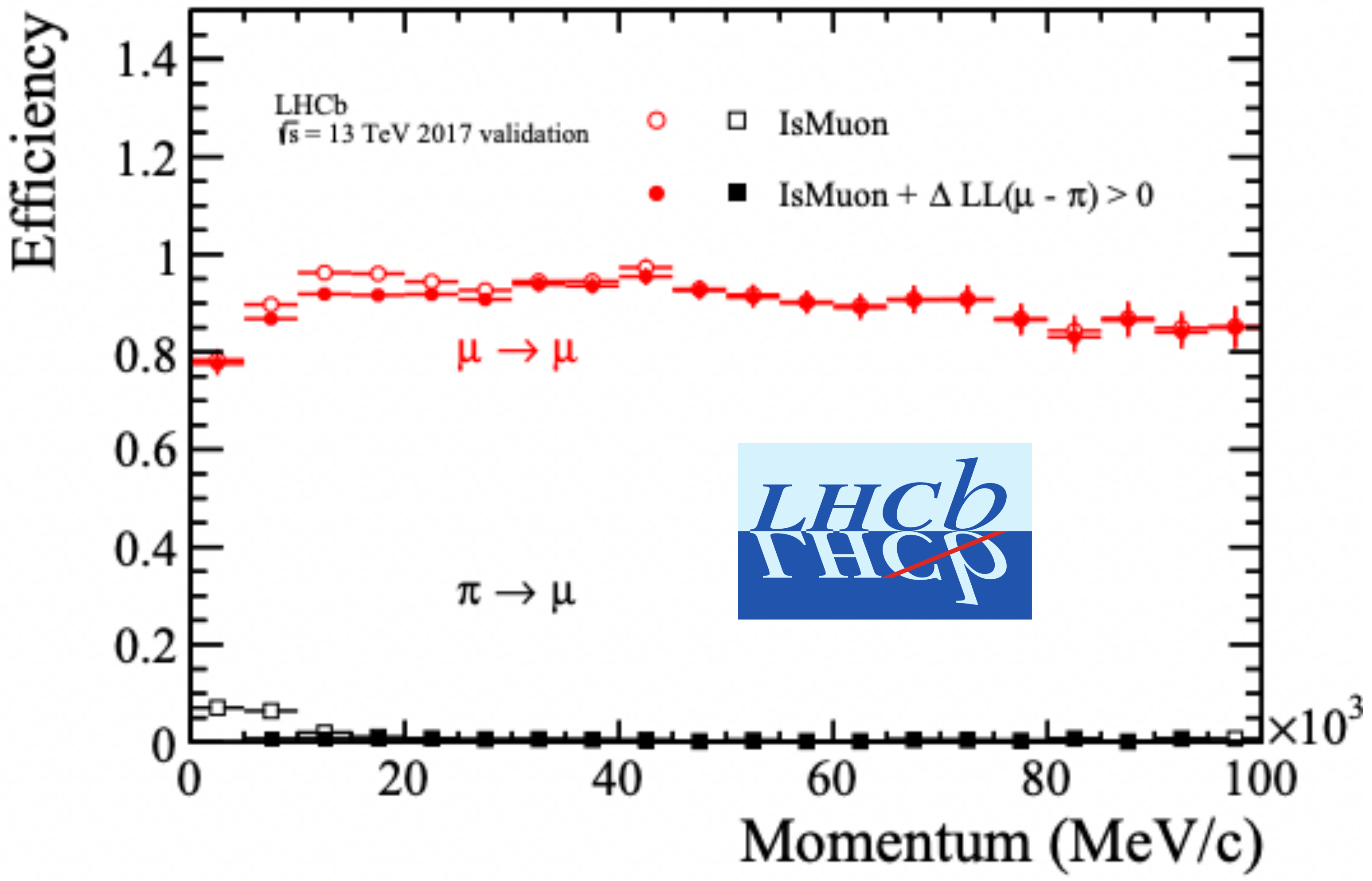

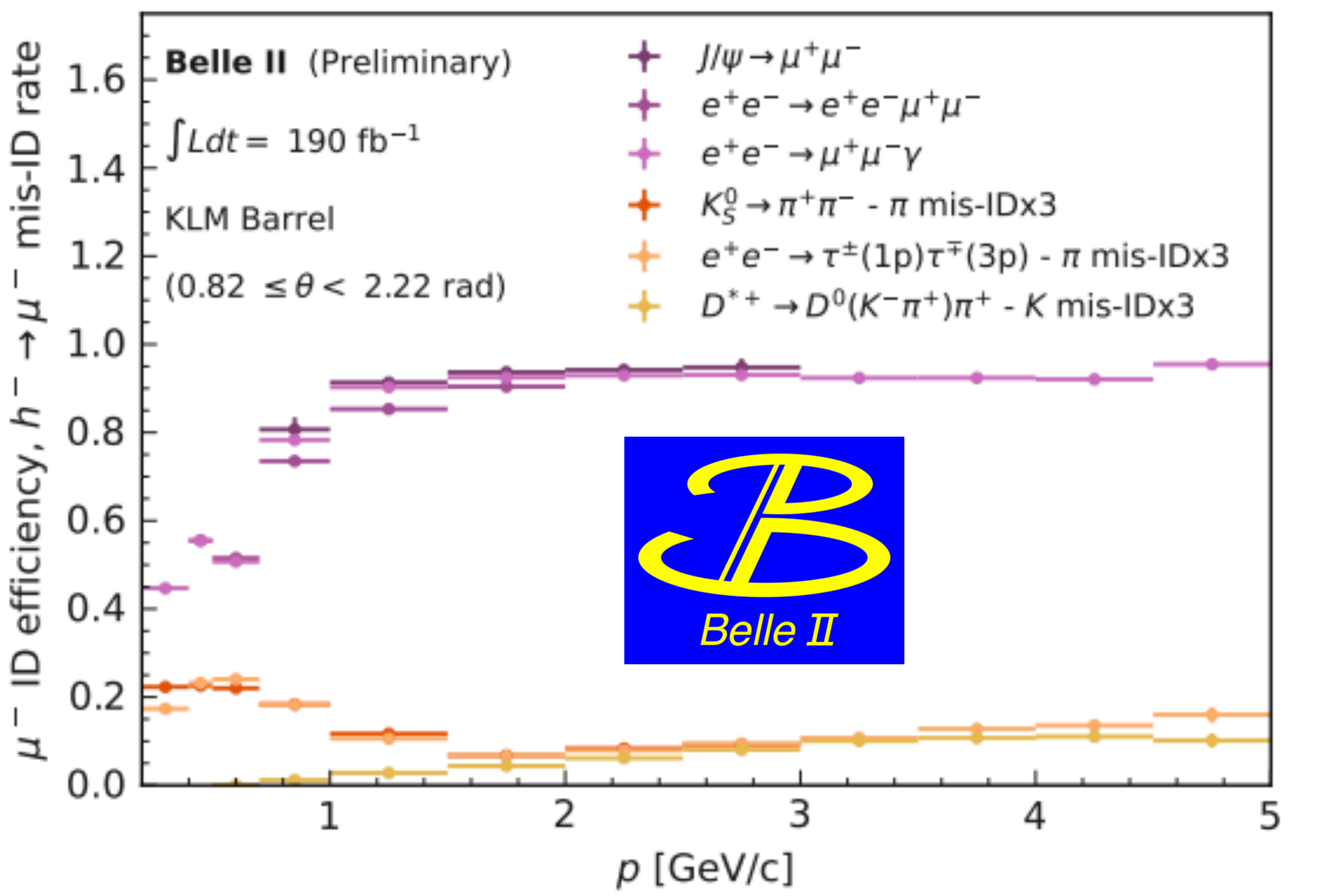

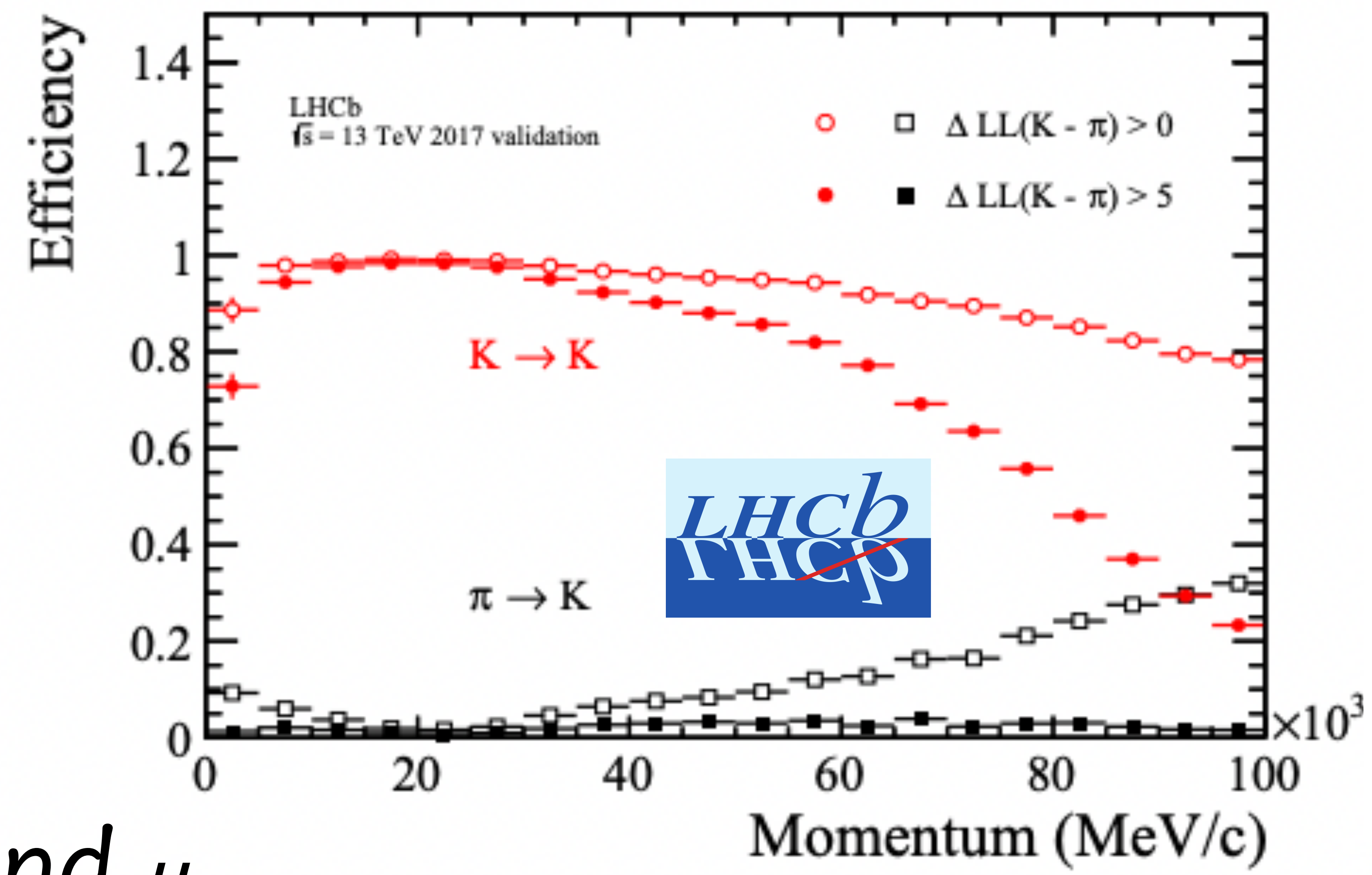

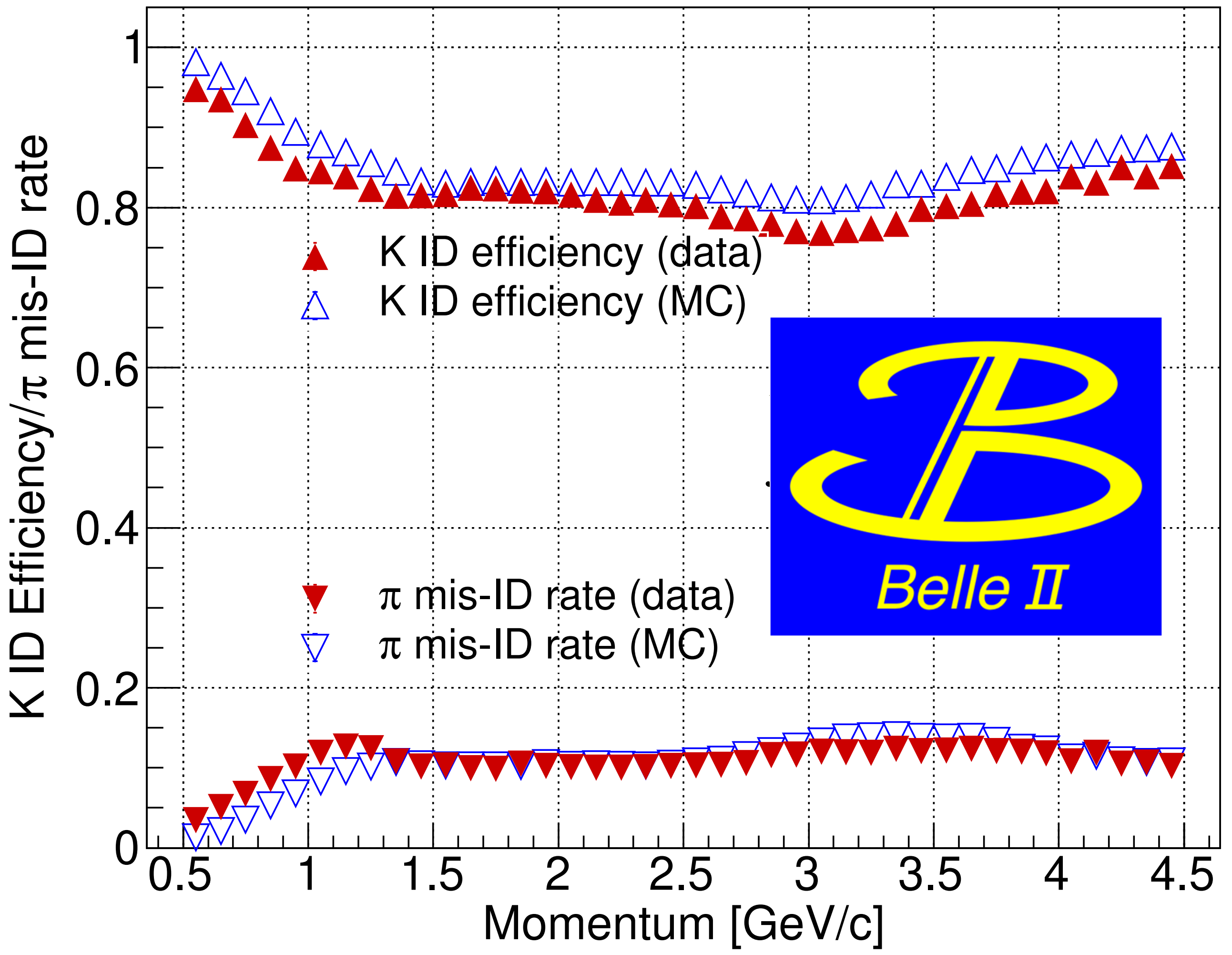

LHCb is very good with muons

Belle II has similar sensitivity for e and μ

Rare B Decays

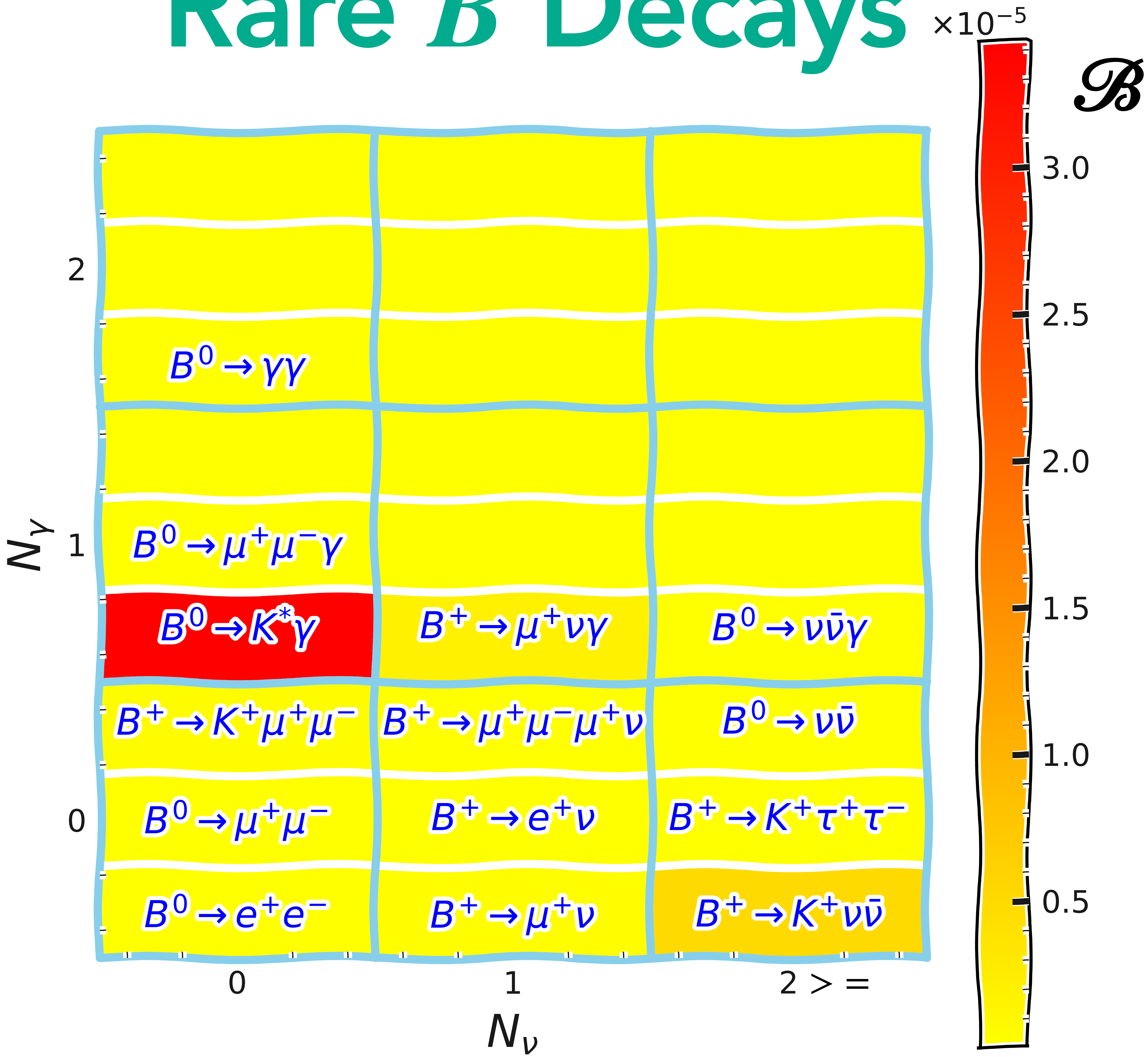

Rare B Decays

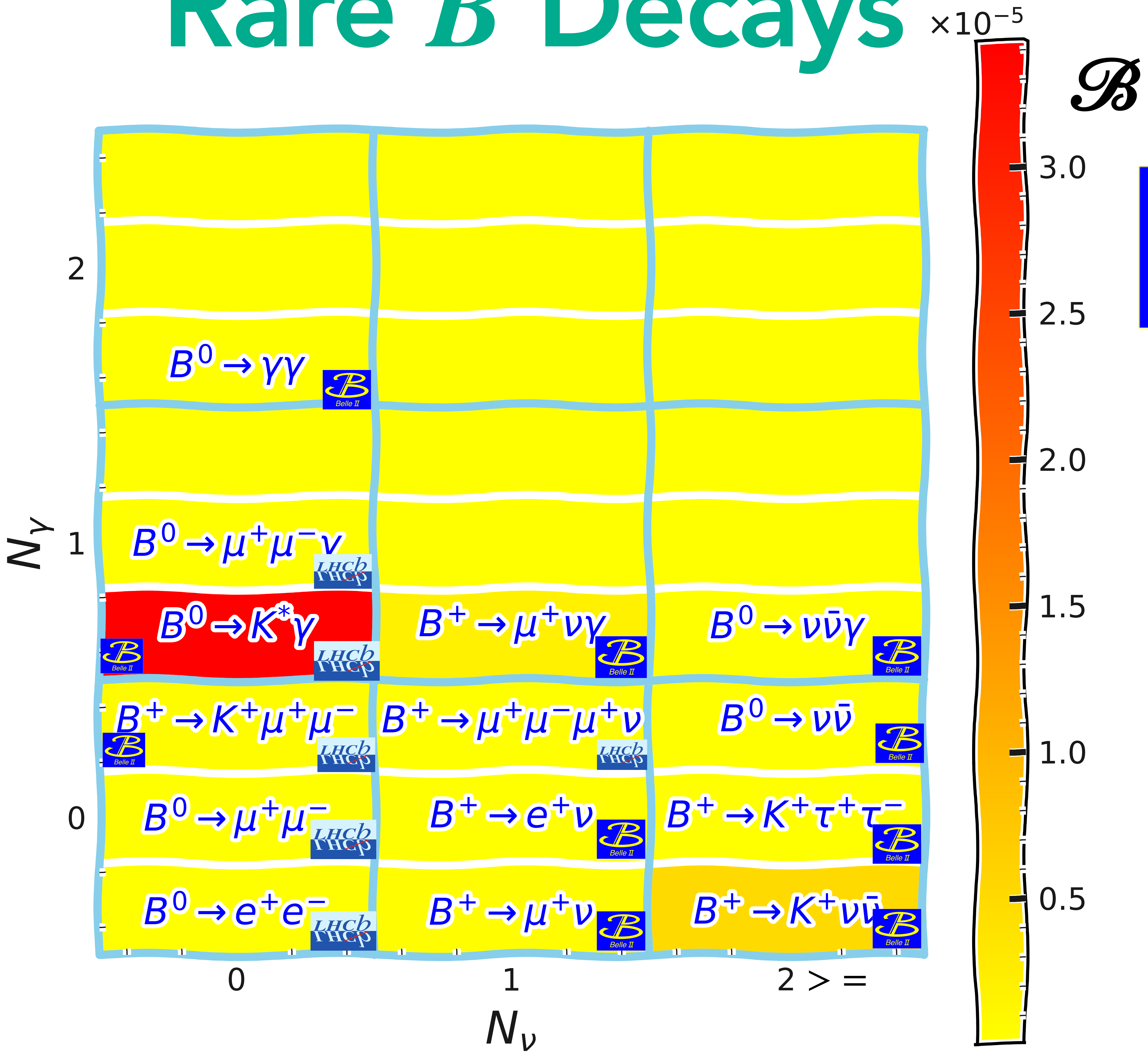

Better with higher number of γ and ν

Better with multiple muons/ charged tracks that can be vertexed

Results

$B \to K^*\gamma$

$B^0 \to \gamma\gamma$

$B_s^0 \to \mu\mu\gamma$

$\Lambda_b^0 \to pK^-\gamma$

$B^+ \to K^+\nu\bar{\nu}$

BRAND NEW

$B \to K^*\gamma$

Belle II

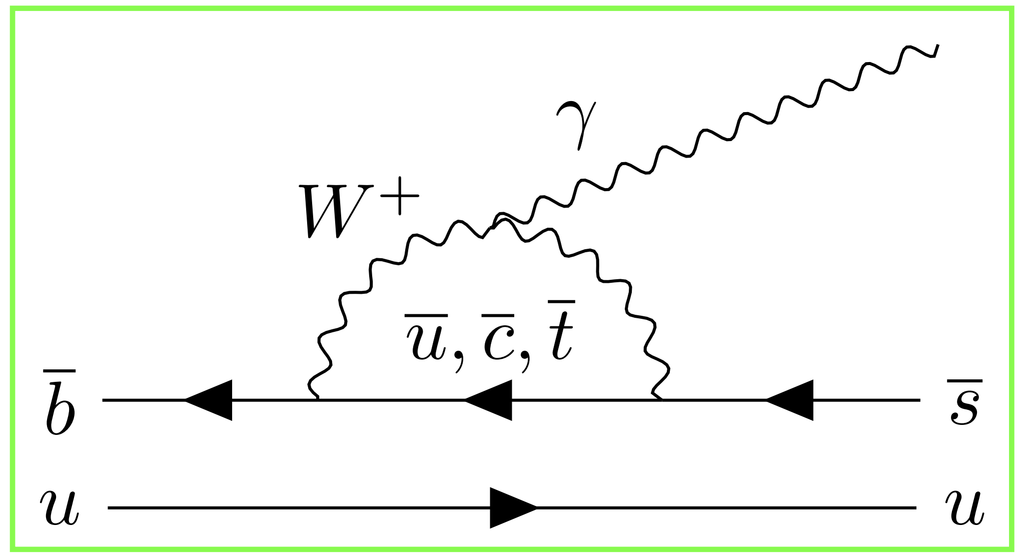

FCNC $b \to s\gamma$ transition:

- **First radiative penguin** to be measured at Belle II
- **Branching fractions** $\mathscr{B}$ have **large theoretical uncertainties** (~20%)
- CP (A_{CP}) and isospin (Δ_{+0}) asymmetries theoretically clean (cancellation of form factors)
- **Latest Belle measurement found evidence** of 3.1σ for the **isospin asymmetry** [PRL 119, 191802 (2017)]
- Belle II wants to measure in addition to $\mathscr{B}$

$$A_{CP} = \frac{\Gamma(\bar{B} \to \overline{K^*}\gamma) - \Gamma(B \to K^*\gamma)}{\Gamma(\bar{B} \to \overline{K^*}\gamma) + \Gamma(B \to K^*\gamma)}$$

SM prediction: A_{CP} is small (~1%)

$$\Delta A_{CP} = A_{CP}(B^0 \to K^{*0}\gamma) + A_{CP}(B^+ \to K^{*+}\gamma)$$

$$\Delta_{+0} = \frac{\Gamma(B^0 \to K^{*0}\gamma) - (B^+ \to K^{*+}\gamma)}{\Gamma(B^0 \to K^{*0}\gamma) + (B^+ \to K^{*+}\gamma)}$$

SM prediction: $\Delta_{+,0}$ range from 2-8% with an uncertainty ~2%

BRAND NEW

$B \to K^* \gamma$

Selection strategy:

- Based on Run 1 Belle II dataset 362 fb^{-1}
- Reconstruct $K^* \to K^+\pi^-, K_s^0\pi^0, K^+\pi^0$ and $K_s^0\pi^+$
- Use **classifiers to reject backgrounds** from $\pi^0 \to \gamma\gamma$ and $\eta \to \gamma\gamma$, continuum events

Fitting strategy:

- Make **2D fit** to ΔE and M_{bc} distributions to extract yields

$$\Delta E = E_B - E_{beam} \qquad M_{bc} = \sqrt{E_{beam}^2 - |\vec{p_B}|^2 - p_B^{*2}}$$

Control samples:

- **$D^+ \to K_s^0\pi^+$ to study K_s^0 reconstruction efficiency**
  - Excellent kinematic coverage
  - Total systematic uncertainty of 1.4% derived in bins of K_s^0 flight distance in $p \in (0.3, 3.1)$ GeV$/c$
- **$D^0 \to K^+\pi^-$ to validate the rest of selection efficiency**

Normalised to same area

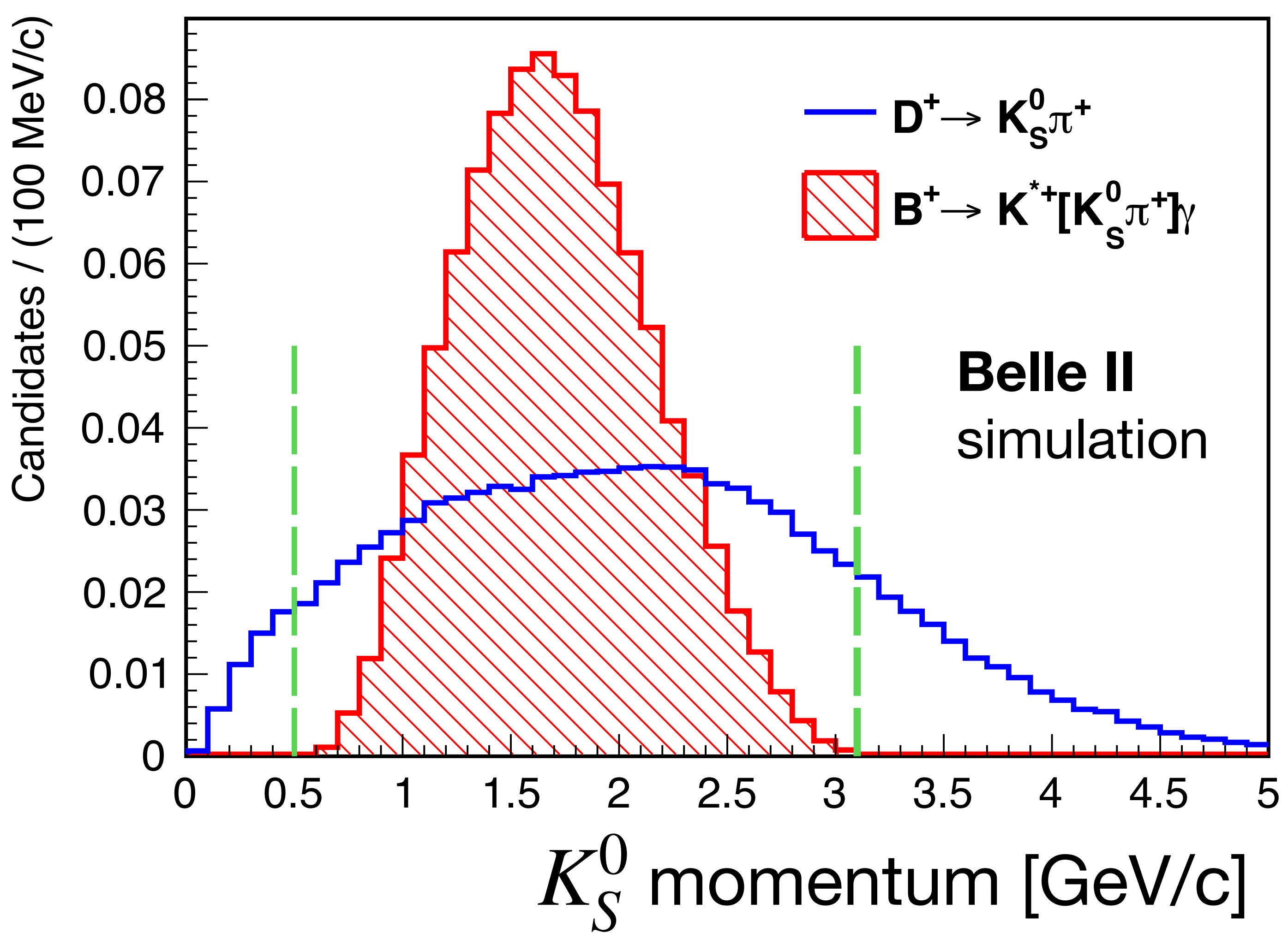

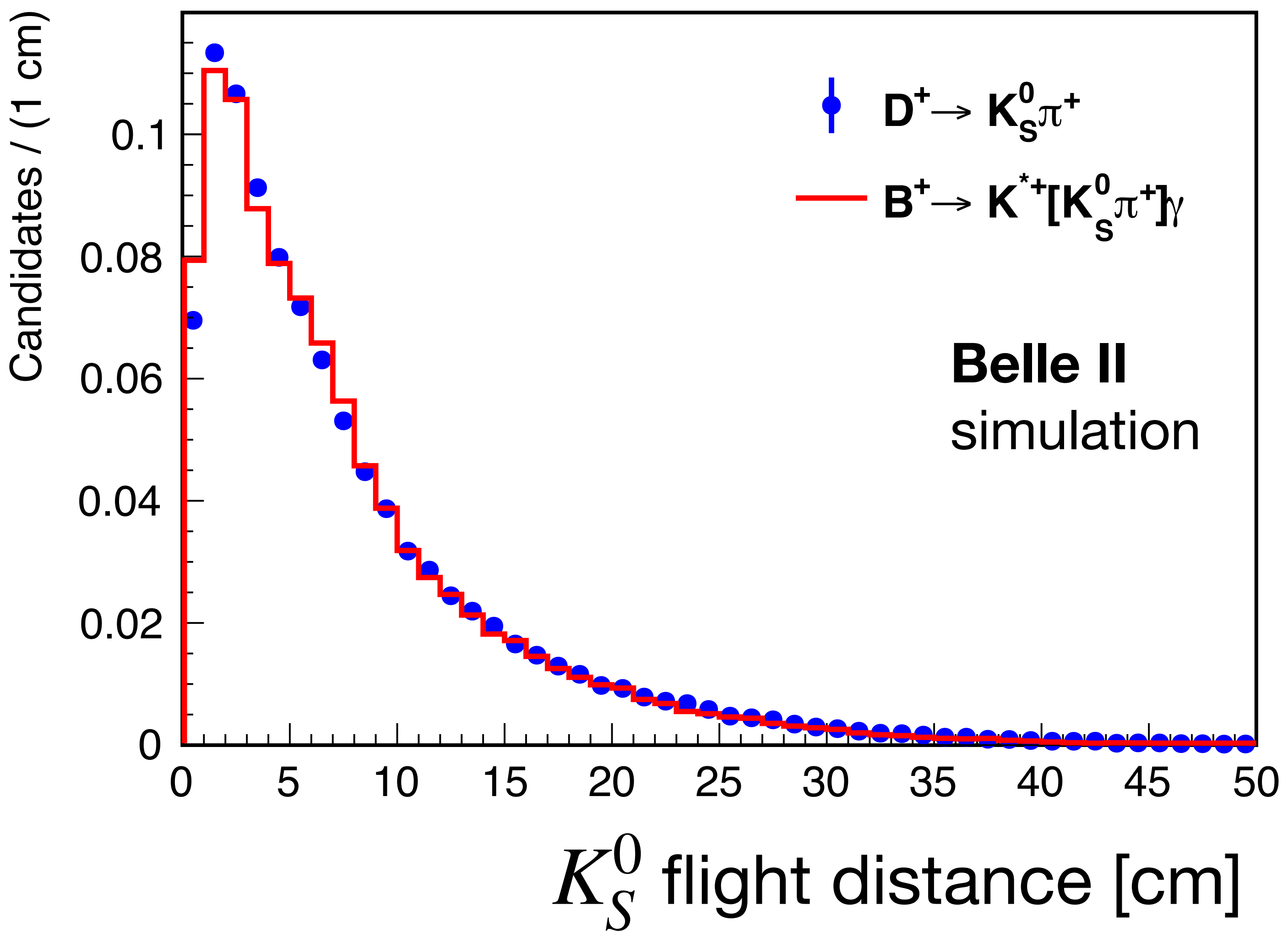

BRAND NEW

$B \to K^{*}\gamma$

Results:

Branching fractions

$$\mathscr{B}[B^0 \to K^{*0}\gamma] = (4.16 \pm 0.10 \pm 0.11) \times 10^{-5}$$

$$\mathscr{B}[B^+ \to K^{*+}\gamma] = (4.04 \pm 0.13 \pm 0.13) \times 10^{-5}$$

$$\mathscr{B}[B \to K^{*}\gamma] = (4.12 \pm 0.08 \pm 0.11) \times 10^{-5}$$

A_{CP}

$$A_{CP}[B^0 \to K^{*0}\gamma] = (-3.2 \pm 2.4 \pm 0.4)\,\%$$

$$A_{CP}[B^+ \to K^{*+}\gamma] = (-1.0 \pm 3.0 \pm 0.6)\,\%$$

$$A_{CP}[B \to K^{*}\gamma] = (-2.3 \pm 1.9 \pm 0.3)\,\%$$

Asymmetries

$$\Delta A_{CP} = (2.2 \pm 3.8 \pm 0.7)\,\%$$

$$\Delta_{0+} = (5.1 \pm 2.0 \pm 1.0 \pm 1.1)\,\%$$

$f^{\pm}/f^{00}$

$\sim 2.0\ \sigma$

Fit projections to M_{bc}

B^0, B^+

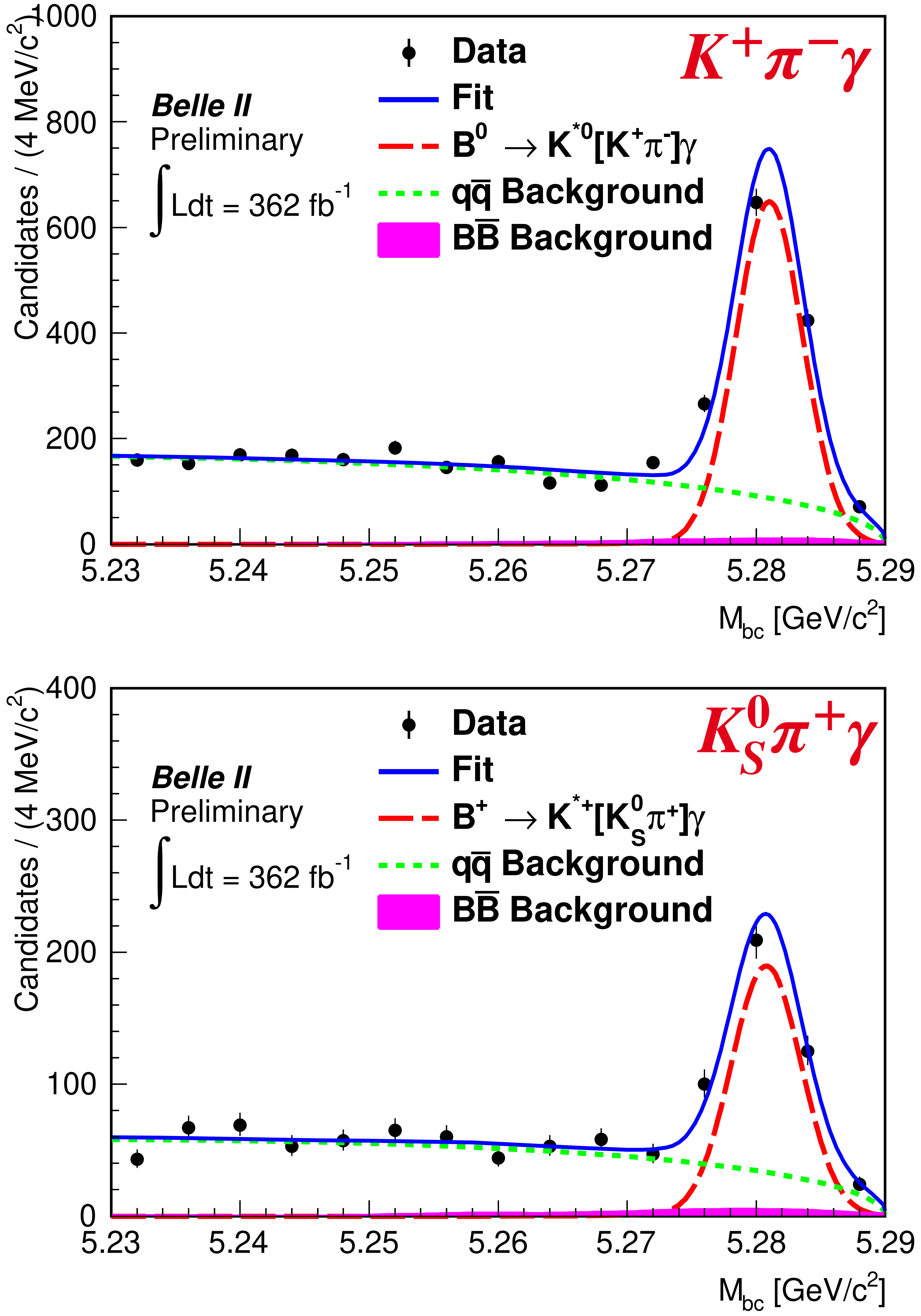

Belle result (3.1σ)

[PRL 119, 191802 (2017)]

$$\Delta_{0+} = [+6.2 \pm 1.5(\text{stat}) \pm 0.6(\text{syst}) \pm 1.2(f_{+-}/f_{00})]\%,$$

Remarks:

- **Consistent with PDG and SM**
- Similar sensitivity to Belle due to improved K_s^0 efficiency and ΔE resolution

BRAND NEW

$B^0 \to \gamma\gamma$

BELLE Belle II

FCNC $b \to d\gamma$ transition:

- Theoretically the $\mathscr{B}$ of this decay mode is expected to be $(1.4^{+1.4}_{-0.8}) \times 10^{-8}$
- Theoretical uncertainty dominated by the uncertainty on λ_b

Previous searches:

- PLB 363 (1995) 137-144
- PRD 73, 051107 (2006)
- PRD 83, 032006 (2011)

Experiment	Integrated Luminosity ($\int \mathcal{L}\, dt$)	Limit @ 90 C.L.
L3	73 pb^{-1}	3.9×10^{-5}
Belle	104 fb^{-1}	6.2×10^{-7}
Babar	426 fb^{-1}	3.2×10^{-7}

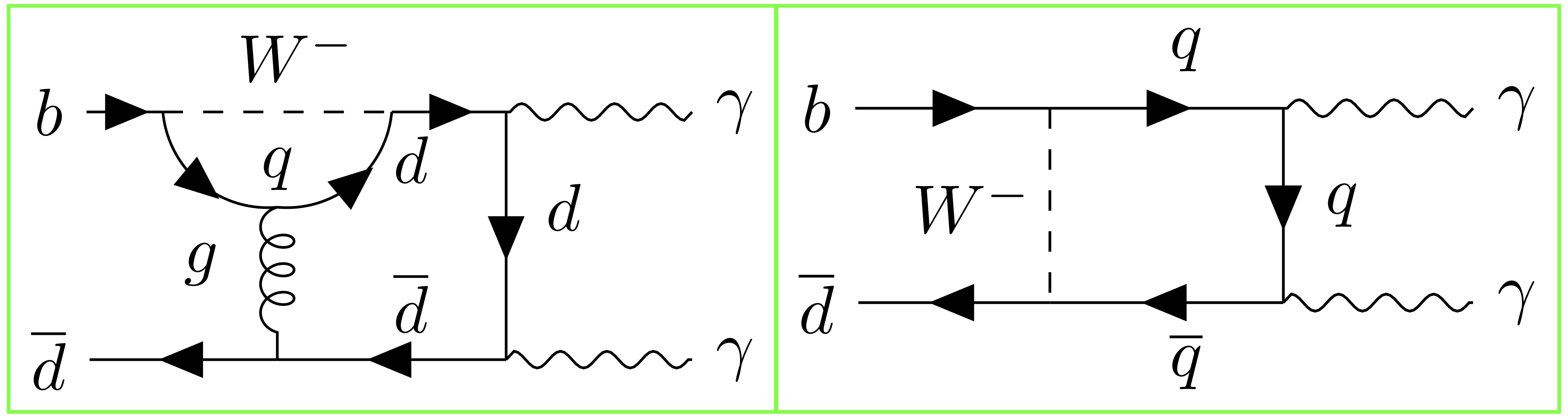

Karlsruhe Institute of Technology

BRAND NEW

$B^0 \to \gamma\gamma$

Selection strategy:

- Based on Belle ($692\ \mathrm{fb}^{-1}$) and Run 1 Belle II ($362\ \mathrm{fb}^{-1}$) dataset
- Reconstruct signal from two photons, where $E_\gamma \in (1.4,\ 3.4)$ GeV
- Use timing cuts to remove peaking back-to-back off-time photons
- Use π^0/η vetos and classifiers (BDTs) to suppress backgrounds
  ($e^+e^- \to q\bar{q}$ (90%) + $B^0 \to \pi^0\pi^0$)

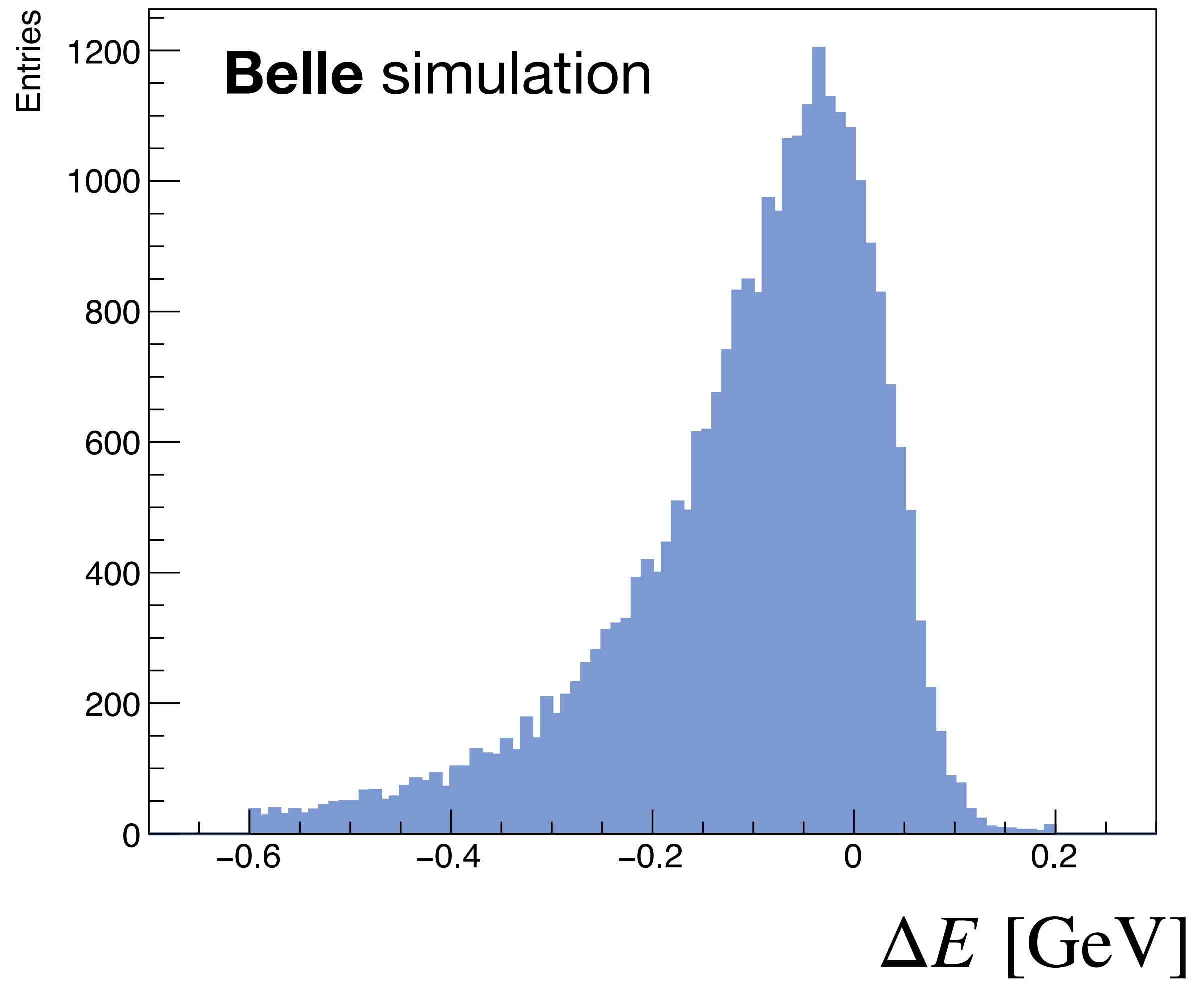

Fitting strategy:

- Simultaneous 3D fit to M_{bc}, ΔE, C'_{BDT} (transformed BDT) with Belle & Belle II data to extract $\mathscr{B}$

Control channel:

- Use partial $B \to K^*\gamma$ data

	Belle	Belle II
Sig efficiency	23%	31%
Exp. bkg/fb-1	~ 0.8	

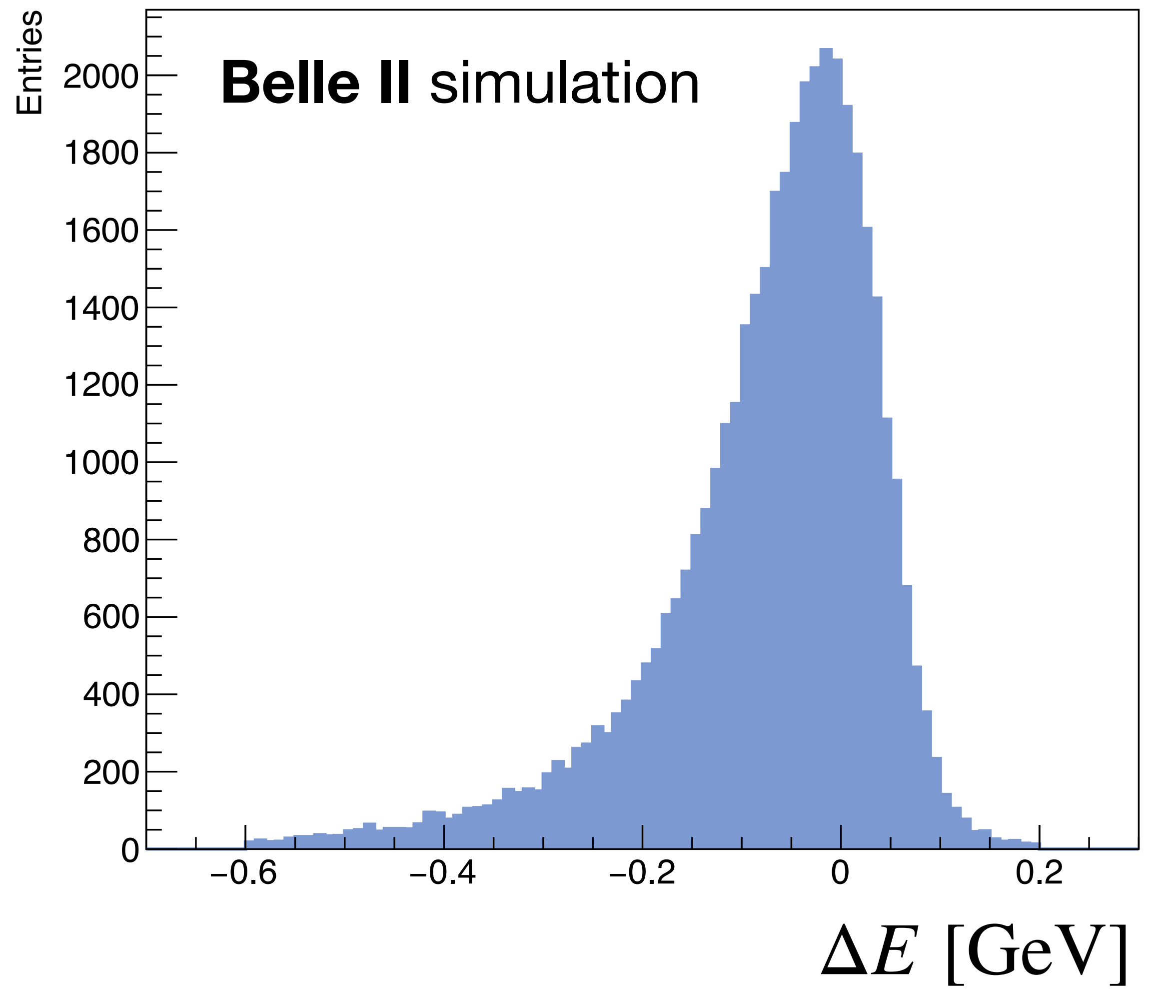

Belle II vs Belle:

- Improved signal efficiency per fb^{-1} background
- Improved ΔE resolution

$B^0 \to \gamma\gamma$

BRAND NEW

BELLE Belle II

Results:

- $11.0^{+6.5}_{-5.5}$ signal events corresponding to 2.5σ significance
- Since no significant signal → set 90% C.L. limits
- Really close to SM expectation

  → **best upper limit with Belle II data**

	$\mathcal{B}(B^0 \to \gamma\gamma)$	$\mathcal{B}(B^0 \to \gamma\gamma)$ (at 90% CL)
Belle	$(5.4^{+3.3}_{-2.6} \pm 0.5) \times 10^{-8}$	$< 9.9 \times 10^{-8}$
Belle II	$(1.7^{+3.7}_{-2.4} \pm 0.3) \times 10^{-8}$	$< 7.4 \times 10^{-8}$
Combined	$(3.7^{+2.2}_{-1.8} \pm 0.7) \times 10^{-8}$	$< 6.4 \times 10^{-8}$

Expected 90 C.L. 4.4×10^{-8}

Fit projections on M_{bc} and C'_{BDT}

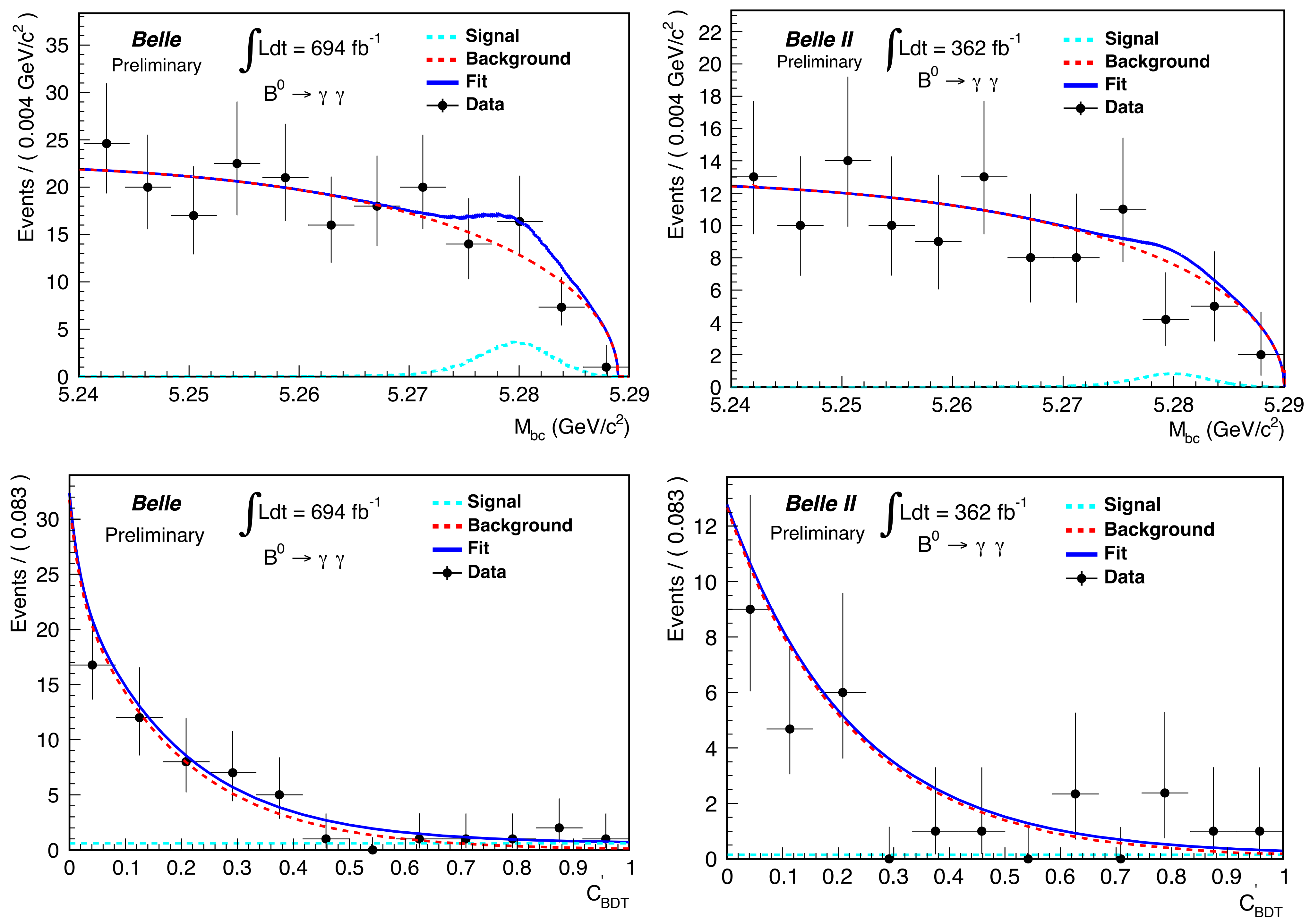

Remarks:

5 x improvement in limit wrt BaBar (previous best result)

- BaBar had upward fluctuation

Karlsruhe Institute of Technology

arxiv: 2403.03710

$\Lambda_b^0 \rightarrow pK^-\gamma$

FCNC $b \rightarrow s\gamma$ transition:

- Used Run 1 + Run 2 LHCb data (9 fb^{-1})
- $m_{pK} < 2.5\ \mathrm{GeV}/c^{-2}$ to reduce $\Lambda_b^0 \rightarrow pK^-\pi^0$
- Veto m_{KK} around ϕ resonance

Selection strategy:

- Strict particle ID for p and K to reduce $B_s^0 \rightarrow K^+K^-\gamma$ and $B^0 \rightarrow K^+\pi^-\gamma$
- BDT to suppress backgrounds (combinatorial)

Remaining contributions:

- Partially reconstructed $\Lambda_b^0 \rightarrow pK^-\pi^0\gamma$
- Combinatorial background
- Signal

Invariant mass (Run 1,2)

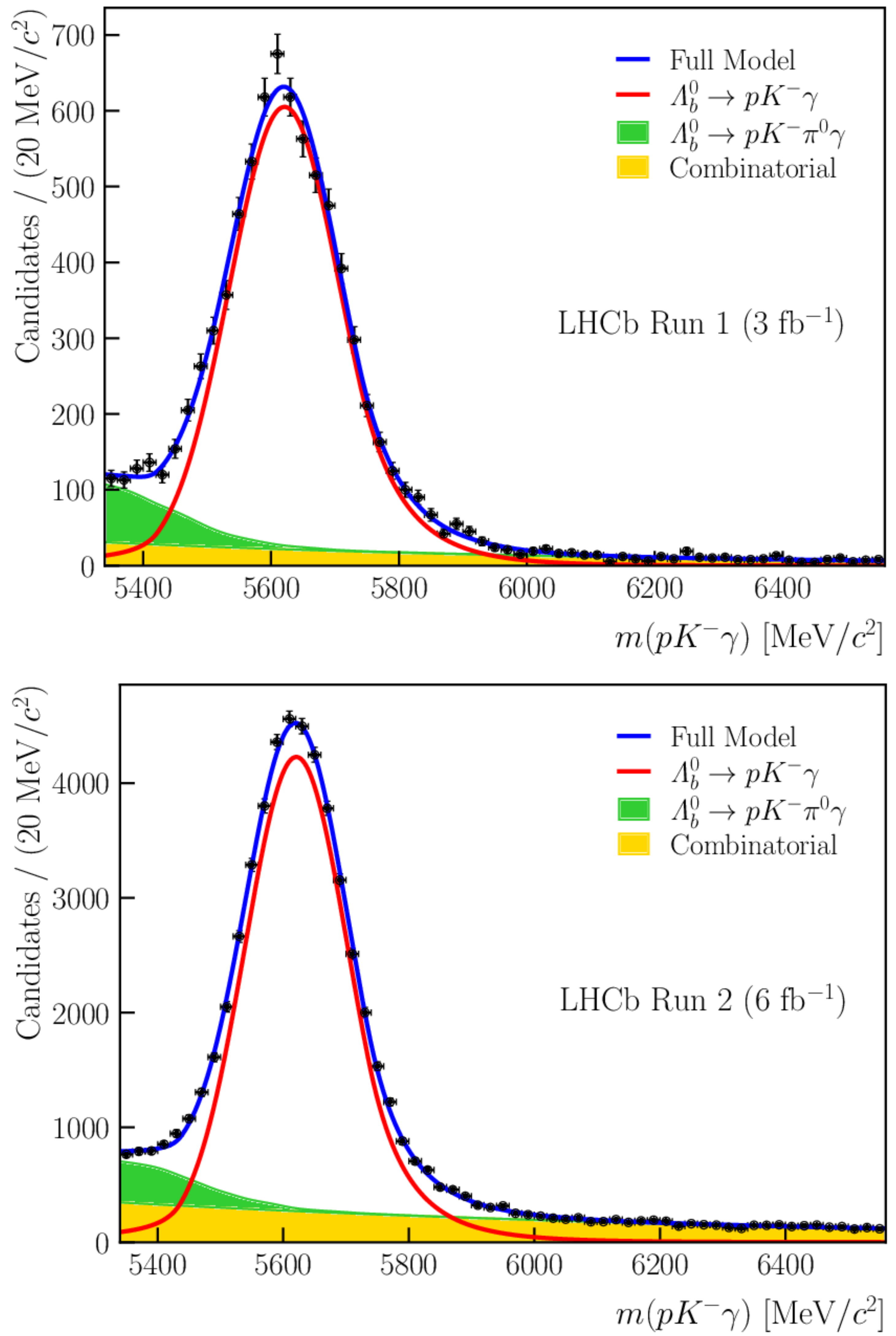

arxiv: 2403.03710

$\Lambda_b^0 \to pK^-\gamma$

Fitting strategy:

- Perform amplitude analysis of $\Lambda_b^0 \to \Lambda^* \to (pK^-)\gamma$ for a defined set of helicities λ_i with unbinned fits to Dalitz plane $m^2(p,K), m^2(p,\gamma)$

$$\underbrace{d^{J_\Lambda}_{\lambda_p \lambda_\Lambda}(\theta_p)}_{\text{Wigner d}} \times \sum_{L=|J_{\Lambda_b^0}-S|}^{|J_{\Lambda_b^0}+S|} \sum_{S=|J_\Lambda - J_\gamma|}^{|J_\Lambda + J_\gamma|} \left[\underbrace{C_1 C_2 C_3}_{\text{Clebsch-Gordans}} \underbrace{h^{\Lambda}_{LS}}_{LS \text{ coupling}} \underbrace{\left(\frac{p}{M_{\Lambda_b^0}}\right)^L \left(\frac{q}{M_\Lambda}\right)^l}_{\text{orb. ang. mom. barriers}} \underbrace{B_L(p) B_l(q) BW_l(m_{pK})}_{\text{line shape with form factors}} \right]$$

connect p and Λ^* helicity frames; fit parameter h^{Λ}_{LS}

[JHEP 06 (2020) 116]

sPlotted Dalitz plane

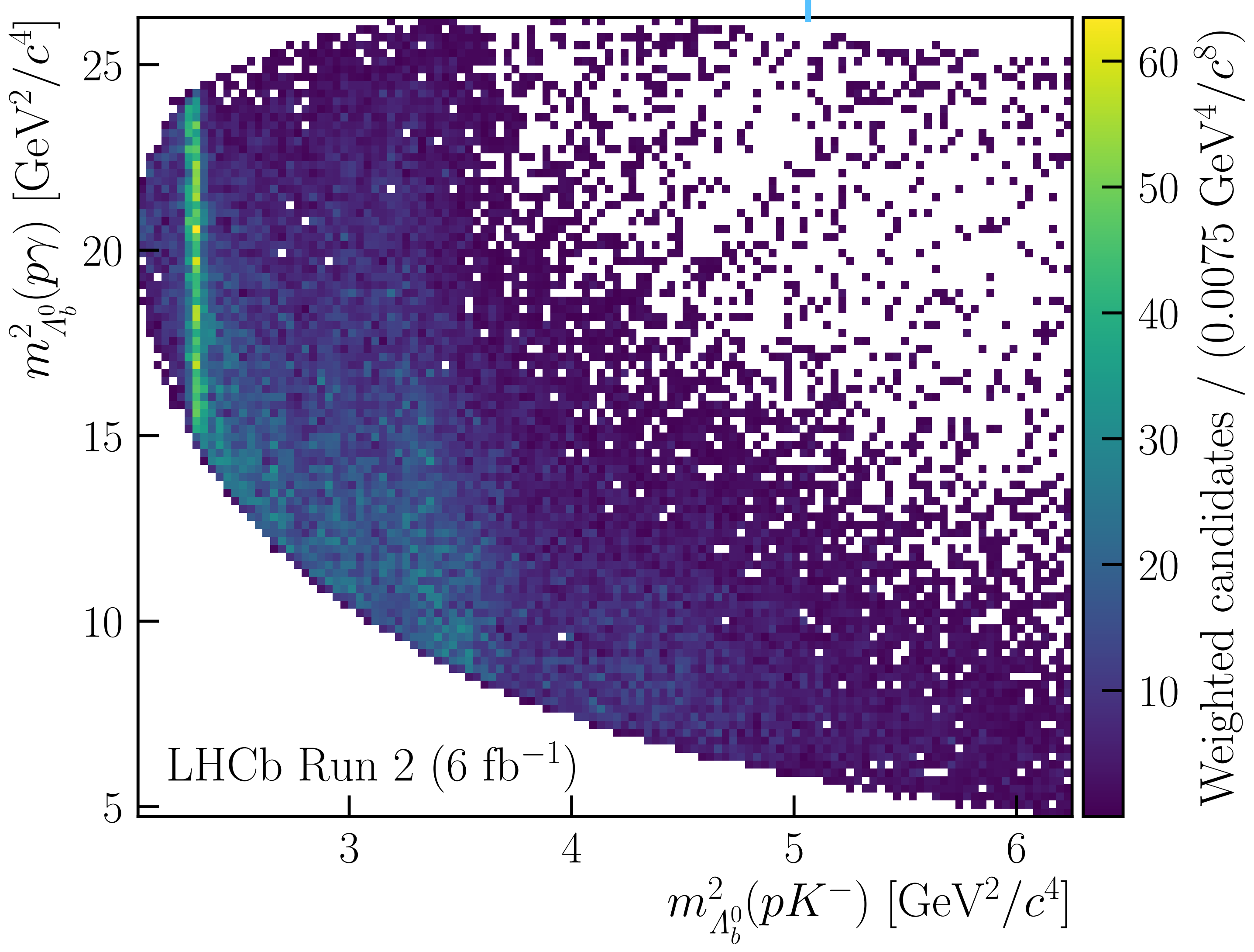

Invariant pK^- mass

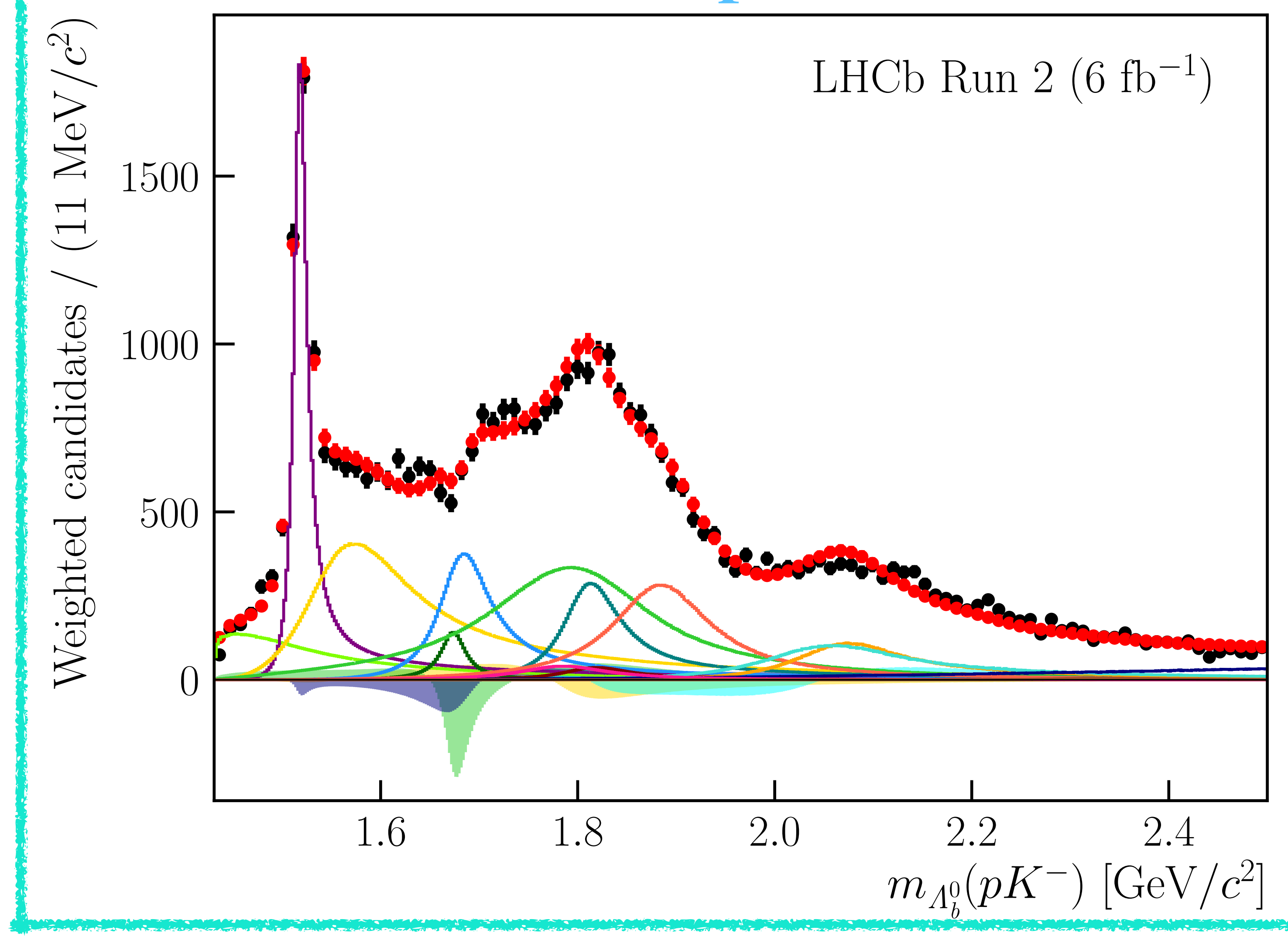

- The default fit model comprises of all known Λ resonances as well as a non-resonant contribution

arxiv: 2403.03710

$\Lambda_b^0 \to pK^-\gamma$

Results:

- Fit and interference fractions between the different components contributing to the final state

Final results

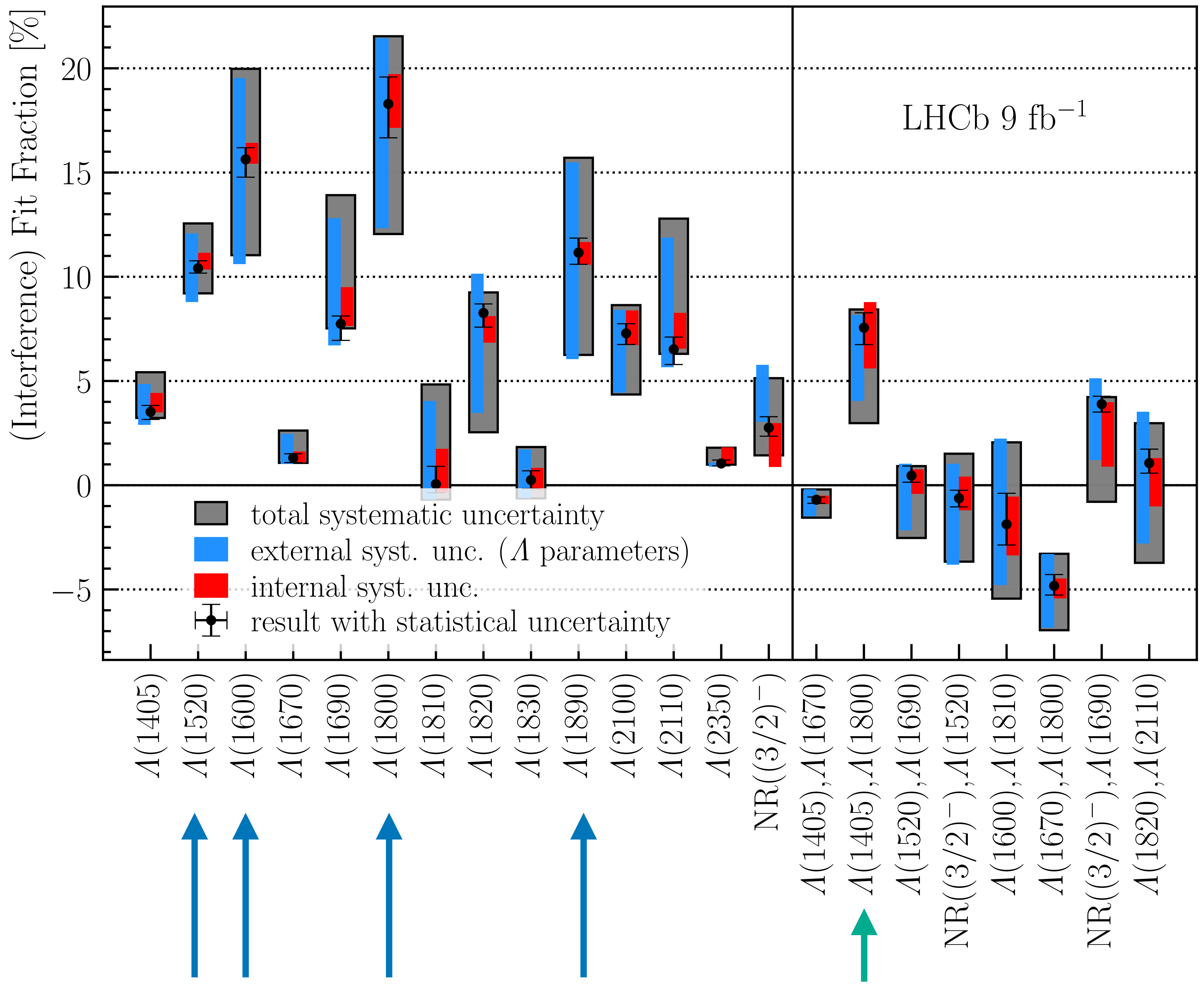

Remarks:

- Largest contributions stem from $\Lambda(1520), \Lambda(1600), \Lambda(1800), \Lambda(1890)$
- Largest interference stems from $\Lambda(1405) + \Lambda(1800)$
- First $\Lambda_b^0 \to pK^-\gamma$ amplitude analysis based on the helicity formalism
-

$B_s^0 \to \mu^+\mu^-\gamma$

FCNC $b \to s\gamma$ transition:

- Radiative counterpart to famous $B_s^0 \to \mu^+\mu^-$
- Theoretically less clean, experimentally also harder
- Aim: perform measurement of $\mathcal{B}$ in three bins of q^2 = invariant dimuon mass squared
- Upper 95 % C.L. limit on $\mathcal{B}(B_s^0 \to \mu^+\mu^-\gamma)$ of 2×10^{-9} for $m_{\mu^+\mu^-} > 4.9\ \mathrm{GeV}/c^2$ by LHCb [PRD 105, 012010 (2019)]

Theoretical predictions [JHEP 11 (2017) 184]

$\mathcal{B}(B_s^0 \to \mu^+\mu^-\gamma) = (8.3 \pm 1.3) \times 10^{-9}$ for $q^2 < 8.64\ \mathrm{GeV}^2/c^4$

$\mathcal{B}(B_s^0 \to \mu^+\mu^-\gamma) = (8.9 \pm 1.0) \times 10^{-10}$ for $q^2 > 15.84\ \mathrm{GeV}^2/c^4$

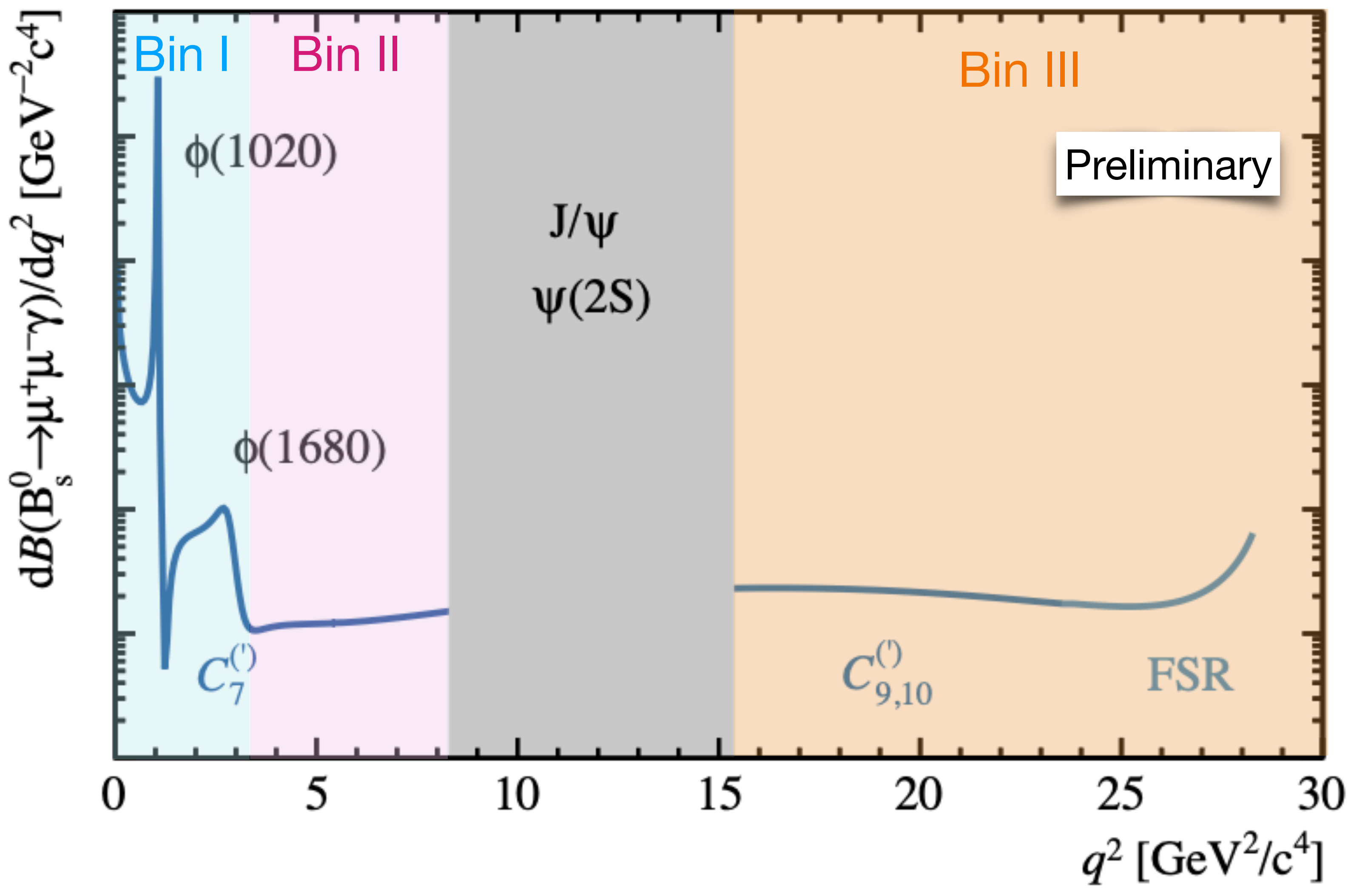

q^2 bin	I	II	III
q^2 [GeV^2/c^4]	$[4\,m_\mu^2, 2.89]$	$[2.89, 8.29]$	$[15.37, m_{B_s^0}^2]$
$m(\mu^+\mu^-)$ [GeV/c^2]	$[2\,m_\mu, 1.70]$	$[1.70, 2.88]$	$[3.92, m_{B_s^0}]$
$10^{10} \times \mathcal{B}(B_s^0 \to \mu^+\mu^-\gamma)$ [8]	82 ± 15	2.54 ± 0.34	9.1 ± 1.1
Fraction of $B_s^0 \to \mu^+\mu^-\gamma$	87%	2.7%	9.8%

Selection strategy:

- Use 5.4 fb^{-1} LHCb data
- **Veto region around ϕ resonance**

$B_s^0 \to \mu^+\mu^-\gamma$

Fit result and limit for q^2 bin

Preliminary

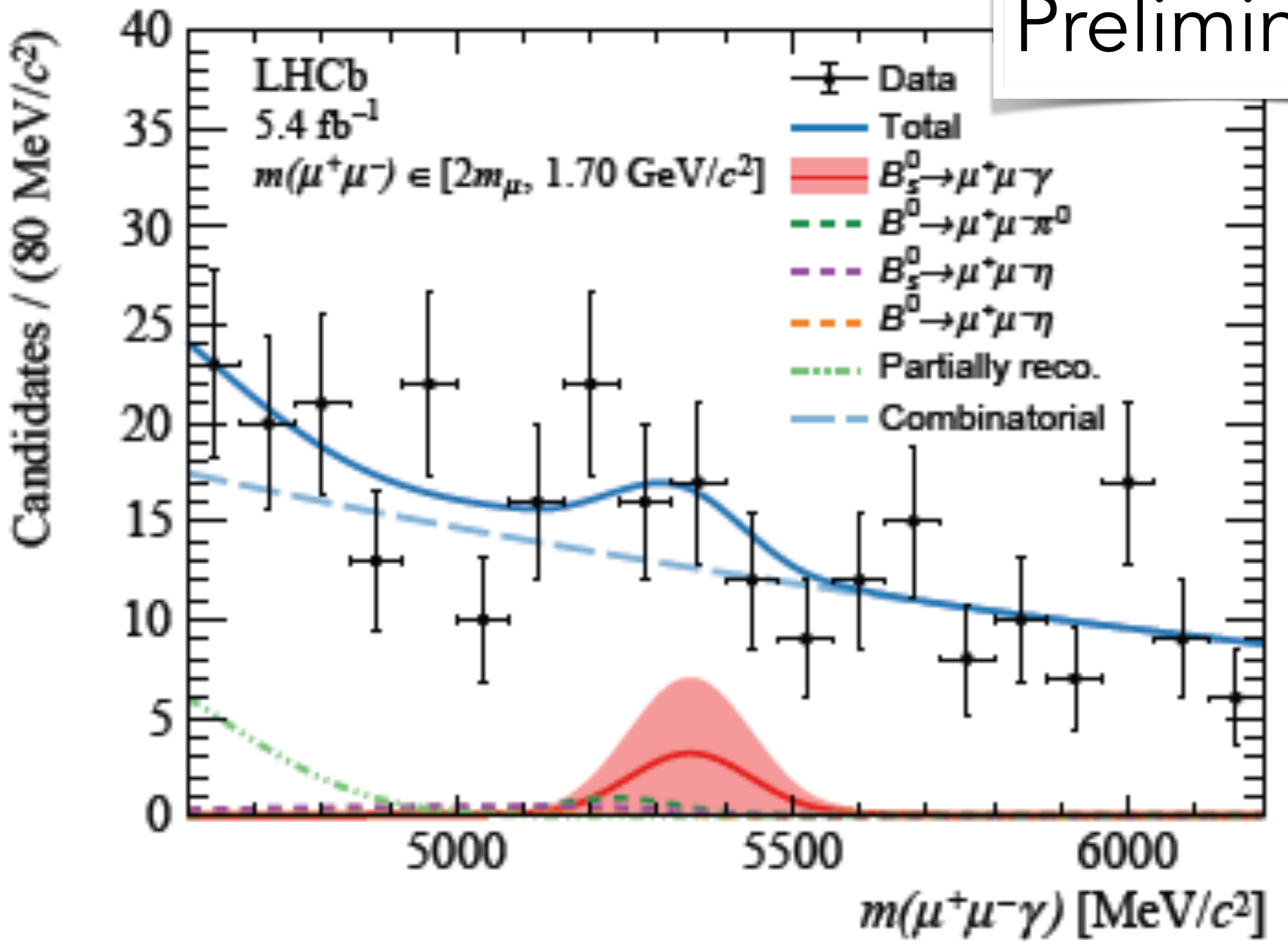

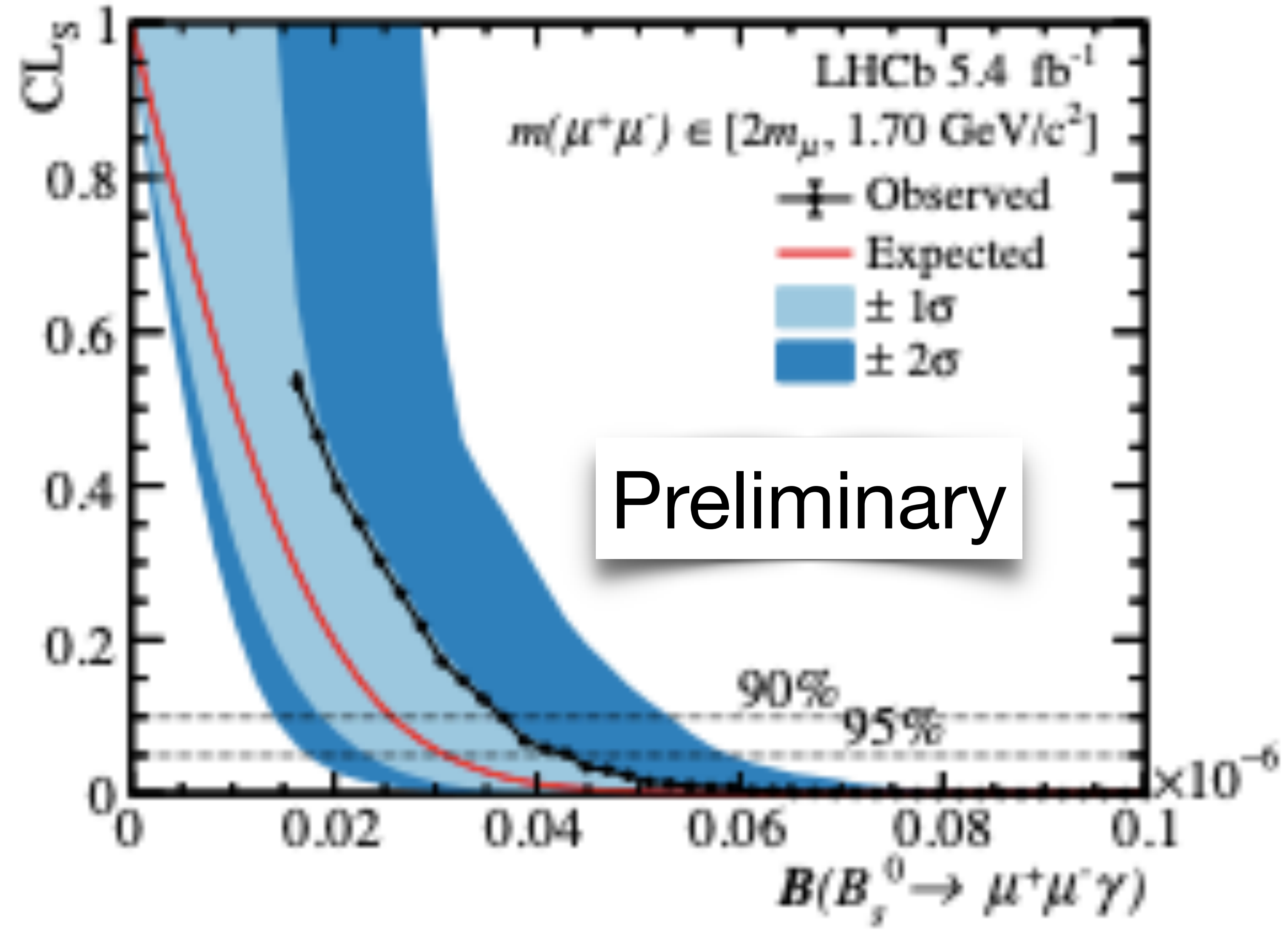

Results:

- No significant signal was observed
- Competitive limits in all of the regions approaching SM have been set:

Preliminary

$$\mathcal{B}(B_s^0 \to \mu^+\mu^-\gamma)_{\text{I}} < 3.6\,(4.2) \times 10^{-8},$$
$$\mathcal{B}(B_s^0 \to \mu^+\mu^-\gamma)_{\text{II}} < 6.5\,(7.7) \times 10^{-8},$$
$$\mathcal{B}(B_s^0 \to \mu^+\mu^-\gamma)_{\text{III}} < 3.4\,(4.2) \times 10^{-8},$$
$$\mathcal{B}(B_s^0 \to \mu^+\mu^-\gamma)_{\text{I},\,\phi\ \text{veto}} < 2.9\,(3.4) \times 10^{-8},$$
$$\mathcal{B}(B_s^0 \to \mu^+\mu^-\gamma)_{\text{comb.}} < 2.5\,(2.8) \times 10^{-8},$$

at 90% (95%) CL.

$B^+ \to K^+ \nu \bar{\nu}$

FCNC $b \to s$ transition:

- precise SM prediction: $\mathscr{B}(B^+ \to K^+ \nu \bar{\nu}) = (5.58 \pm 0.37) \times 10^{-6}$
  [PRD 107, 1324 014511 (2023), PRD 107, 119903 (2023)]
  - dominated by form factor uncertainty

- **NP scenarios:**
  - **Light :** axions [PRD 102, 015023 (2020)], dark scalars [PRD 101, 095006 (2020)], axion-like particles [JHEP 04 (2023) 131]
  - **Heavy :** Z' [PL B 821 (2021) 136607], leptoquarks [PRD 98, 055003 (2018)]

Experimental status:

- Previous limits order of magnitude above SM expectation

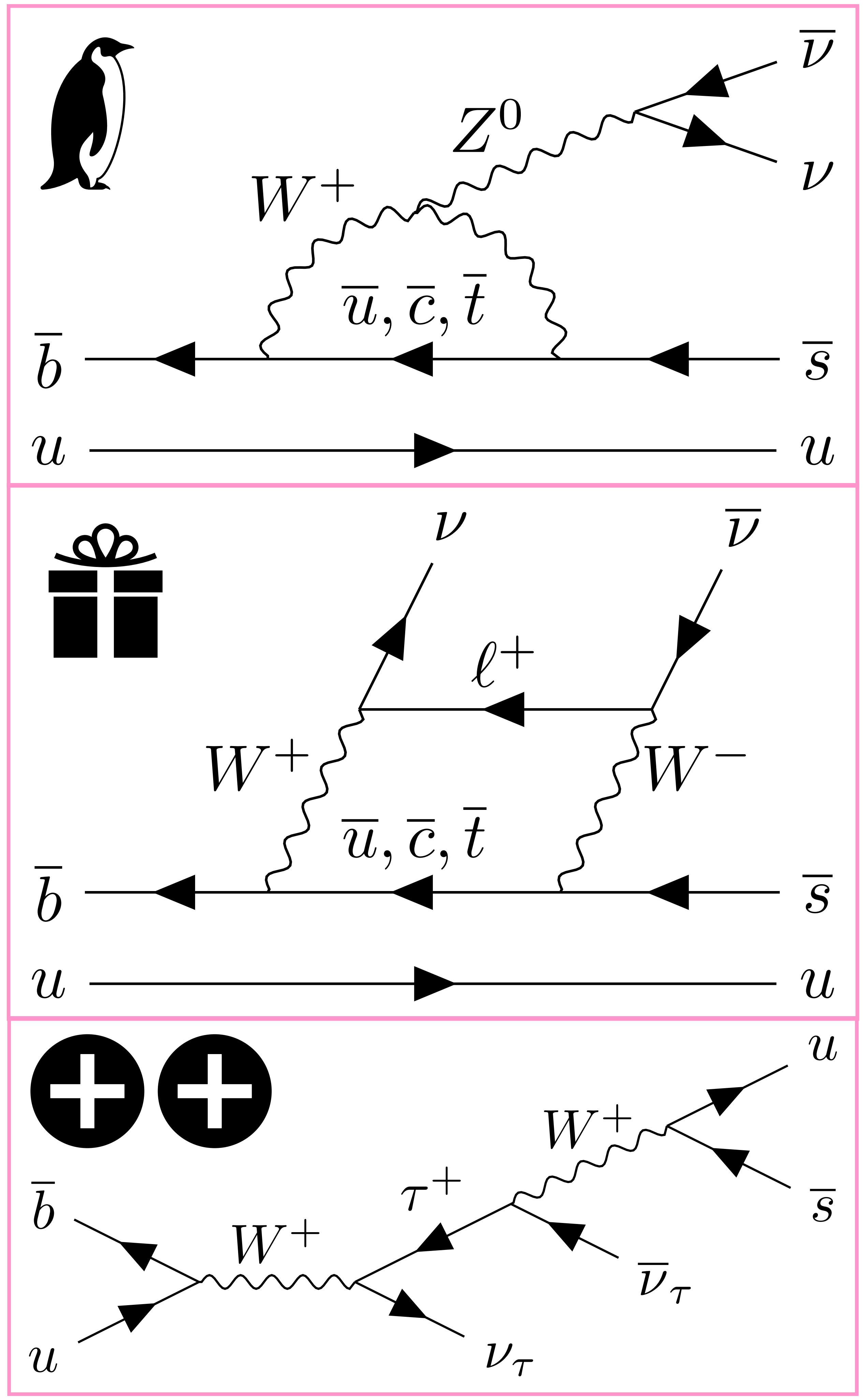

$B^+ \to K^+\nu\bar{\nu}$: Reconstruction

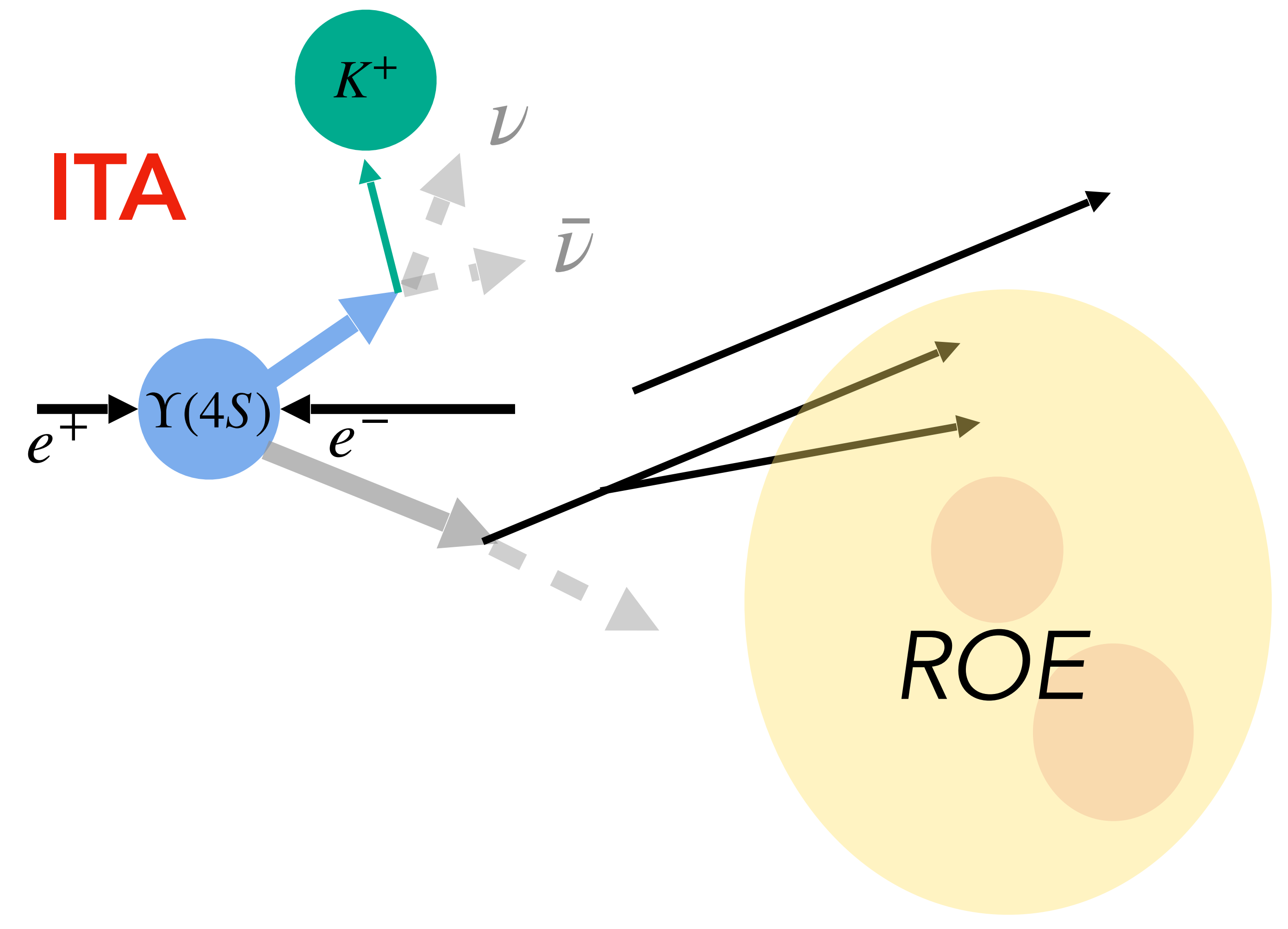

q^2_{rec} = mass squared of the neutrino pair

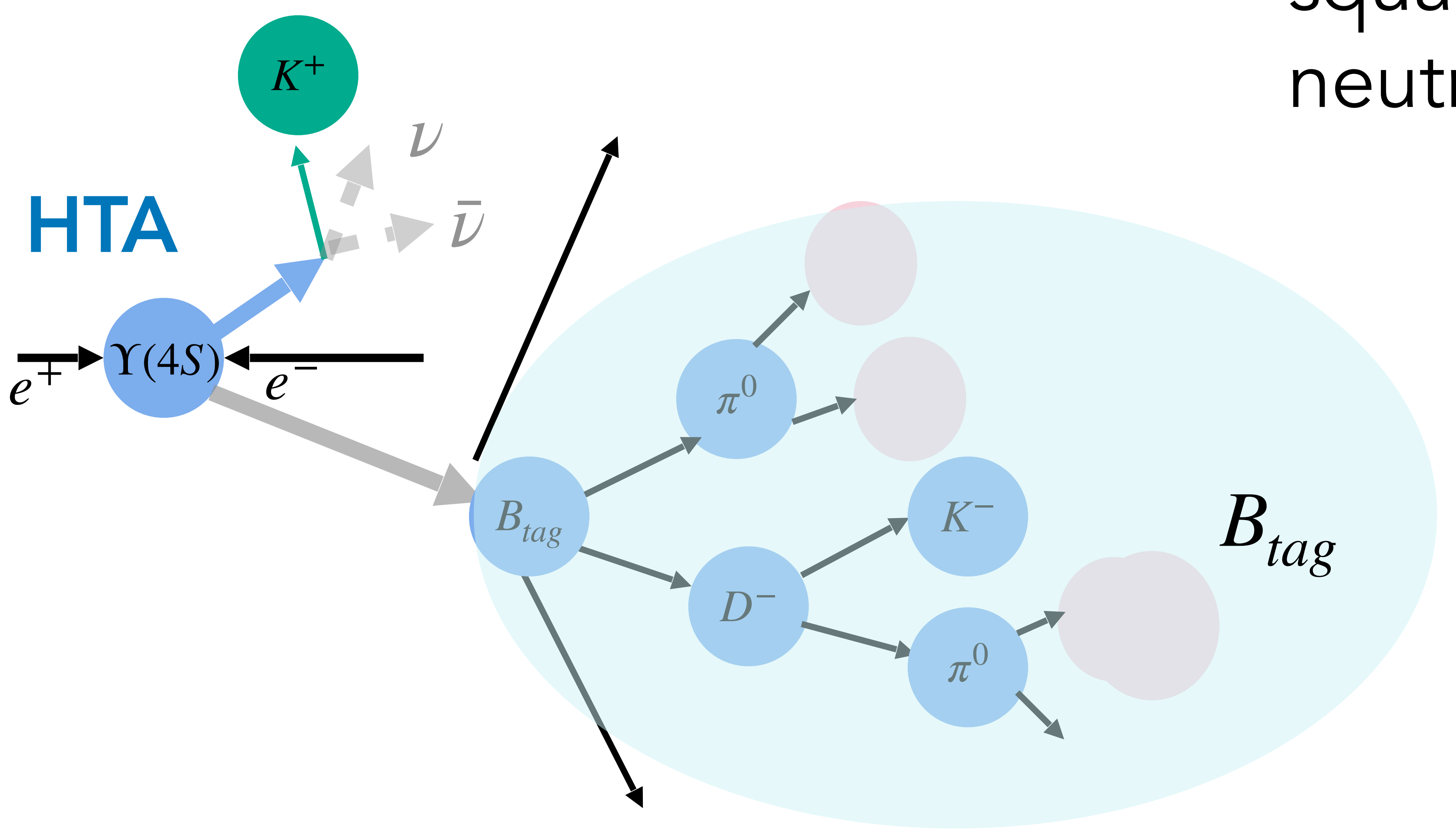

Measurement strategy:

- Use Run 1 Belle II ($362\ \mathrm{fb}^{-1}$) dataset
- Use inclusive tagging + hadronic tagging
  (*most sensitive*) (*conventional*)

ITA

1. Perform basic reconstruction (tracks and clusters)
2. Reconstruct signal kaon
3. Identify rest-of-event object (ROE)

$$q^2_{rec} = \frac{s}{4} + M_K^2 - \sqrt{s}E_K^*$$

$*$ = c.m frame

HTA

1. Perform basic reconstruction (tracks and clusters)
2. Reconstruct hadronic tag (B_{tag})
3. Reconstruct signal kaon

$B^+ \to K^+\nu\bar{\nu}$: Signal Region

Selection Strategy:

- **ITA:** two consecutive BDTs to suppress the continuum and $B\bar{B}$ background → **ITA signal efficiency = 8%; purity = 0.9%**
- **HTA:** one BDT to suppress the continuum and $B\bar{B}$ background → **HTA signal efficiency = 0.4%; purity = 3.5%**

ITA background composition

- 40% $q\bar{q}$ backgrounds
- 60% $B\bar{B}$ backgrounds

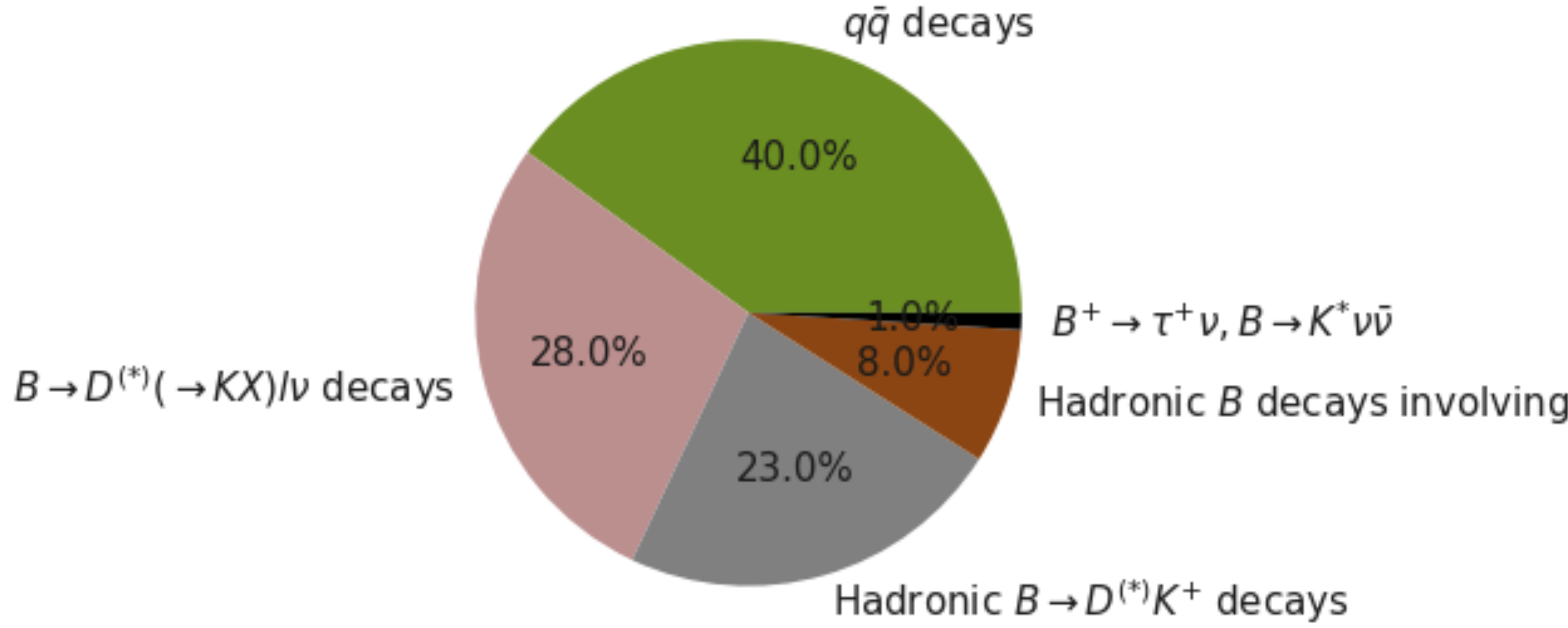

Fitting Strategy:

- Binned maximum likelihood fit to extract parameter of interest signal strength μ

$$\mu = \frac{\mathscr{B}(B^+ \to K^+\nu\bar{\nu})}{\mathscr{B}_{SM}(B^+ \to K^+\nu\bar{\nu})} \text{ with } \mathscr{B}_{SM} = 4.97 \times 10^{-6}$$

- **ITA fit variable:** classifier output $\eta(\mathrm{BDT}_2)$ and mass squared of the neutrino pair q^2_{rec}
- **HTA fit variable:** classifier output $\eta(\mathrm{BDTh})$

arxiv: 2311.14647

$B^+ \to K^+\nu\bar{\nu}$: Validation

1. **Signal efficiency checked with signal embedded $B^+ \to K^+J/\psi(\to \mu^+\mu^-)$ events:** remove J/ψ and correct the kaon kinematics to match that of signal

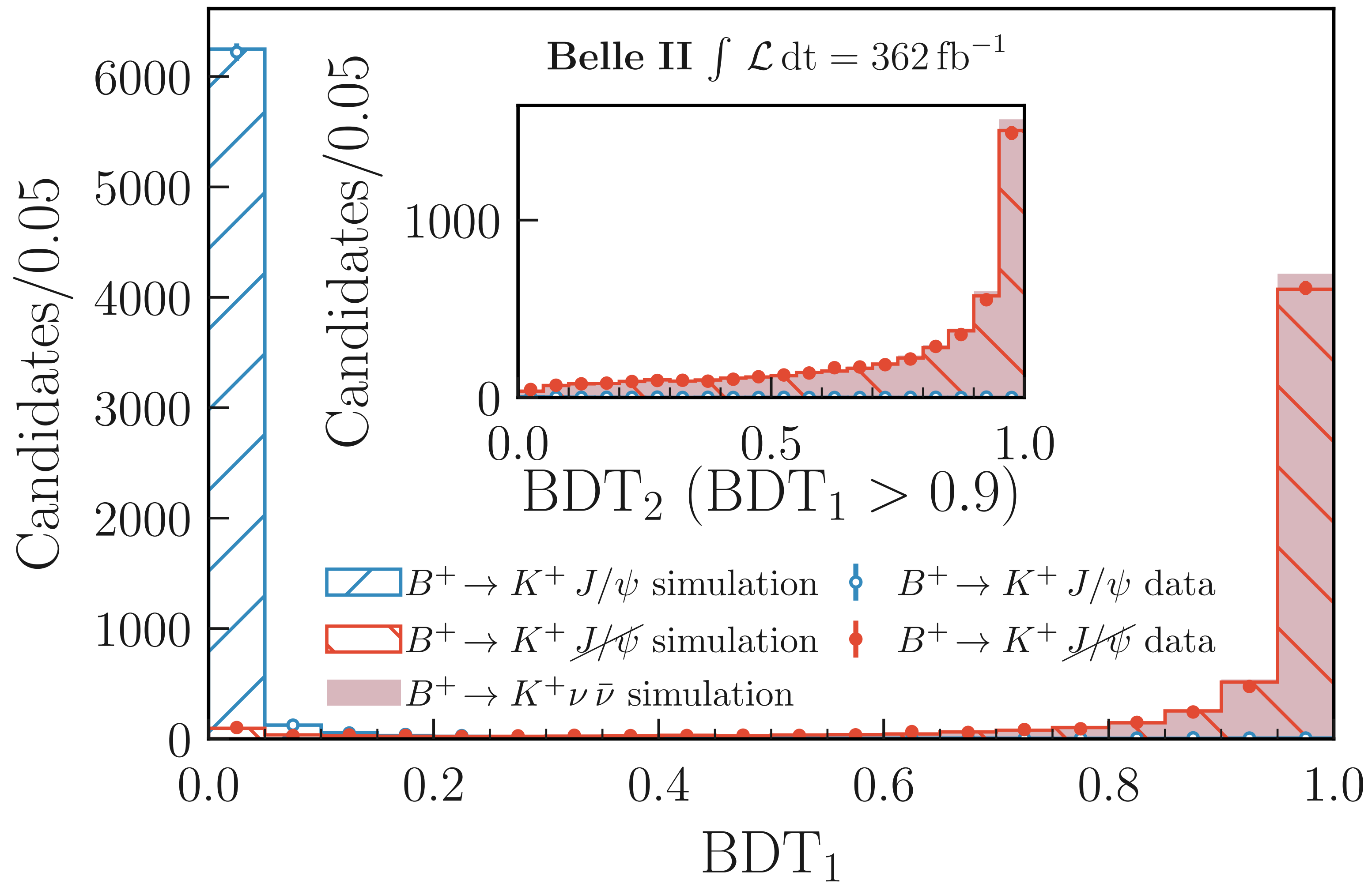

2. **$q\bar{q}$ background physics modelling validated with off-resonance data**

3. **$B \to X_c(\to K_L^0)$ physics modelling validated using pion-enriched sideband:**
   - Scale up the $B \to X_c(\to K_L^0)$ simulated decays by 30%

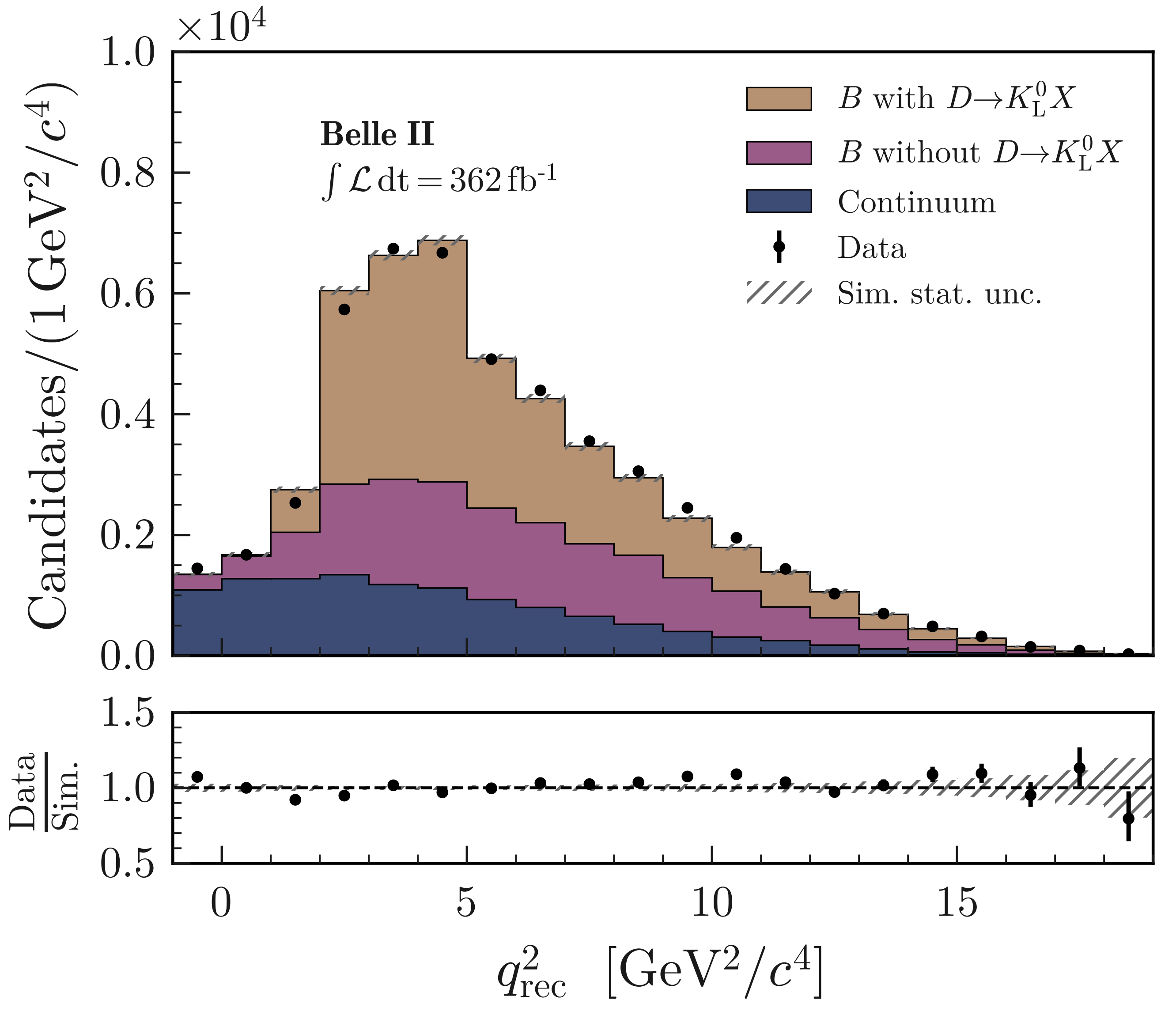

4. **Modelling the signal-like $B^+ \to K^+K_L^0K_L^0$ decays checked with $B^+ \to K^+K_S^0K_S^0$ decays** [PRD 85 112010]
   - Similar treatment for $B^+ \to K^+K_S^0K_L^0$, $B^+ \to K^+n\bar{n}$

arxiv: 2311.14647

$B^+ \to K^+ \nu\bar{\nu}$: Results

ITA

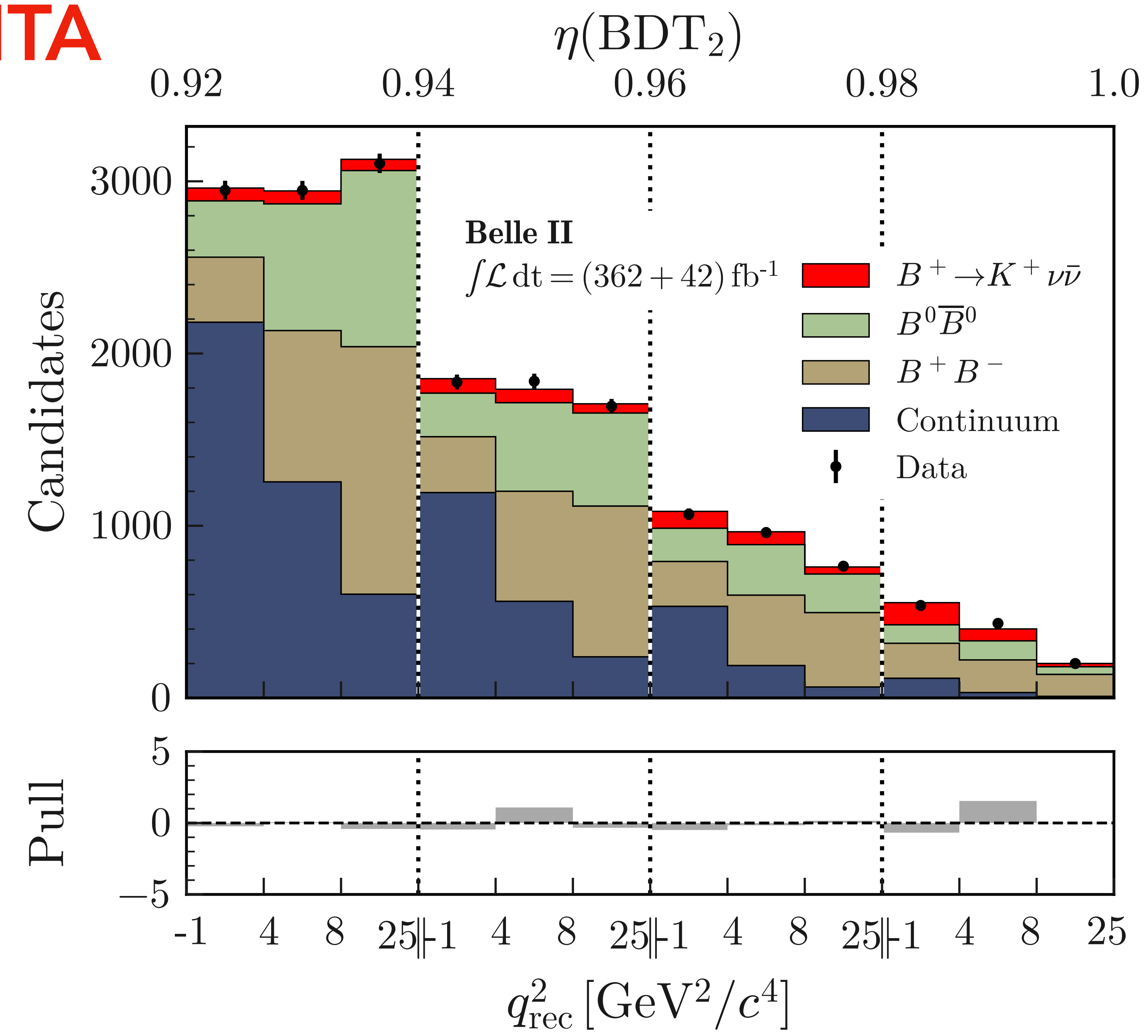

$\mu = 5.4 \pm 1.0(\mathrm{stat}) \pm 1.1(\mathrm{syst})$

corresponding to

$\mathcal{B}(B^+ \to K^+\nu\bar{\nu}) = 2.7 \pm 0.5(\mathrm{stat}) \pm 0.5(\mathrm{syst}) \times 10^{-5}$

- $3.5\ \sigma$ compatibility wrt bkg only
- $2.9\ \sigma$ compatibility wrt to the SM

HTA

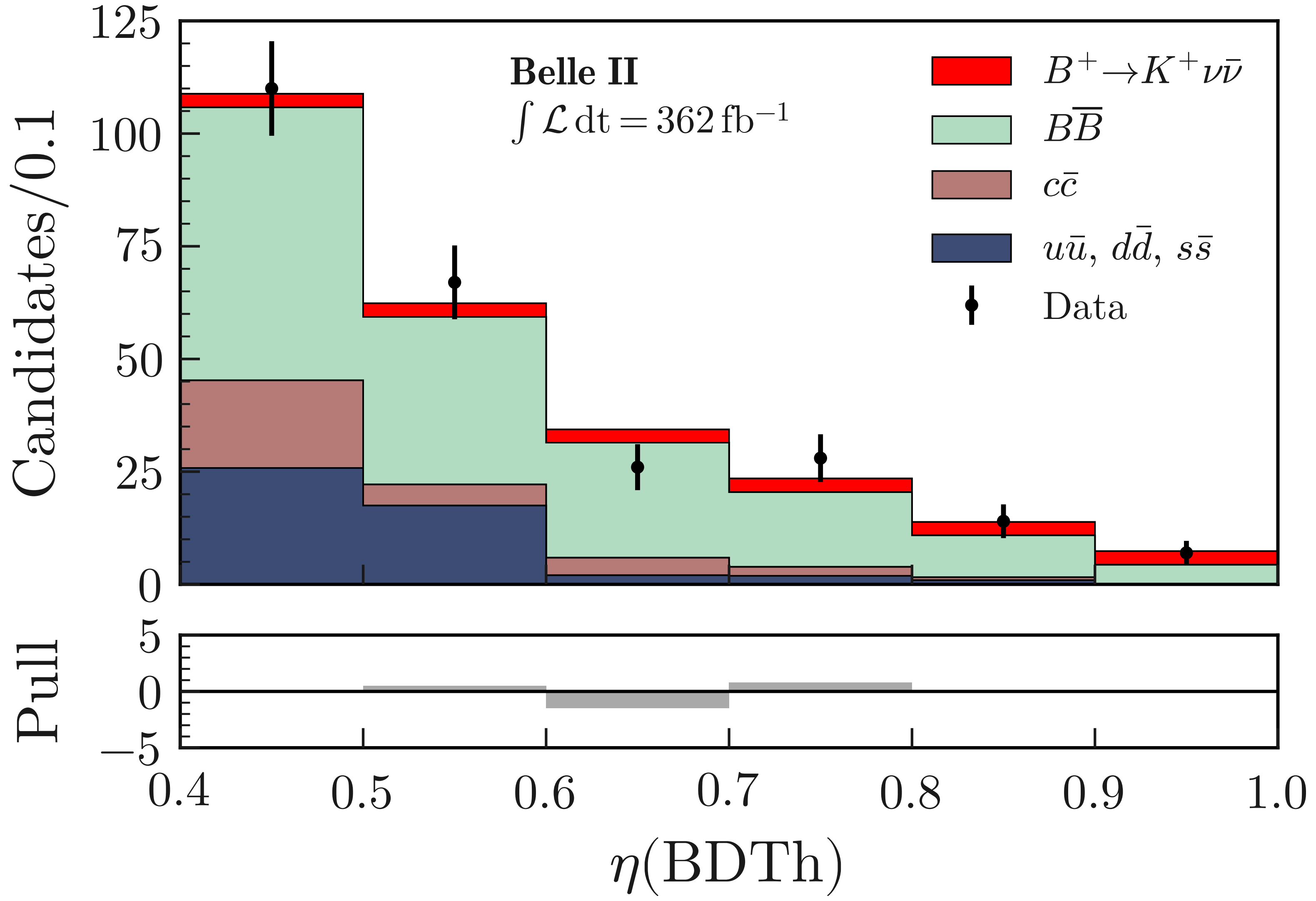

$\mu = 2.2^{+1.8}_{-1.7}(\mathrm{stat})^{+1.6}_{-1.1}(\mathrm{syst})$

corresponding to

$\mathcal{B}(B^+ \to K^+\nu\bar{\nu}) = [1.1^{+0.9}_{-0.8}(\mathrm{stat})^{+0.8}_{-0.5}(\mathrm{syst})] \times 10^{-5}$

- $1.1\ \sigma$ compatibility wrt bkg only
- $0.6\ \sigma$ compatibility wrt to the SM

Combination

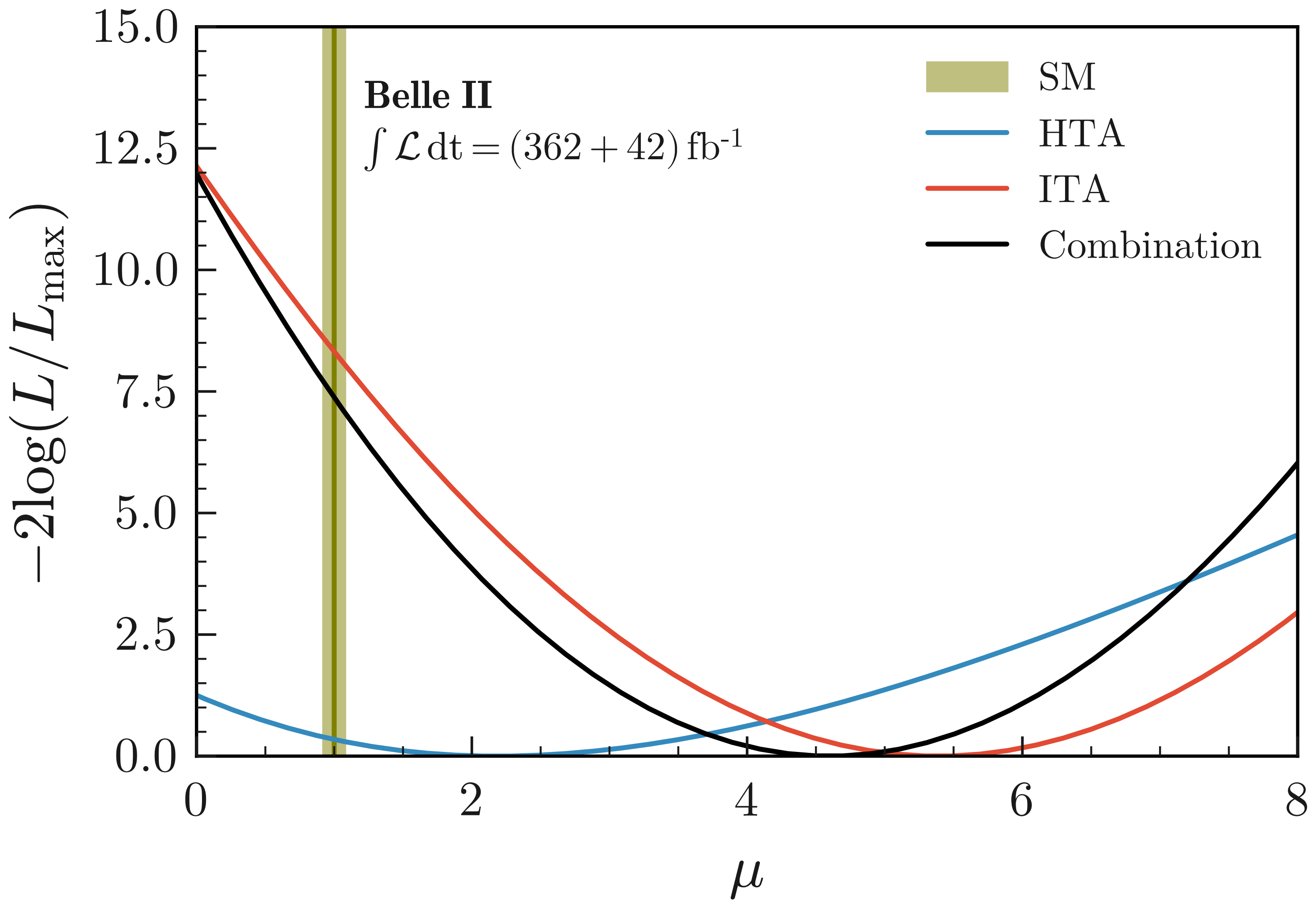

$\mu = 4.6 \pm 1.0(\mathrm{stat}) \pm 0.9(\mathrm{syst})$

corresponding to

$\mathcal{B}(B^+ \to K^+\nu\bar{\nu}) = [2.3 \pm 0.5(\mathrm{stat})^{+0.5}_{-0.4}(\mathrm{syst})] \times 10^{-5}$

- Combination improves the ITA-only precision by 10%
- $3.5\ \sigma$ significance wrt bkg
- $2.7\ \sigma$ significance wrt SM

arxiv: 2311.14647

$B^+ \to K^+ \nu\bar{\nu}$: Results

→ first evidence of the $B^+ \to K^+\nu\bar{\nu}$ process

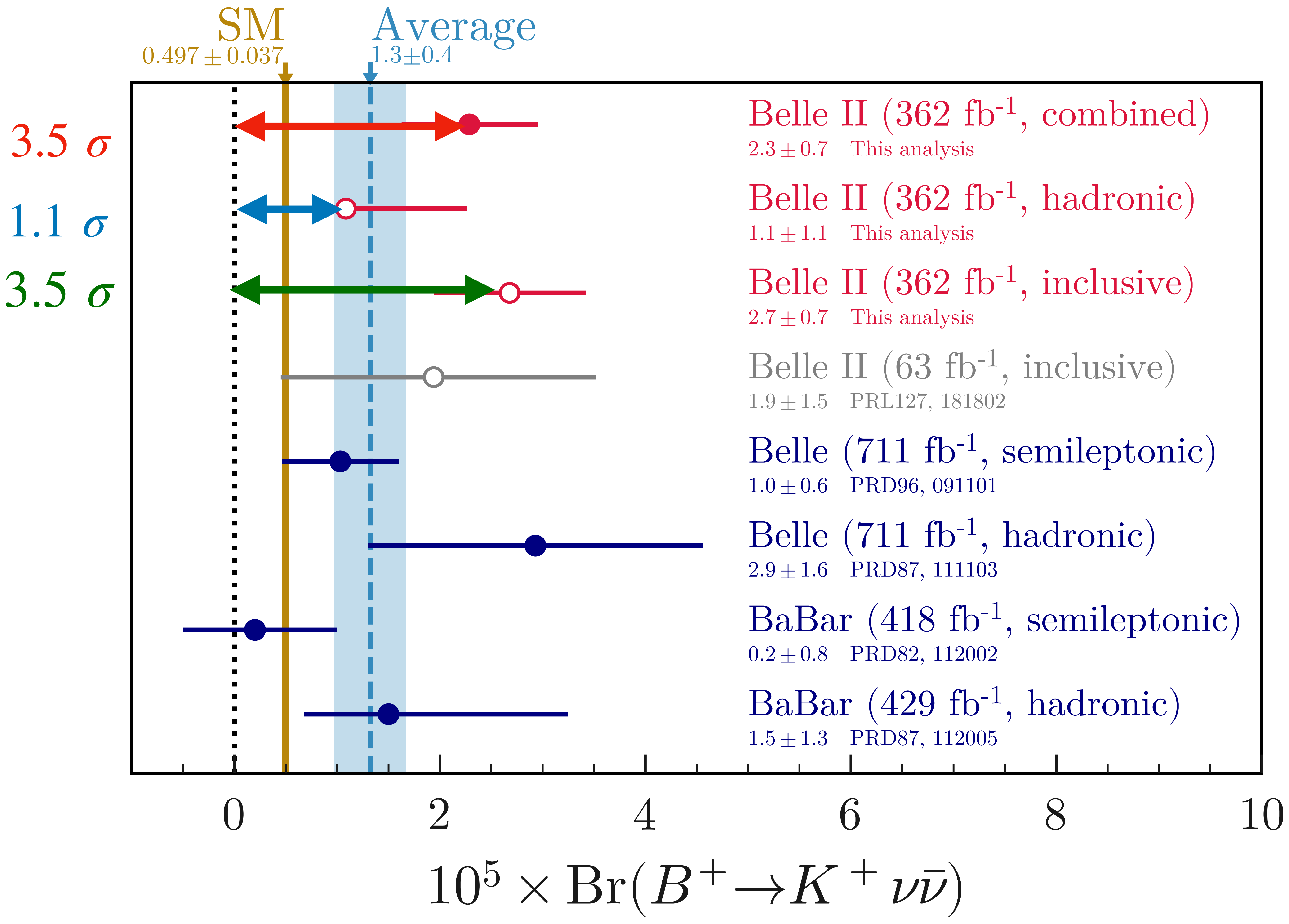

Accepted by PRD!

Conclusion

Both LHCb and Belle (II) are producing world-leading results in rare *B* decays:

- $\boldsymbol{B \to K^*\gamma}$: measurement consistent with SM and PDG
- $\boldsymbol{B^0 \to \gamma\gamma}$: best upper limit, rarest decay measured with Belle II data so far, close to SM
- $\boldsymbol{\Lambda_b^0 \to pK^-\gamma}$: first $\Lambda_b^0 \to pK^-\gamma$ amplitude analysis based on the helicity formalism [arxiv: 2403.03710]
- $\boldsymbol{B_s^0 \to \mu^+\mu^-\gamma}$: first direct search, and first low q^2 search [LHCb-PAPER-2023-045]
- $\boldsymbol{B^+ \to K^+\nu\bar{\nu}}$: first evidence for this decay with $2.7\ \sigma$ compatibility with SM [arxiv: 2311.14647, to appear in PRD]

Most of the measurements are statistically limited → bigger datasets are of particular interest!

Stay tuned for future :)

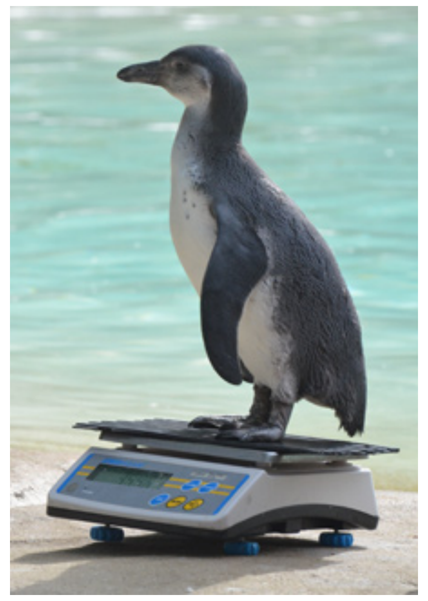

Prospects

$B \to K^*\gamma$

Belle II Physics Book

Observables	Belle II $5\,\mathrm{ab}^{-1}$	Belle II $50\,\mathrm{ab}^{-1}$
$\Delta_{0+}(B \to K^*\gamma)$	0.70%	0.53%
$A_{CP}(B^0 \to K^{*0}\gamma)$	0.58%	0.21%
$A_{CP}(B^+ \to K^{*+}\gamma)$	0.81%	0.29%
$\Delta A_{CP}(B \to K^*\gamma)$	0.98%	0.36%

$\Lambda_b^0 \to pK^-\gamma$

Improved knowledge of the different Λ baryons and more data will result in a significant reduction of the uncertainties

$B^0 \to \gamma\gamma$

Belle II Physics Book

Observables	Belle II $5\,\mathrm{ab}^{-1}$	Belle II $50\,\mathrm{ab}^{-1}$
$\mathrm{Br}(B_d \to \gamma\gamma)$	30%	9.6%
$A_{CP}(B_d \to \gamma\gamma)$	78%	25%
$\mathrm{Br}(B_s \to \gamma\gamma)$	23%	–

$B_s^0 \to \mu\mu\gamma$

more data will result in a observation of this decay

$B^+ \to K^+\nu\bar{\nu}$

Belle II snowmass paper : 2 scenarios baseline (improved*) assuming SM

Decay	$1\,\mathrm{ab}^{-1}$	$5\,\mathrm{ab}^{-1}$	$10\,\mathrm{ab}^{-1}$	$50\,\mathrm{ab}^{-1}$
$B^+ \to K^+\nu\bar{\nu}$	0.55 (0.37)	0.28 (0.19)	0.21 (0.14)	0.11 (0.08)
$B^0 \to K_S^0\nu\bar{\nu}$	2.06 (1.37)	1.31 (0.87)	1.05 (0.70)	0.59 (0.40)
$B^+ \to K^{*+}\nu\bar{\nu}$	2.04 (1.45)	1.06 (0.75)	0.83 (0.59)	0.53 (0.38)
$B^0 \to K^{*0}\nu\bar{\nu}$	1.08 (0.72)	0.60 (0.40)	0.49 (0.33)	0.34 (0.23)

Backup

General

Detectors

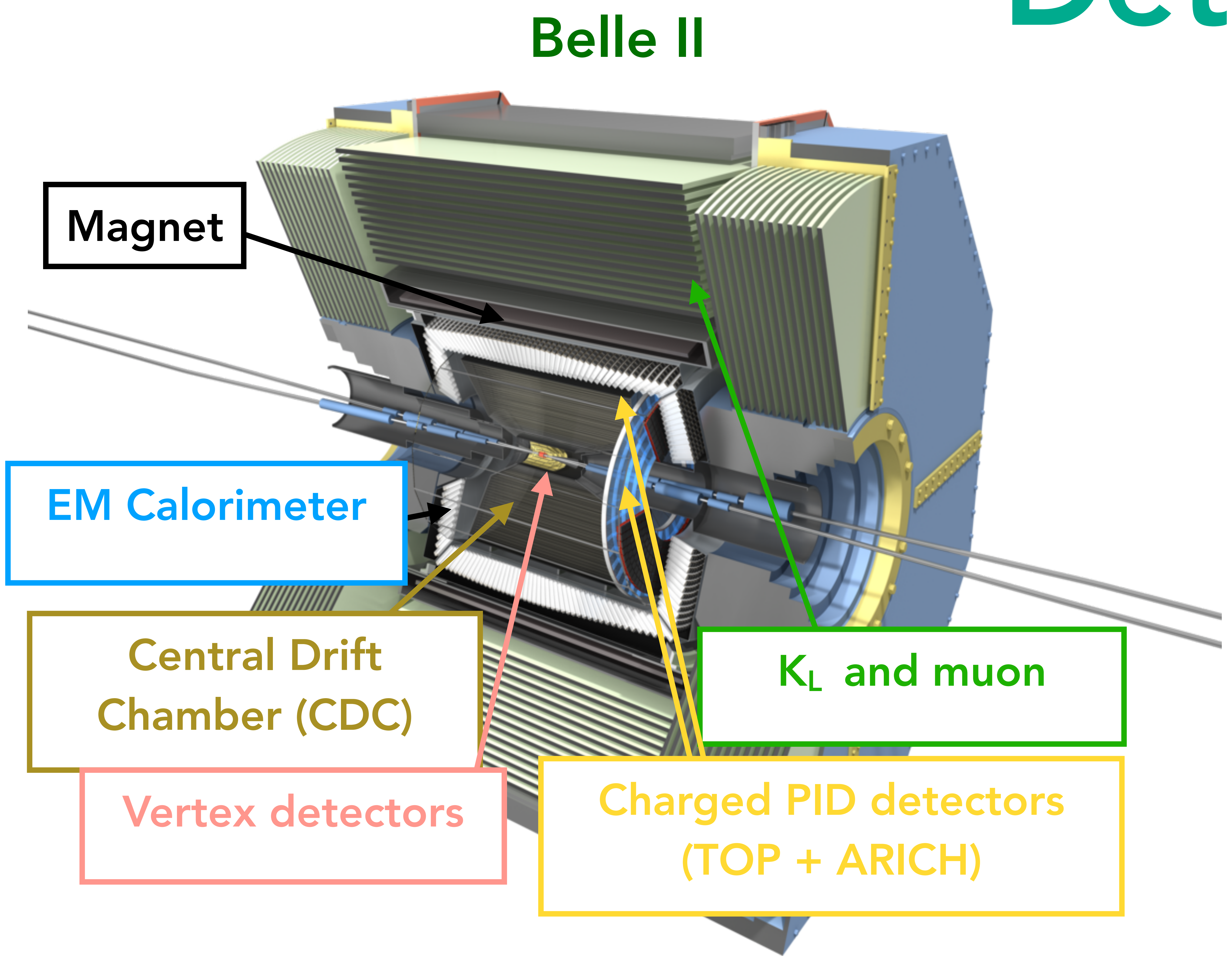

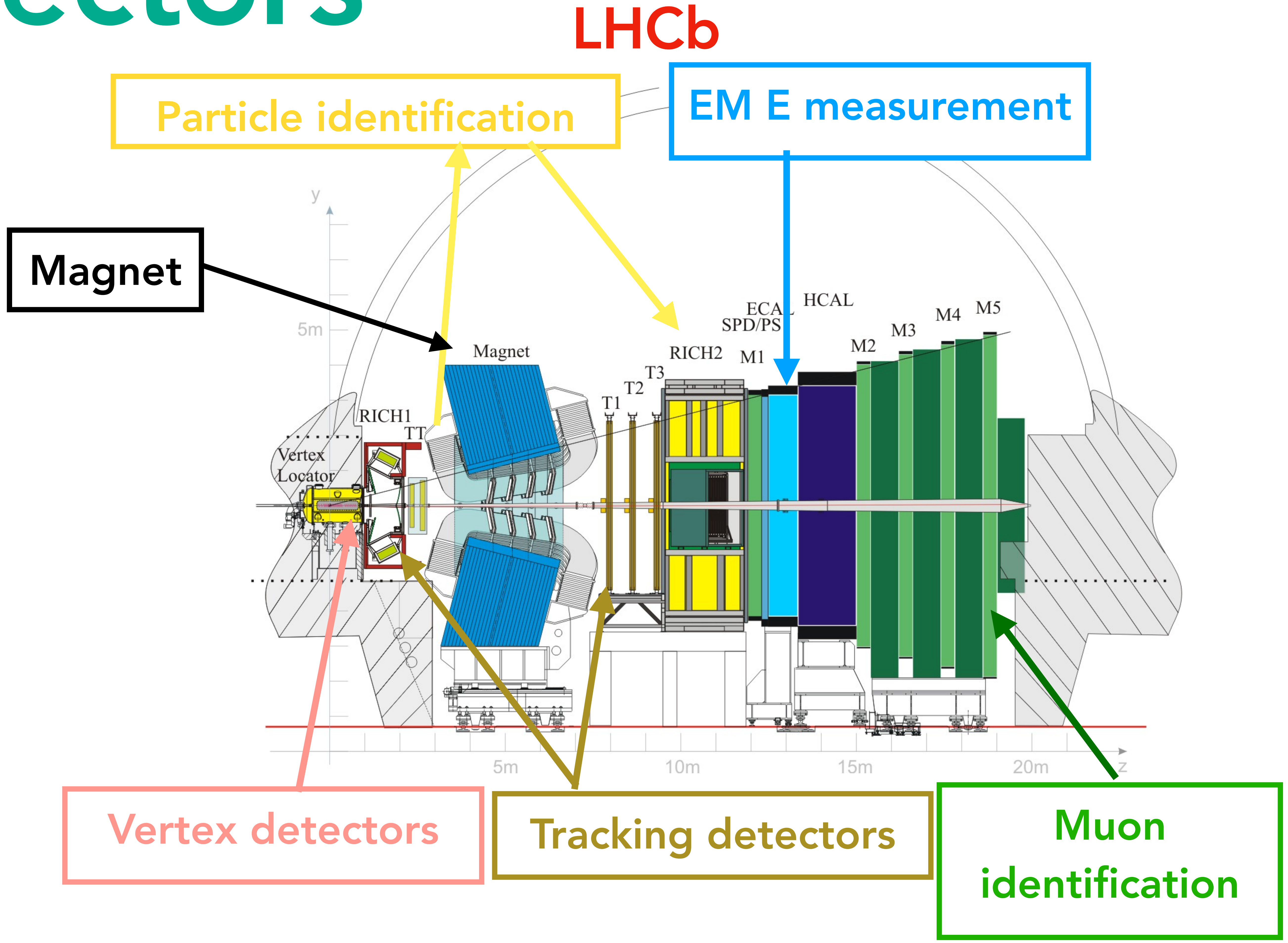

- Hermetic detector
- Sensitive to lower energy/charge deposits
- Known initial state kinematics

- Single arm spectrometer
- Longitudinal momentum of the B not known

SuperKEKB vs KEKB

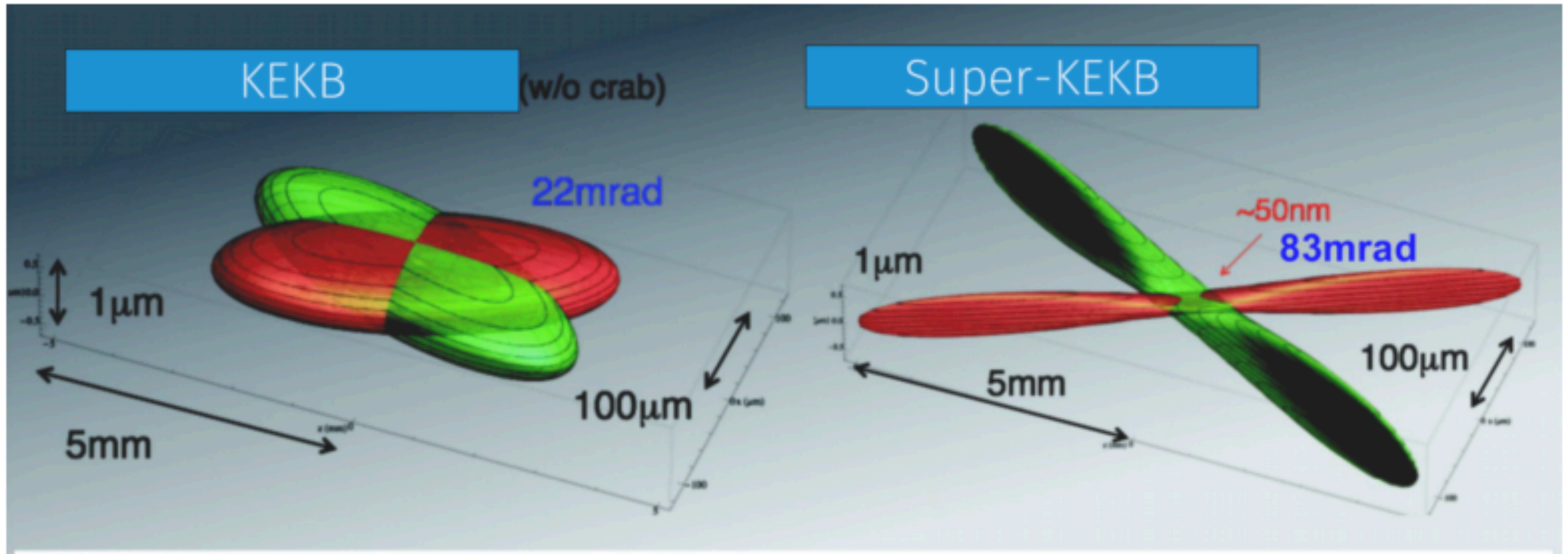

	E (GeV) LER/HER	β^*_y (mm) LER/HER	β^*_x (cm) LER/HER	φ (mrad)	I (A) LER/HER	L ($cm^{-2}s^{-1}$)
KEKB	3.5/8.0	5.9/5.9	120/120	11	1.6/1.2	2.1 x 10^{34}
SuperKEKB	4.0/7.0	0.27/0.30	3.2/2.5	41.5	3.6/2.6	80 x 10^{34}

factor 20 factor 2-3

	KEKB		**SuperKEKB (Juni 2022)**		SuperKEKB Ziel	
	LER	HER	**LER**	**HER**	LER	HER
Energie [GeV]	3.5	8	**4**	**7**	4	7
#Bunches	1584		**2249**		1800	
β^*_x/β^*_y [mm]	1200/5.9	1200/5.9	**80/1.0**	**60/1.0**	32/0.27	25/0.3
I [A]	1.64	1.19	**1.46**	**1.15**	2.8	2.0
Luminosität [10^{34} $cm^{-2}s^{-1}$]	2.1		**4.65 (Rekord!)**		60	
Int. Luminosität [ab^{-1}]	1		**0.43**		50	

Belle II Long Shutdown 1

Belle II stopped taking data in Summer 2022 for a long shutdown

- replacement of beam-pipe
- replacement of photomultipliers of the central PID detector (TOP)
- installation of 2-layered pixel vertex detector
- improved data-quality monitoring and alarm system
- completed transition to new DAQ boards (PCIe40)
- accelerator improvements: injection, non-linear collimators, monitoring
- replacement of aging components
- additional shielding and increased resilience against beam bckg

Related to $B \to K^{*}\gamma$

Systematic Uncertainties

$\mathcal{B}$

Source	$K^{*0}[K^+\pi^-]\gamma$	$K^{*0}[K^0_S\pi^0]\gamma$	$K^{*+}[K^+\pi^0]\gamma$	$K^{*+}[K^0_S\pi^+]\gamma$
B counting	1.5	1.5	1.5	1.5
$f^{\pm}/f^{00}$	1.6	1.6	1.6	1.6
γ selection	0.9	0.9	0.9	0.9
π^0 veto	0.7	0.7	0.7	0.7
η veto	0.2	0.2	0.2	0.2
Tracking efficiency	0.5	0.5	0.2	0.7
π^+ selection	0.2	–	–	0.2
K^+ selection	0.4	–	0.4	–
K^0_S reconstruction	–	1.4	–	1.4
π^0 reconstruction	–	3.9	3.9	–
χ^2 selection	0.2	1.0	0.2	1.0
CSBDT selection	0.3	0.4	0.4	0.3
Candidate selection	0.1	1.0	0.6	0.2
Fit bias	0.1	0.9	0.5	0.2
Signal PDF model	0.1	0.4	0.3	0.2
KDE PDF model	0.1	0.8	0.6	0.2
Simulation sample size	0.2	0.8	0.4	0.5
Misreconstructed signal	–	1.0	1.0	–
Total	2.6	5.4	4.9	3.2

A_{CP}

Source	$K^{*0}[K^+\pi^-]\gamma$	$K^{*+}[K^+\pi^0]\gamma$	$K^{*+}[K^0_S\pi^+]\gamma$
Fit bias	0.1	0.2	0.2
Signal PDF model	0.1	0.1	0.1
KDE modelling	0.1	0.4	0.2
BCS	0.1	0.5	0.2
K^+ asymmetry	–	0.6	–
π^+ asymmetry	–	–	0.6
$K^+\pi^-$ asymmetry	0.3	–	–
Total	0.4	0.9	0.7

Related to $B^0 \rightarrow \gamma\gamma$

Systematic Uncertainties

Signal yield

Source	Belle (%)	Belle II (%)
Photon Detection Efficiency	4.0	2.7
Reconstruction Efficiency (ϵ_{rec})	0.6	0.5
Number of $B\overline{B}$	1.3	1.5
f^{00}	2.5	2.5
C_{BDT} requirement	0.4	0.9
π^0/η veto	0.3	0.4
Timing requirement efficiency	2.8	–
Total (sum in quadrature)	5.7	4.1

Signal efficiencies

Source	Belle (events)	Belle II (events)
Fit bias	$+0.16$	$+0.12$
PDF parameterization	$^{+0.56}_{-0.48}$	$^{+0.30}_{-0.32}$
Shape Modeling	$+0.06$	$+0.04$
Total (sum in quadrature)	$^{+0.58}_{-0.48}$	$^{+0.30}_{-0.32}$

Related to $\Lambda_b^0 \to pK^-\gamma$

Systematic Uncertainties

Table 3: Fit fractions (top) and interference fit fractions (bottom) determined using the amplitude model. The values are given in %. The uncertainties from internal and external sources, determined by the numerical convolution procedure are labelled $\sigma_{\rm syst}^{\rm internal}$ and $\sigma_{\rm syst}^{\rm external}$.

Observable	Value	$\sigma_{\rm stat}$	$\sigma_{\rm syst}^{\rm internal}$	$\sigma_{\rm syst}^{\rm external}$	$\sigma_{\rm syst}$
$\Lambda(1405)$	3.5	$^{+0.3}_{-0.4}$	$^{+0.9}_{-0.0}$	$^{+1.3}_{-0.6}$	$^{+1.9}_{-0.3}$
$\Lambda(1520)$	10.4	$^{+0.4}_{-0.2}$	$^{+0.7}_{-0.0}$	$^{+1.7}_{-1.6}$	$^{+2.2}_{-1.2}$
$\Lambda(1600)$	15.6	$^{+0.6}_{-0.9}$	$^{+0.8}_{-0.2}$	$^{+3.9}_{-5.0}$	$^{+4.3}_{-4.6}$
$\Lambda(1670)$	1.3	$^{+0.2}_{-0.2}$	$^{+0.3}_{-0.2}$	$^{+1.2}_{-0.3}$	$^{+1.3}_{-0.2}$
$\Lambda(1690)$	7.7	$^{+0.4}_{-0.8}$	$^{+1.8}_{-0.1}$	$^{+5.1}_{-1.0}$	$^{+6.2}_{-0.2}$
$\Lambda(1800)$	18.3	$^{+1.3}_{-1.6}$	$^{+1.4}_{-1.1}$	$^{+3.2}_{-6.0}$	$^{+3.2}_{-6.2}$
$\Lambda(1810)$	0.1	$^{+0.9}_{-0.4}$	$^{+1.7}_{-0.4}$	$^{+4.0}_{-0.7}$	$^{+4.8}_{-0.7}$
$\Lambda(1820)$	8.3	$^{+0.4}_{-0.7}$	$^{-0.2}_{-1.4}$	$^{+1.9}_{-4.8}$	$^{+1.0}_{-5.7}$
$\Lambda(1830)$	0.3	$^{+0.4}_{-0.4}$	$^{+0.6}_{-0.5}$	$^{+1.5}_{-0.9}$	$^{+1.6}_{-0.9}$
$\Lambda(1890)$	11.2	$^{+0.7}_{-0.6}$	$^{+0.5}_{-0.6}$	$^{+4.3}_{-5.1}$	$^{+4.6}_{-4.9}$
$\Lambda(2100)$	7.3	$^{+0.5}_{-0.5}$	$^{+1.1}_{-0.6}$	$^{+1.1}_{-2.8}$	$^{+1.4}_{-2.9}$
$\Lambda(2110)$	6.5	$^{+0.6}_{-0.7}$	$^{+1.7}_{-0.0}$	$^{+5.4}_{-0.9}$	$^{+6.3}_{-0.2}$
$\Lambda(2350)$	1.0	$^{+0.2}_{-0.1}$	$^{+0.8}_{-0.0}$	$^{+0.0}_{-0.2}$	$^{+0.8}_{-0.1}$
NR($3/2^-$)	2.8	$^{+0.5}_{-0.4}$	$^{+0.2}_{-1.9}$	$^{+3.0}_{+0.3}$	$^{+2.4}_{-1.3}$
$\Lambda(1405), \Lambda(1670)$	−0.7	$^{+0.1}_{-0.2}$	$^{+0.2}_{-0.2}$	$^{+0.5}_{-0.8}$	$^{+0.5}_{-0.9}$
$\Lambda(1405), \Lambda(1800)$	7.6	$^{+0.7}_{-0.8}$	$^{+1.2}_{-2.0}$	$^{+0.6}_{-3.5}$	$^{+0.9}_{-4.6}$
$\Lambda(1520), \Lambda(1690)$	0.5	$^{+0.5}_{-0.3}$	$^{+0.3}_{-0.9}$	$^{+0.6}_{-2.6}$	$^{+0.5}_{-3.0}$
$\Lambda(1520)$, NR($3/2^-$)	−0.6	$^{+0.4}_{-0.4}$	$^{+1.0}_{-0.6}$	$^{+1.6}_{-3.2}$	$^{+2.1}_{-3.0}$
$\Lambda(1600), \Lambda(1810)$	−1.9	$^{+1.5}_{-1.0}$	$^{+1.3}_{-1.5}$	$^{+4.1}_{-2.9}$	$^{+3.9}_{-3.6}$
$\Lambda(1670), \Lambda(1800)$	−4.8	$^{+0.5}_{-0.4}$	$^{+0.4}_{-0.6}$	$^{+1.5}_{-2.0}$	$^{+1.5}_{-2.1}$
$\Lambda(1690)$, NR($3/2^-$)	3.9	$^{+0.4}_{-0.4}$	$^{+0.1}_{-3.0}$	$^{+1.2}_{-2.7}$	$^{+0.3}_{-4.7}$
$\Lambda(1820), \Lambda(2110)$	1.1	$^{+0.7}_{-0.5}$	$^{+0.2}_{-2.1}$	$^{+2.5}_{-3.9}$	$^{+1.9}_{-4.8}$

18

- The uncertainties for most observables are dominated by external inputs: specifically the masses and widths of the Λ states. A future measurement including improved knowledge of the different Λ baryons and more data will result in a significant reduction of the uncertainties.
- $\mathscr{B}(\Lambda_b^0 \to \Lambda^{*0}\gamma) \sim 3 \times 10^{-5}$

Related to $B_s^0 \to \mu^+\mu^-\gamma$

Selection details

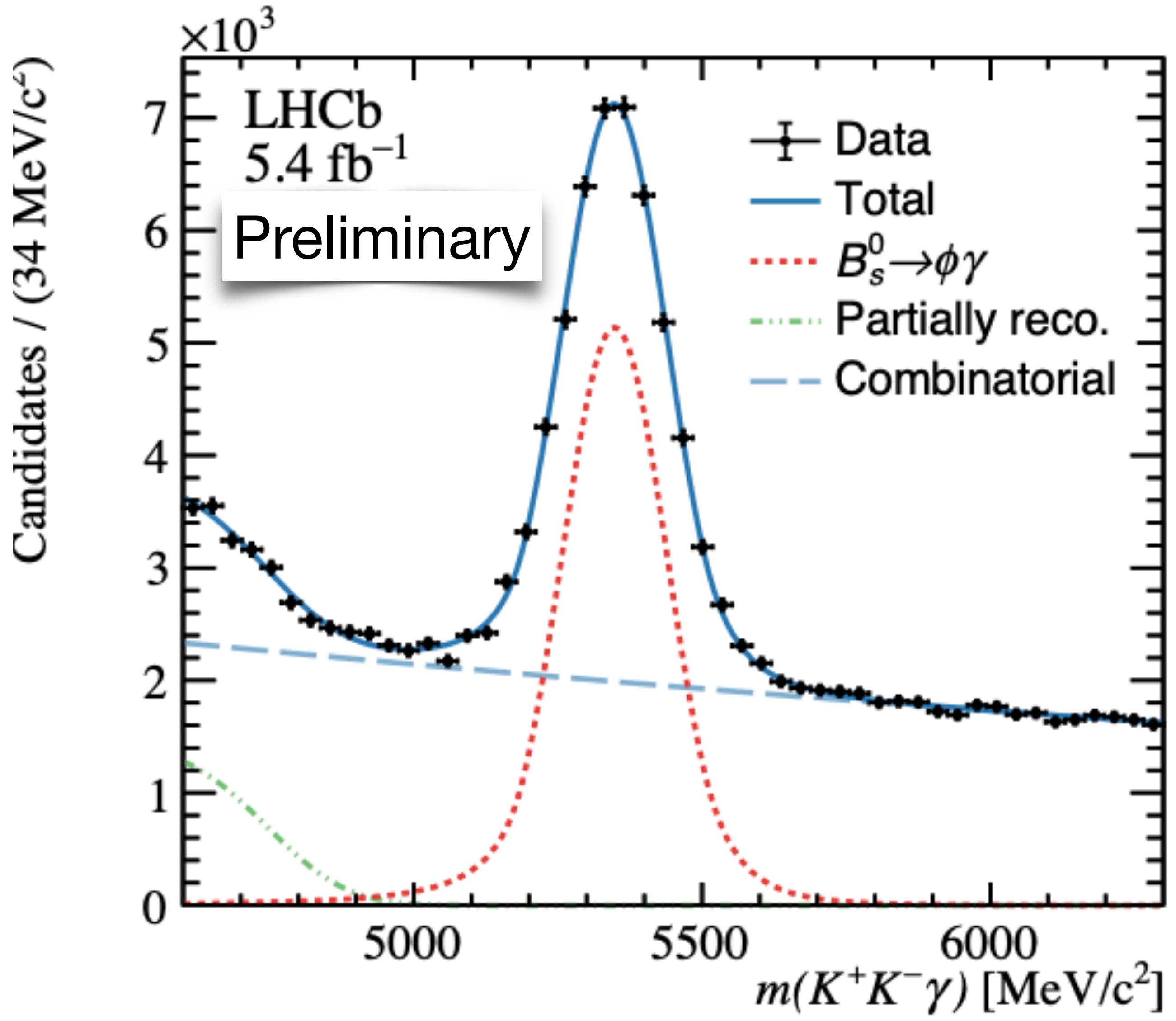

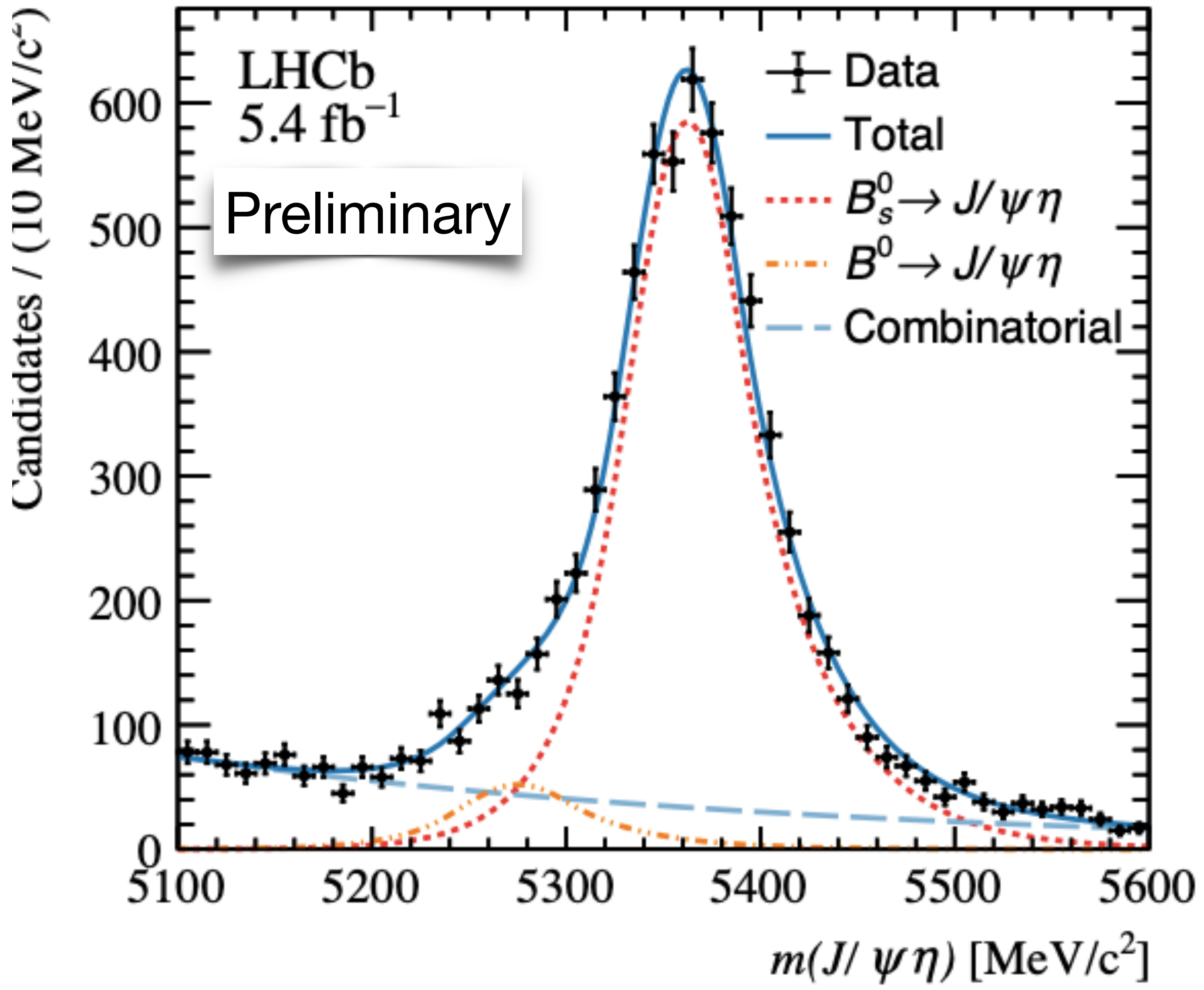

- Use two MLP classifiers to reduce backgrounds (optimised for each q^2 region)
- Double mis-ID, partially reconstructed, $B \to \mu\mu\pi^0$, $B \to \mu\mu\eta$
- Control channel: $B_s^0 \to \phi(\to K^+K^-)\gamma$
- Normalisation channel: $B_s^0 \to J/\psi(\to \mu^+\mu^-)\eta(\to \gamma\gamma)$

More Results

Preliminary

$$
\begin{aligned}
\mathcal{B}(B_s^0 \to \mu^+\mu^-\gamma)_{\mathrm{I}} &= (1.34 \pm 1.60 \pm 0.28) \times 10^{-8}, \\
\mathcal{B}(B_s^0 \to \mu^+\mu^-\gamma)_{\mathrm{II}} &= (0.76 \pm 3.55 \pm 0.30) \times 10^{-8}, \\
\mathcal{B}(B_s^0 \to \mu^+\mu^-\gamma)_{\mathrm{III}} &= (-2.55 \pm 2.25 \pm 0.41) \times 10^{-8}, \\
\mathcal{B}(B_s^0 \to \mu^+\mu^-\gamma)_{\mathrm{I},\,\phi\ \mathrm{veto}} &= (0.72 \pm 1.56 \pm 0.29) \times 10^{-8}.
\end{aligned}
$$

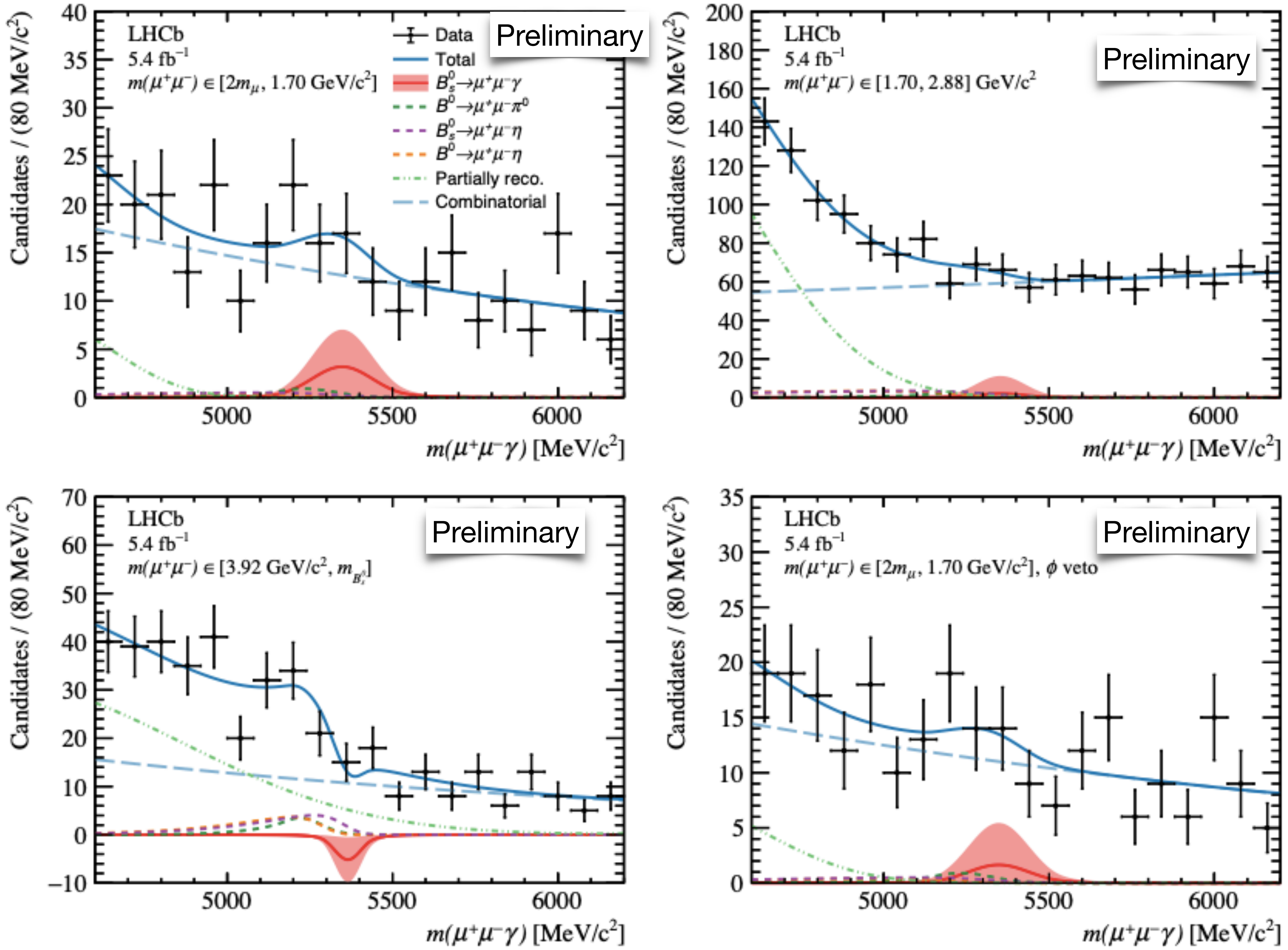

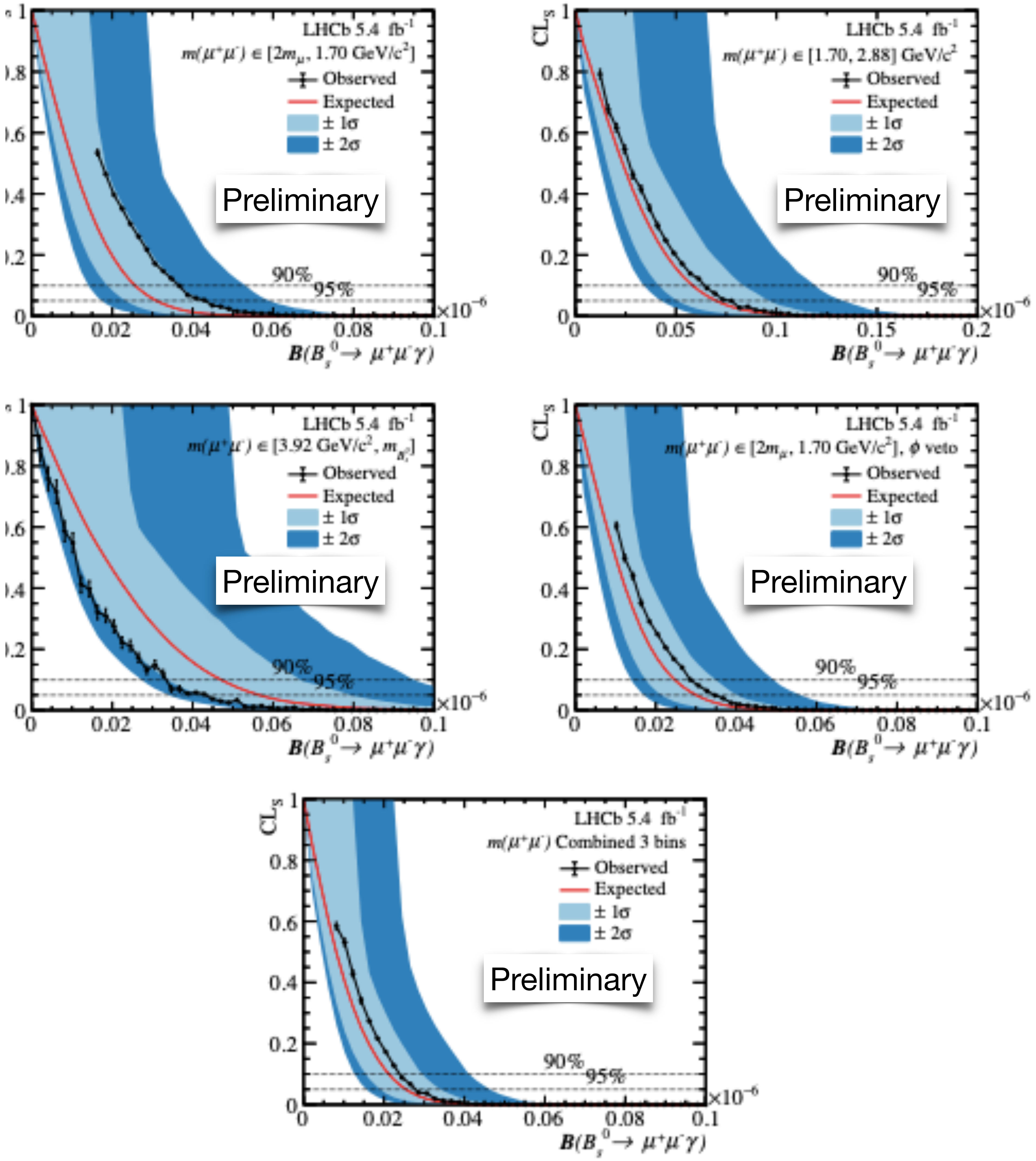

Comparison

- Indirect search in $B_s^0 \to \mu^+\mu^-$ = no photon reconstruction
- Only sensitive to high q^2 region

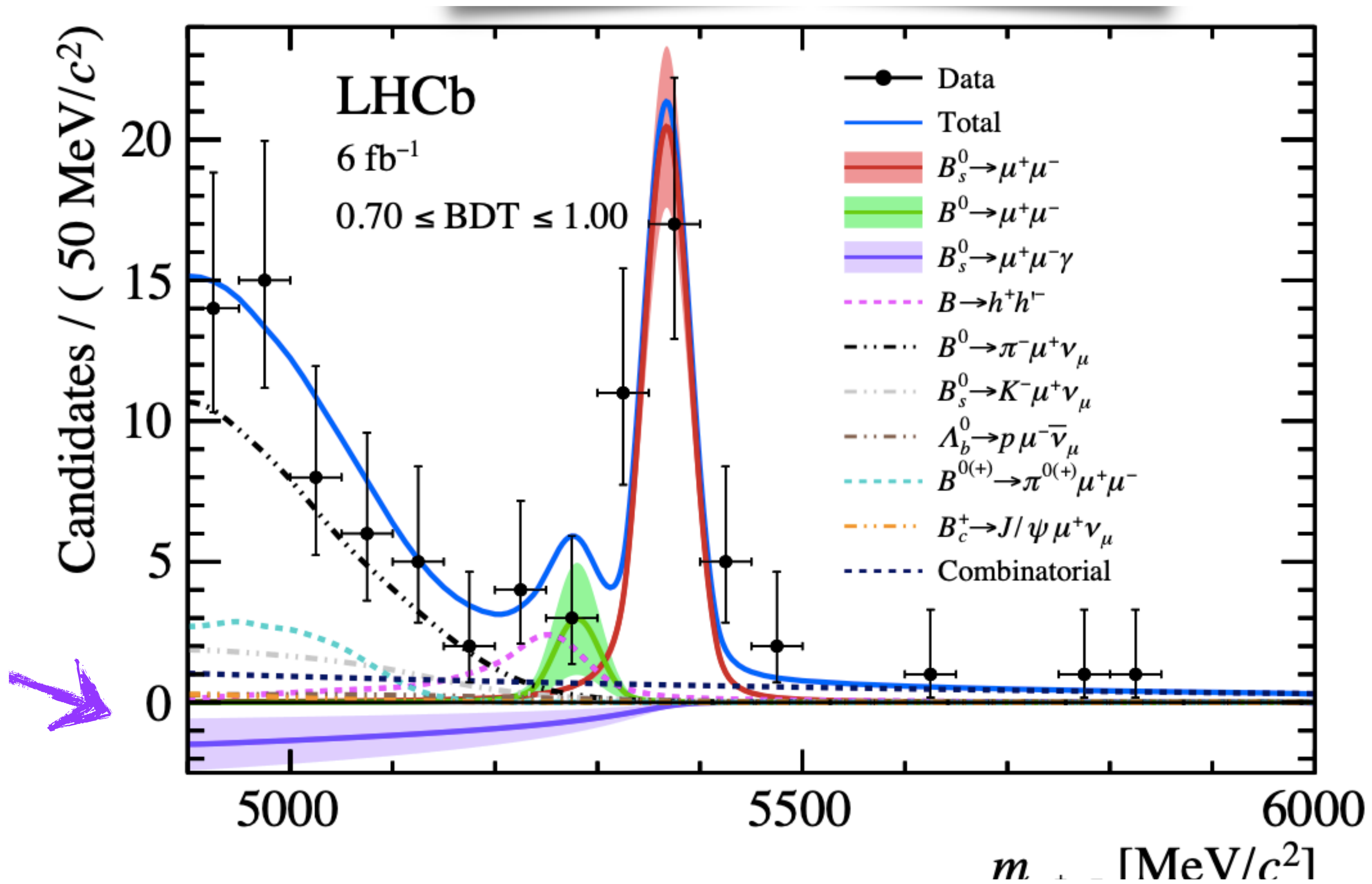

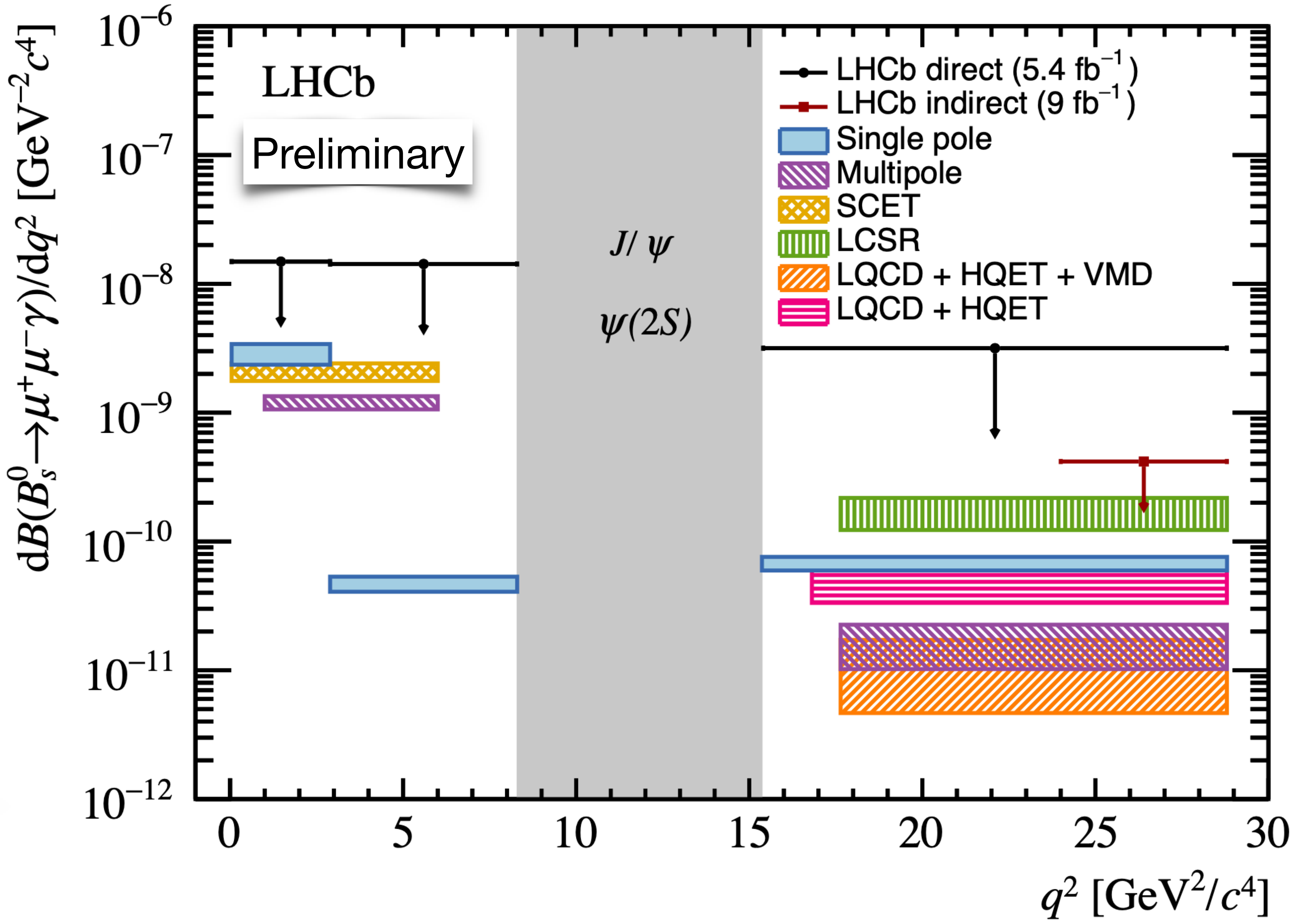

Related to $B^+ \to K^+ \nu\bar{\nu}$

$B^+ \to K^+\nu\bar{\nu}$: Variables

Seven major backgrounds categories:

- $B^0\overline{B}^0$
- B^+B^-

} $B\bar{B}$ *backgrounds*

- $c\bar{c}$
- $s\bar{s}$
- $u\bar{u}$
- $d\bar{d}$

} $q\bar{q}$ *continuum*

- $\tau^+\tau^-$

ITA discriminating variables: signal kinematics, two/three-track vertices, general event topology (**e.g sphericity**) →

HTA discriminating variables: signal kinematics, B_{tag}, other track and cluster information

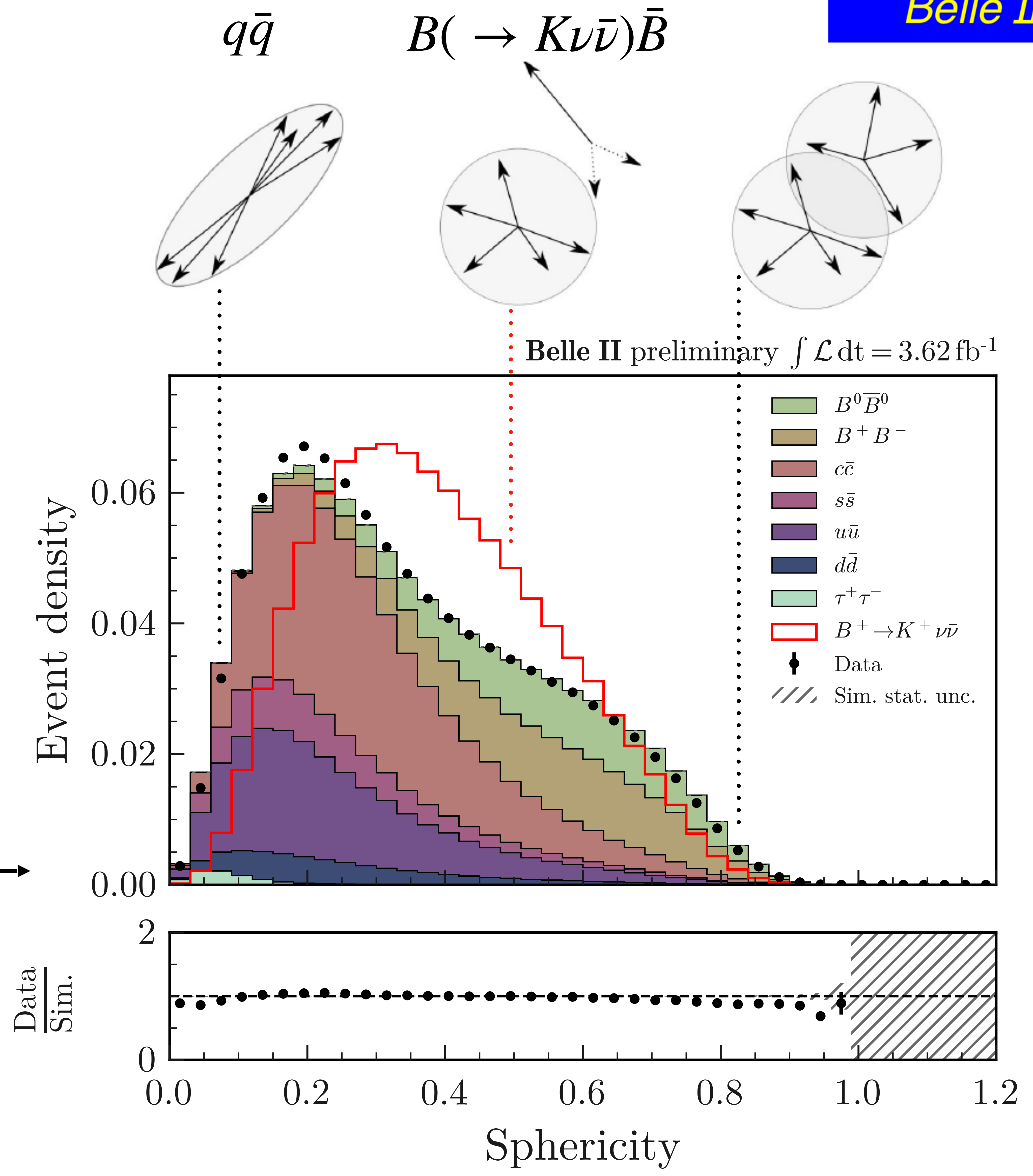

Reconstruction Techniques

Efficiency

$\epsilon \sim 0.1 - 1\,\%$ $\epsilon \sim 1 - 3\,\%$ $\epsilon \sim 1 - 100\,\%$

Exclusive hadronic (HAD)

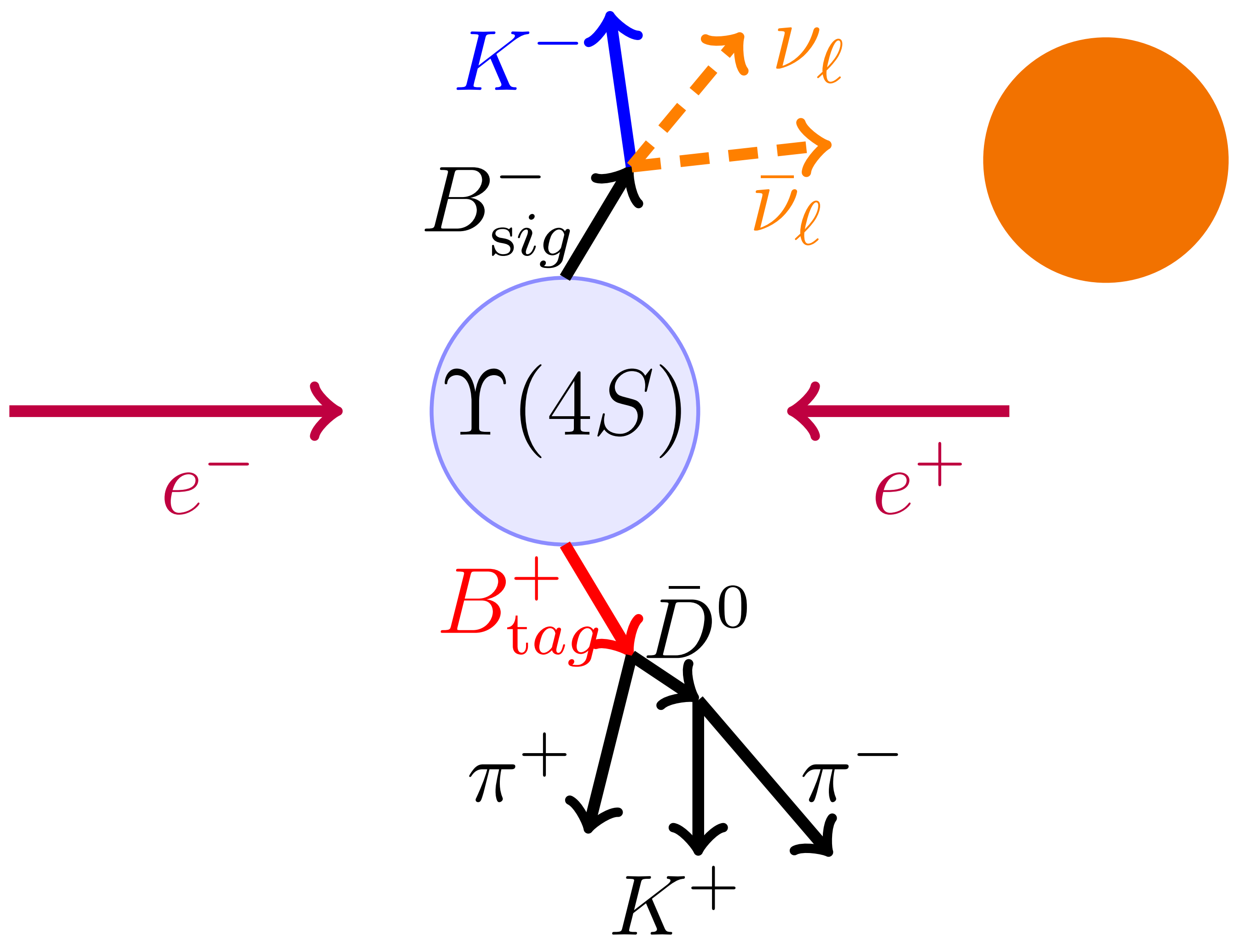

Exclusive semileptonic

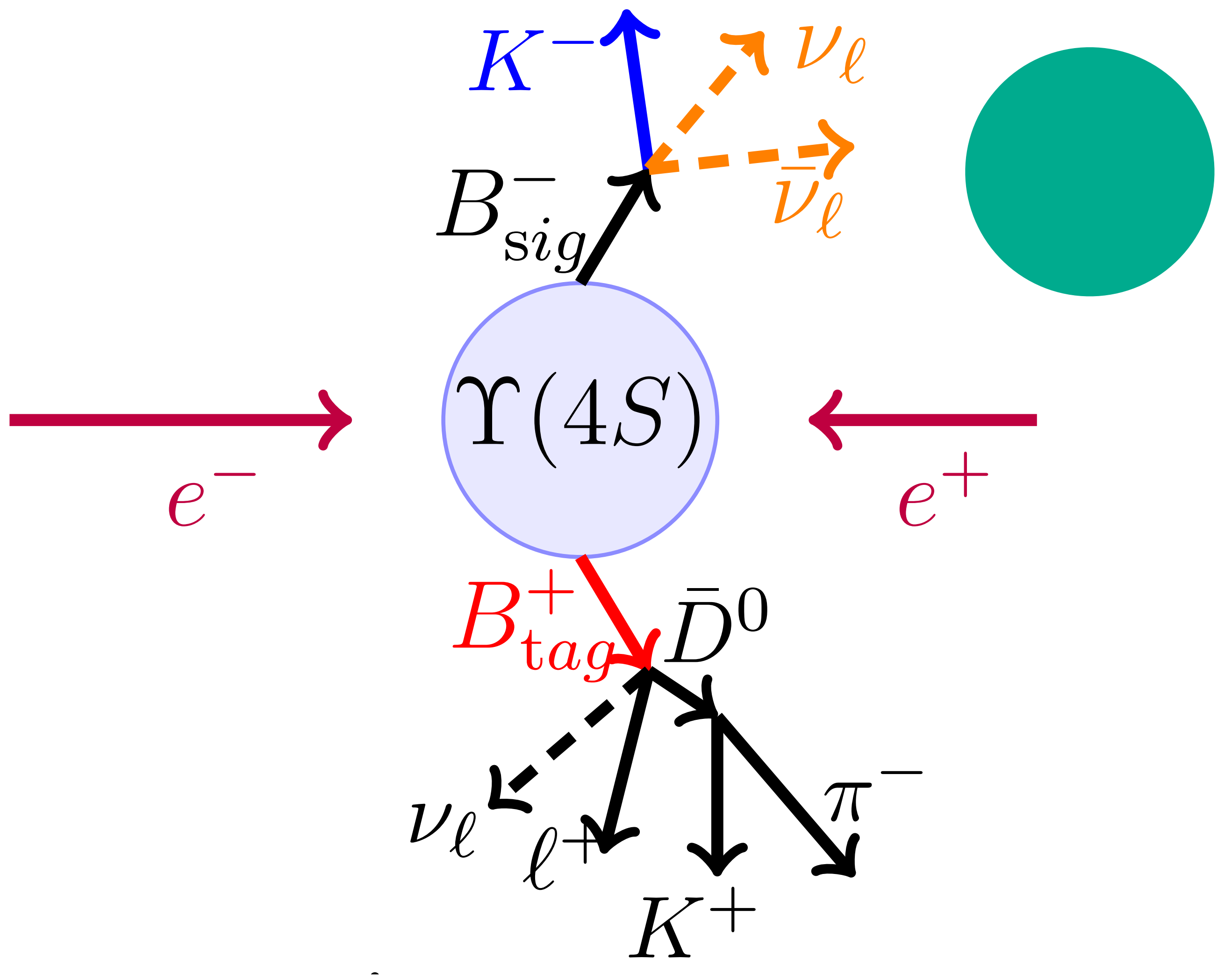

Inclusive (ITA)

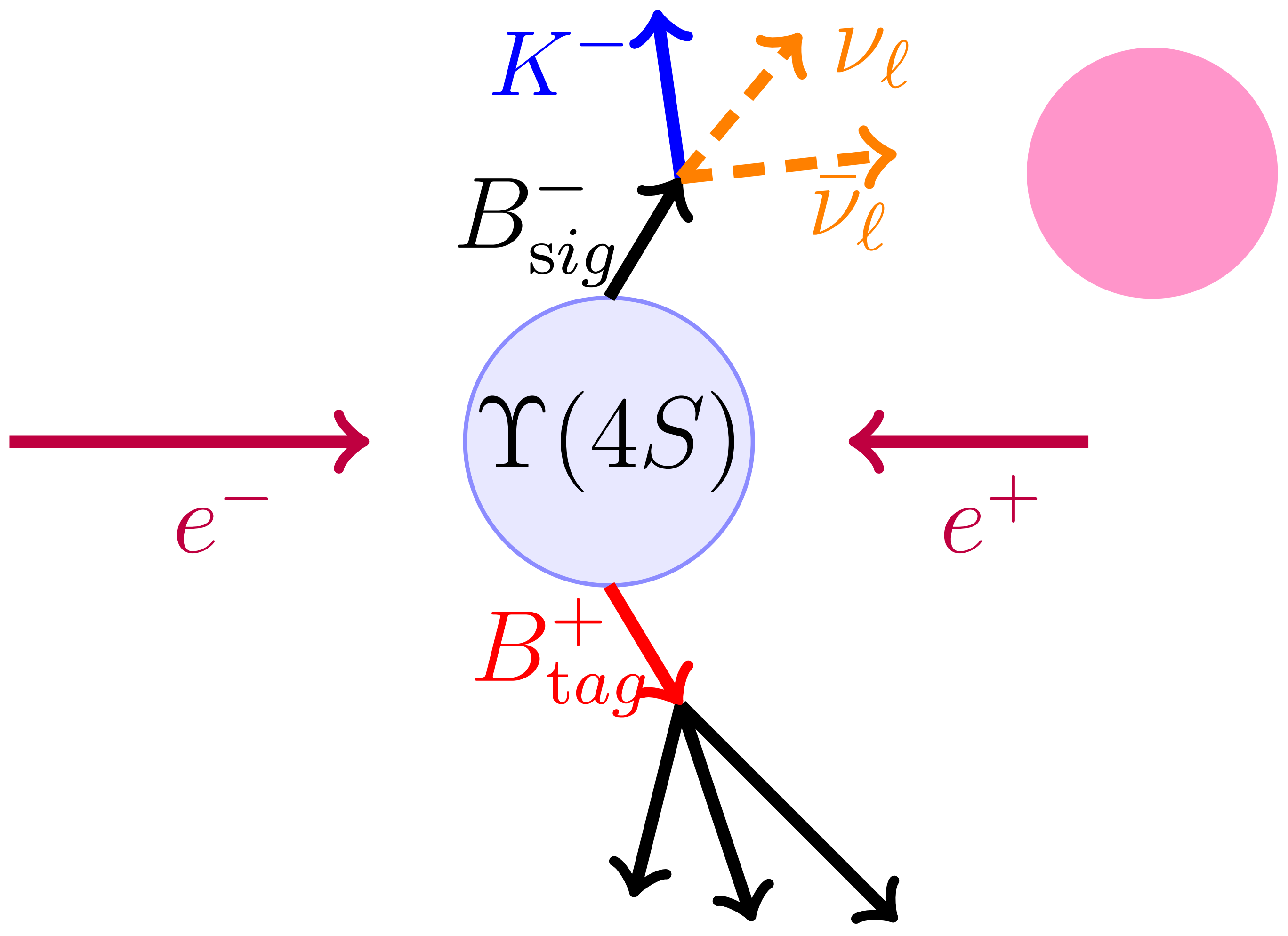

Purity, Resolution

Different reconstruction techniques lead to nearly orthogonal data samples

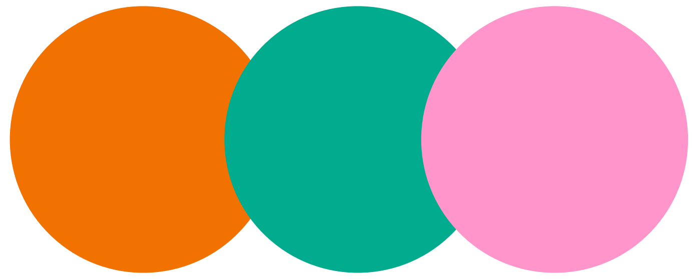

q^2 distribution

- Default signal model → PHSP model with SM form factor reweighting [arXiv:1409.4557]
- At low q^2 maximum signal efficiency of 13%
- No sensitivity for $q^2 > 16\ \mathrm{GeV}^2/\mathrm{c}^2$

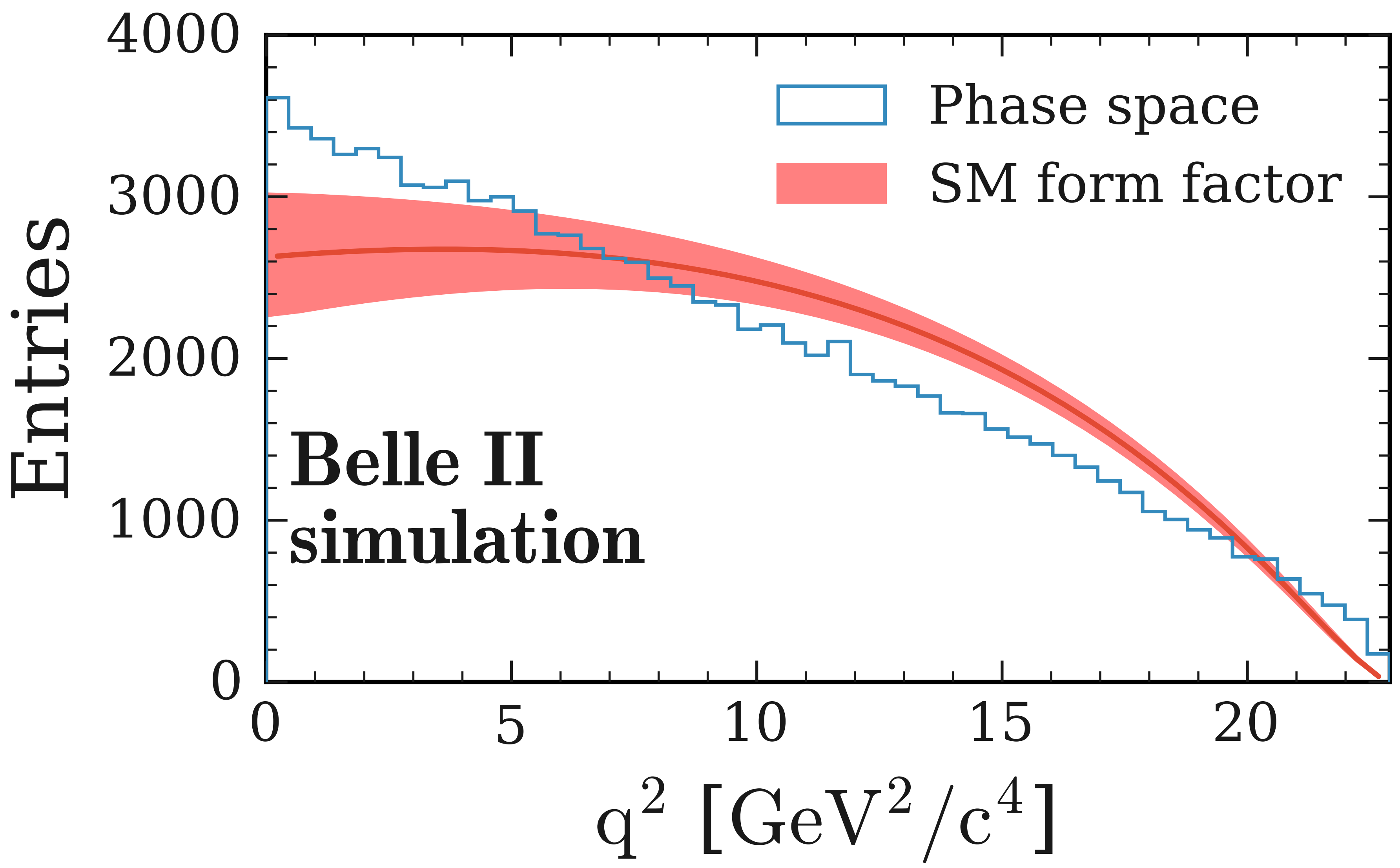

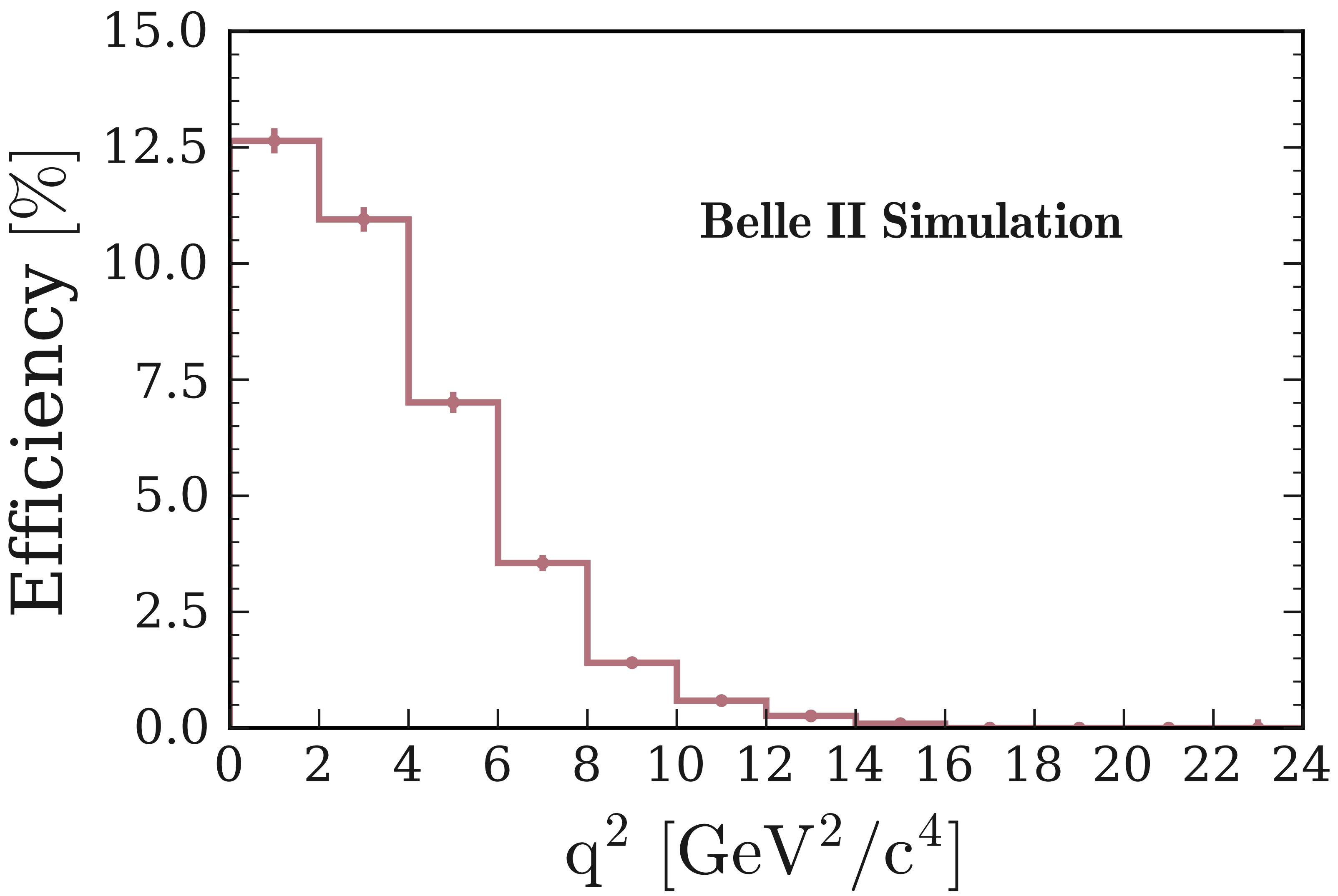

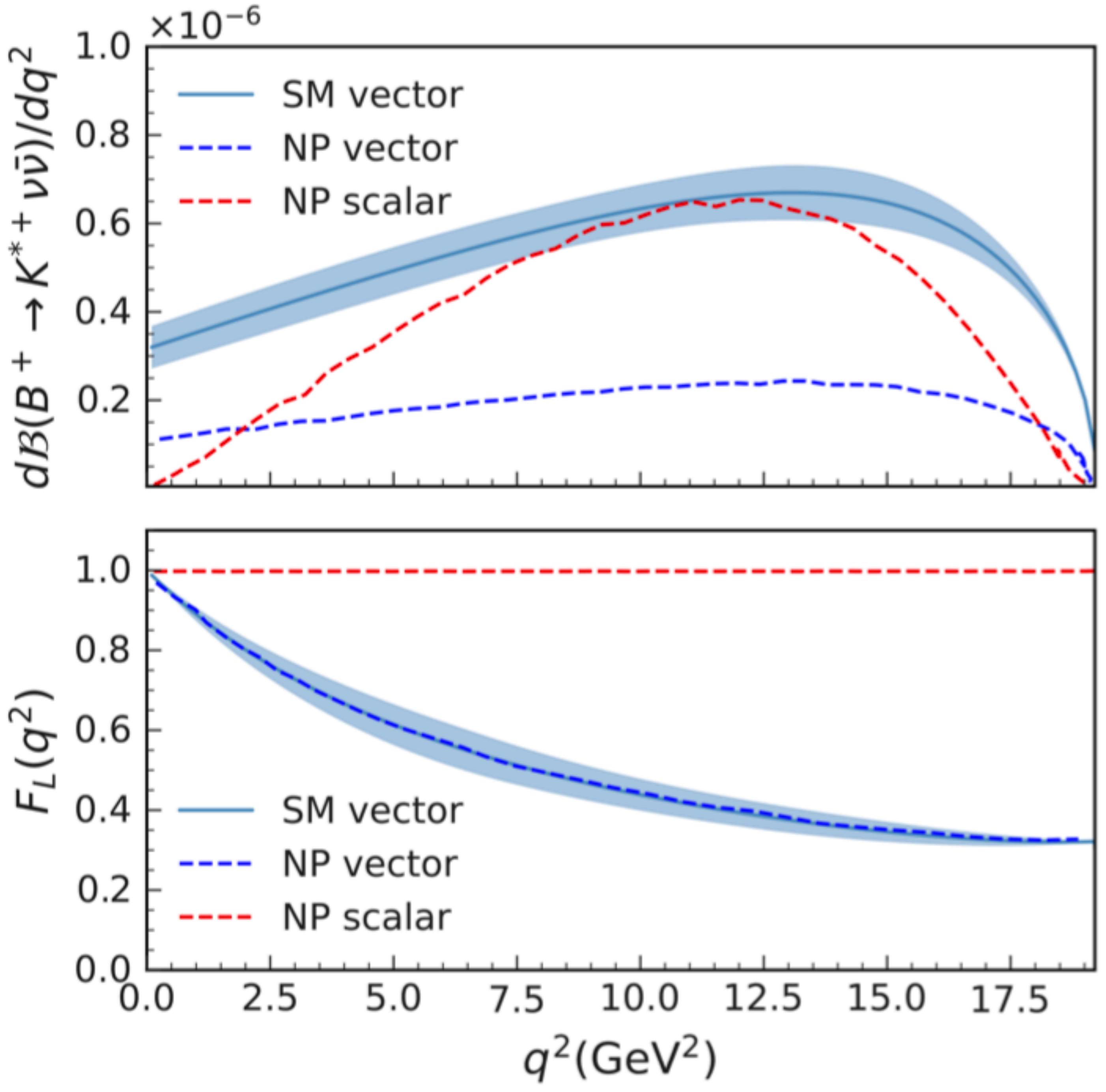

[PRL 127, 181802 (2021)]

Selection Efficiency as a fn. q^2

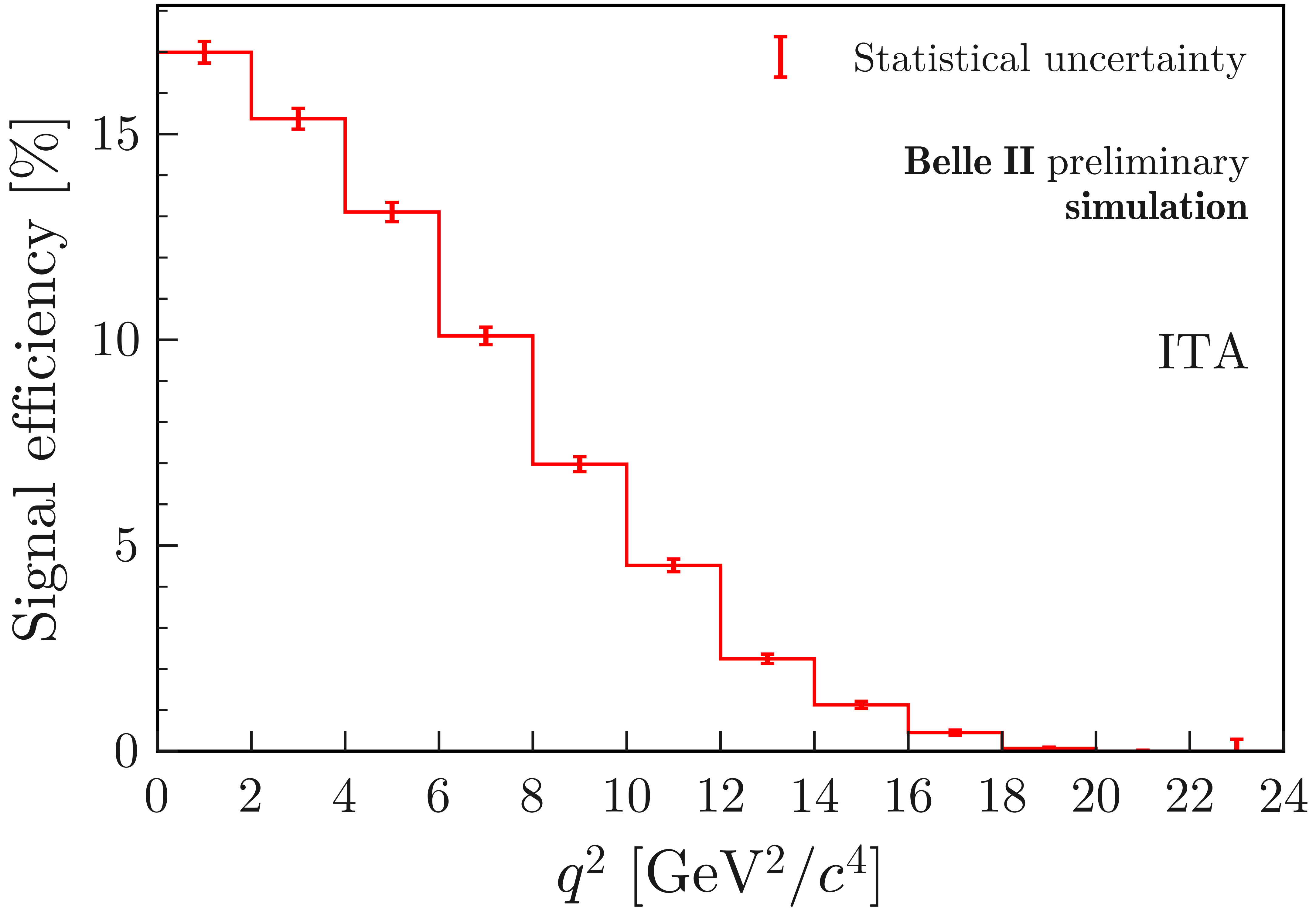

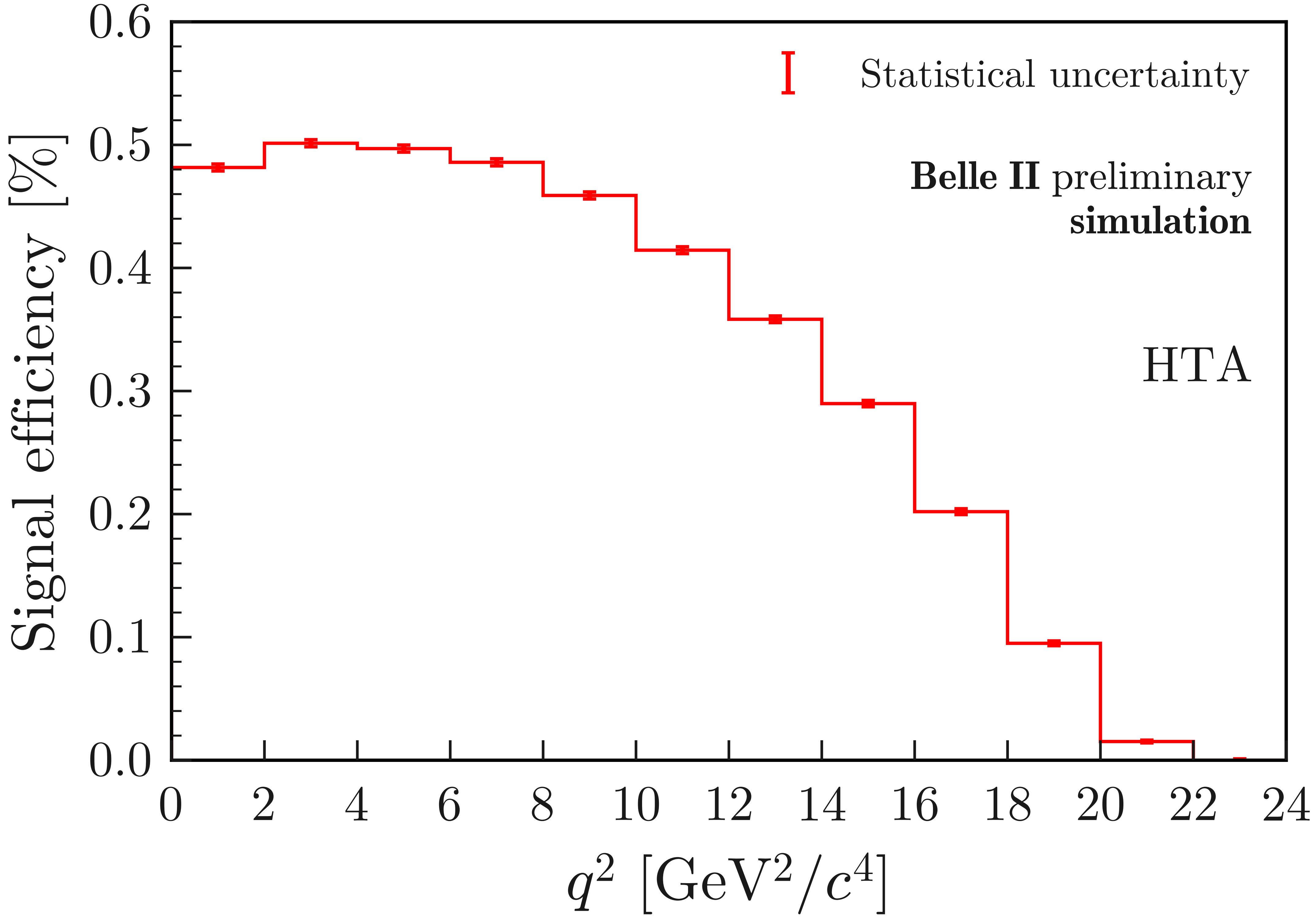

HTA much lower efficiency w.r.t. ITA analysis, but a smaller variation in q^2

arxiv: 2311.14647

Slavomira Stefkova, slavomira.stefkova@kit.edu

Systematic Uncertainties

Source	Uncertainty size	Impact on σ_μ	
Normalization of $B\bar{B}$ background	50%	0.88	1.
Normalization of continuum background	50%	0.10	
Leading B-decays branching fractions	$O(1\%)$	0.22	
Branching fraction for $B^+ \to K^+ K^0_L K^0_L$	20%	0.49	3.
p-wave component for $B^+ \to K^+ K^0_S K^0_L$	30%	0.02	
Branching fraction for $B \to D^{(**)}$	50%	0.42	
Branching fraction for $B^+ \to n\bar{n}K^+$	100%	0.20	
Branching fraction for $D \to K_L X$	10%	0.14	
Continuum background modeling, $\mathrm{BDT_c}$	100% of correction	0.01	
Integrated luminosity	1%	< 0.01	
Number of $B\bar{B}$	1.5%	0.02	
Off-resonance sample normalization	5%	0.05	
Track finding efficiency	0.3%	0.20	
Signal kaon PID	$O(1\%)$	0.07	
Photon energy scale	0.5%	0.08	
Hadronic energy scale	10%	0.36	
K^0_L efficiency in ECL	8%	0.21	
Signal SM form factors	$O(1\%)$	0.02	
Global signal efficiency	3%	0.03	
MC statistics	$O(1\%)$	0.52	2.

statistical uncertainty on μ = 1.1

Systematic Uncertainties

Source	Uncertainty size	Impact on σ_μ	
Normalization $B\bar{B}$ background	30%	0.91	1.
Normalization continuum background	50%	0.58	
Leading B-decays branching fractions	$O(1\%)$	0.10	
Branching fraction for $B^+ \to K^+ K_L^0 K_L^0$	20%	0.20	
Branching fraction for $B \to D^{(**)}$	50%	< 0.01	
Branching fraction for $B^+ \to K^+ n\bar{n}$	100%	0.05	
Branching fraction for $D \to K_L X$	10%	0.03	
Continuum background modeling, $\mathrm{BDT_c}$	100% of correction	0.29	
Number of $B\bar{B}$	1.5%	0.07	
Track finding efficiency	0.3%	0.01	
Signal kaon PID	$O(1\%)$	< 0.01	
Extra photon multiplicity	$O(20\%)$	0.61	2.
K_L^0 efficiency	17%	0.31	
Signal SM form factors	$O(1\%)$	0.06	
Signal efficiency	16%	0.42	
Simulated sample size	$O(1\%)$	0.60	3.

statistical uncertainty on μ = 2.3

ITA Results: Post-fit distributions

Belle II

$\mu(BDT_2) > 0.92$

$\mu(BDT_2) > 0.98$

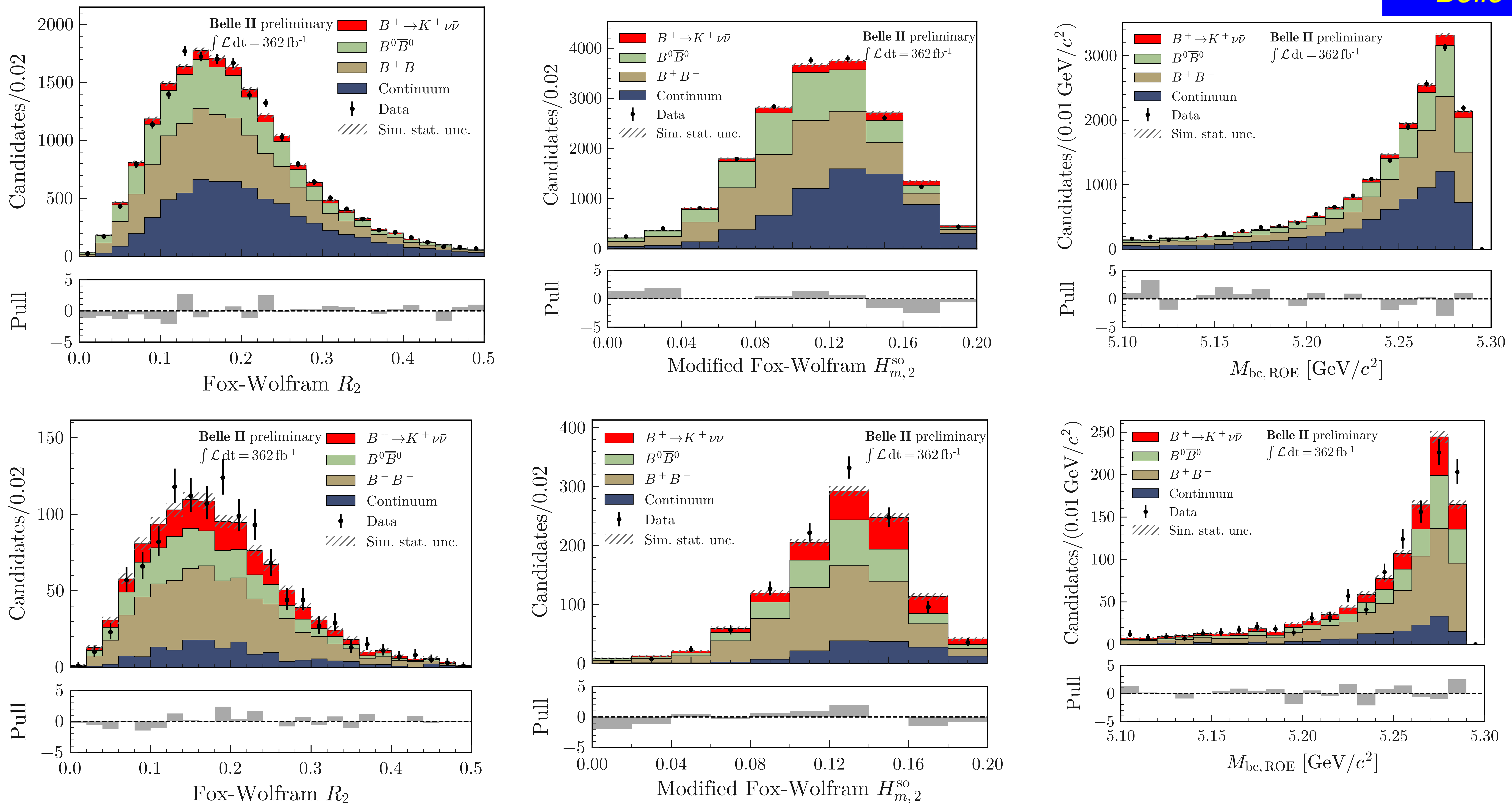

Slavomira Stefkova, slavomira.stefkova@kit.edu

KIT Karlsruhe Institute of Technology

ITA Results: Post-fit distributions

$\eta(\mathrm{BDT}_2) > 0.92$

$\eta(\mathrm{BDT}_2) > 0.98$

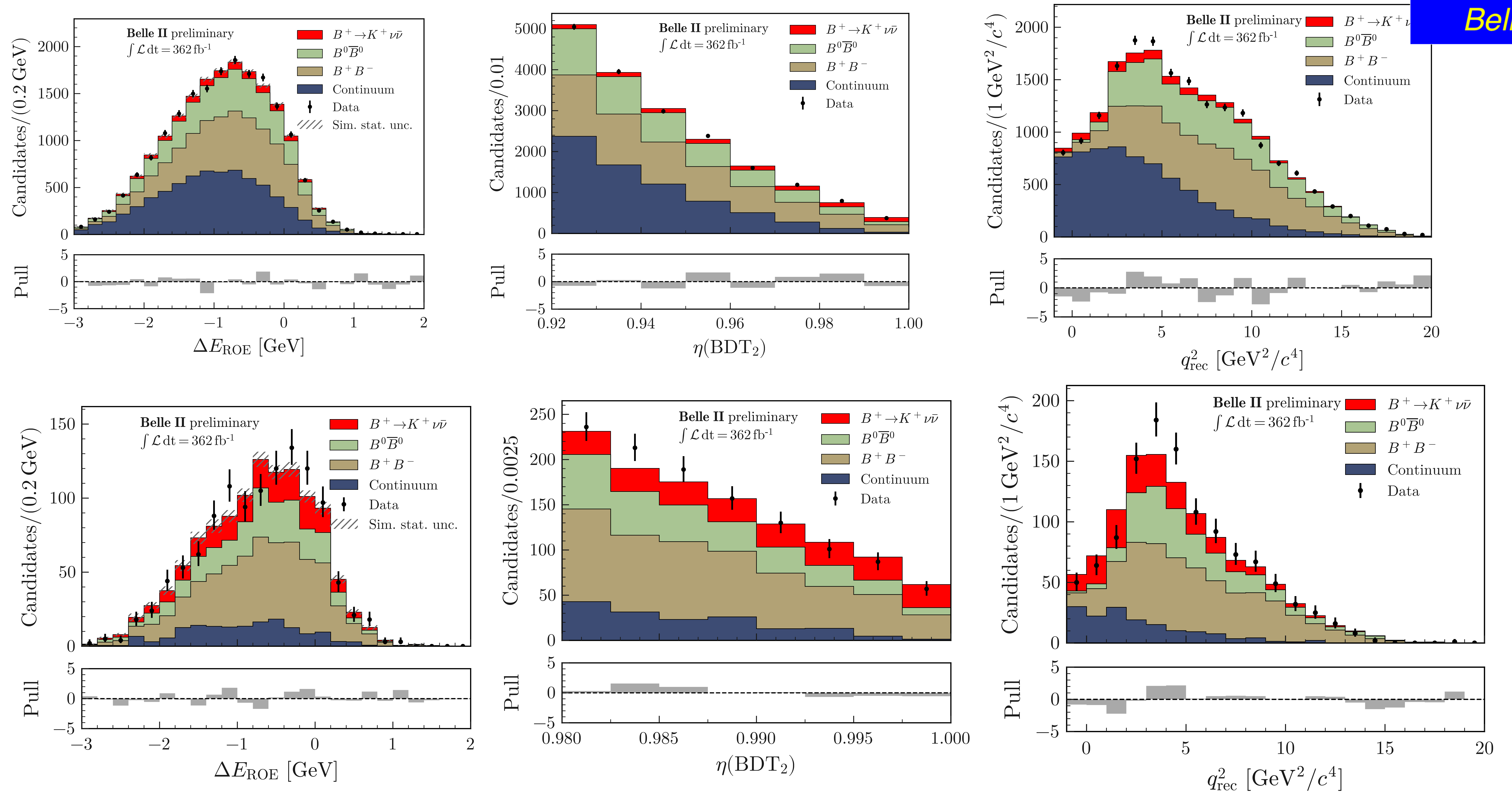

HTA Results: Post-fit distributions

HTA Signal region $\eta(\mathrm{BDTh}) > 0.4$

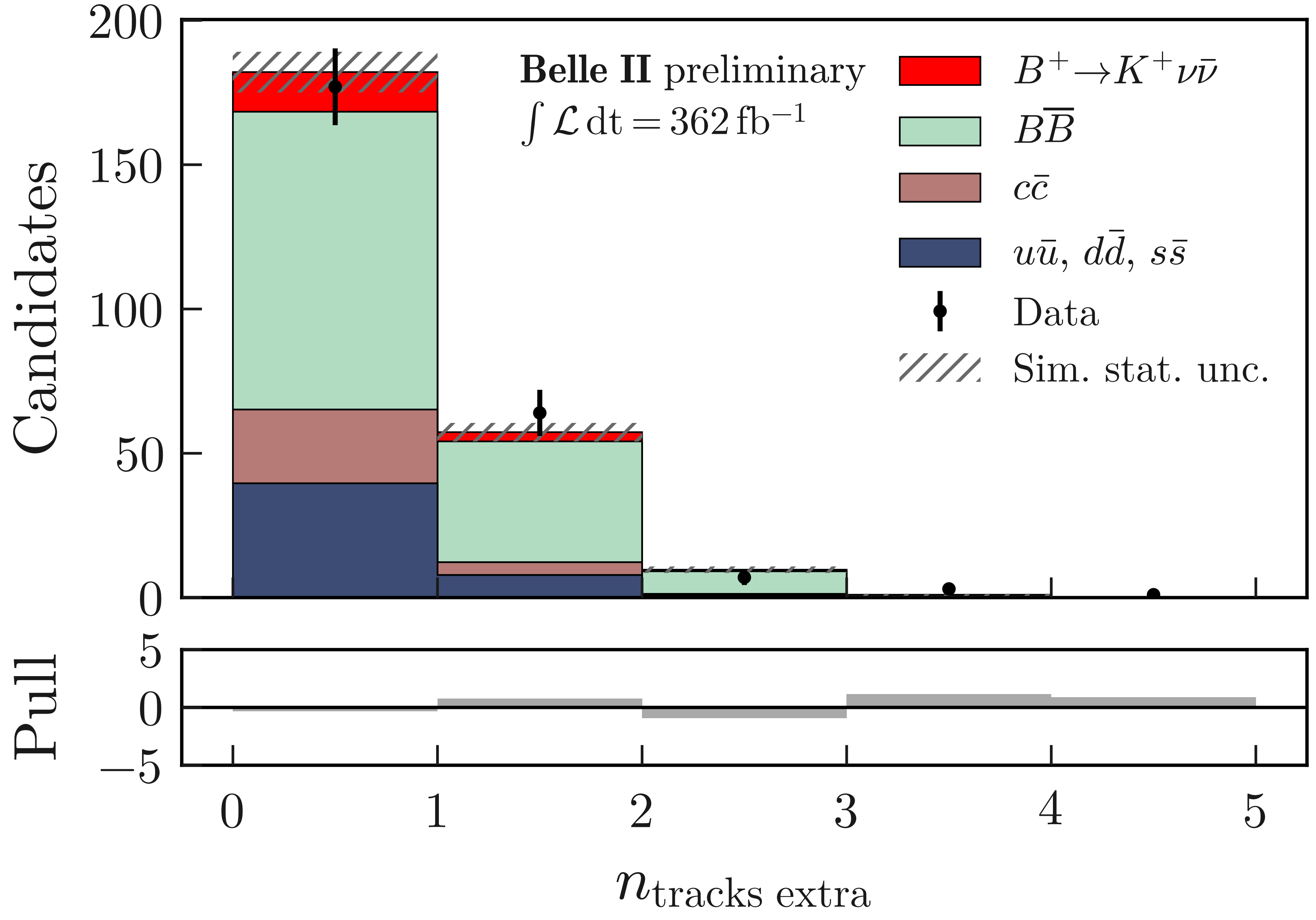

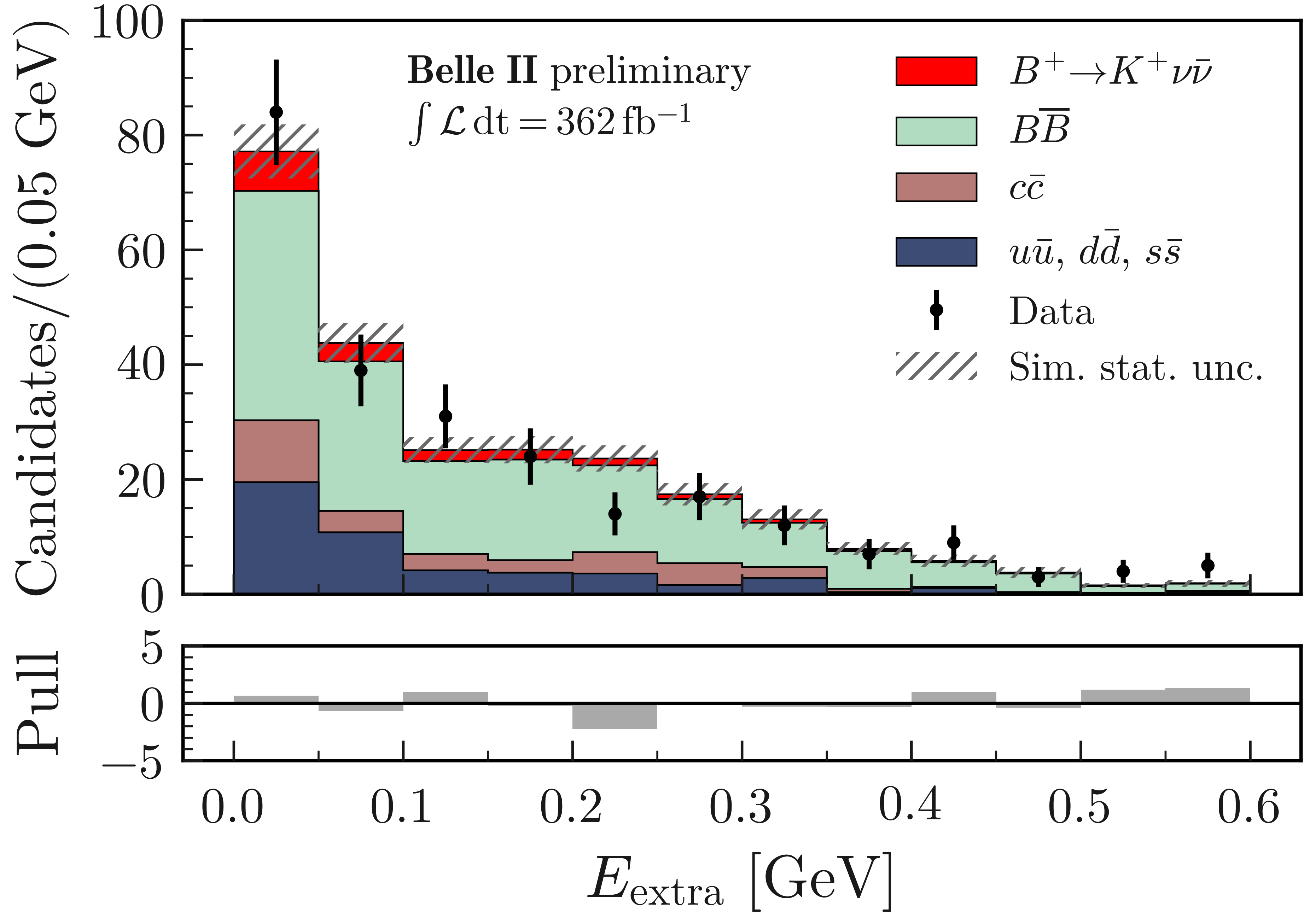

HTA Results: Post-fit distributions

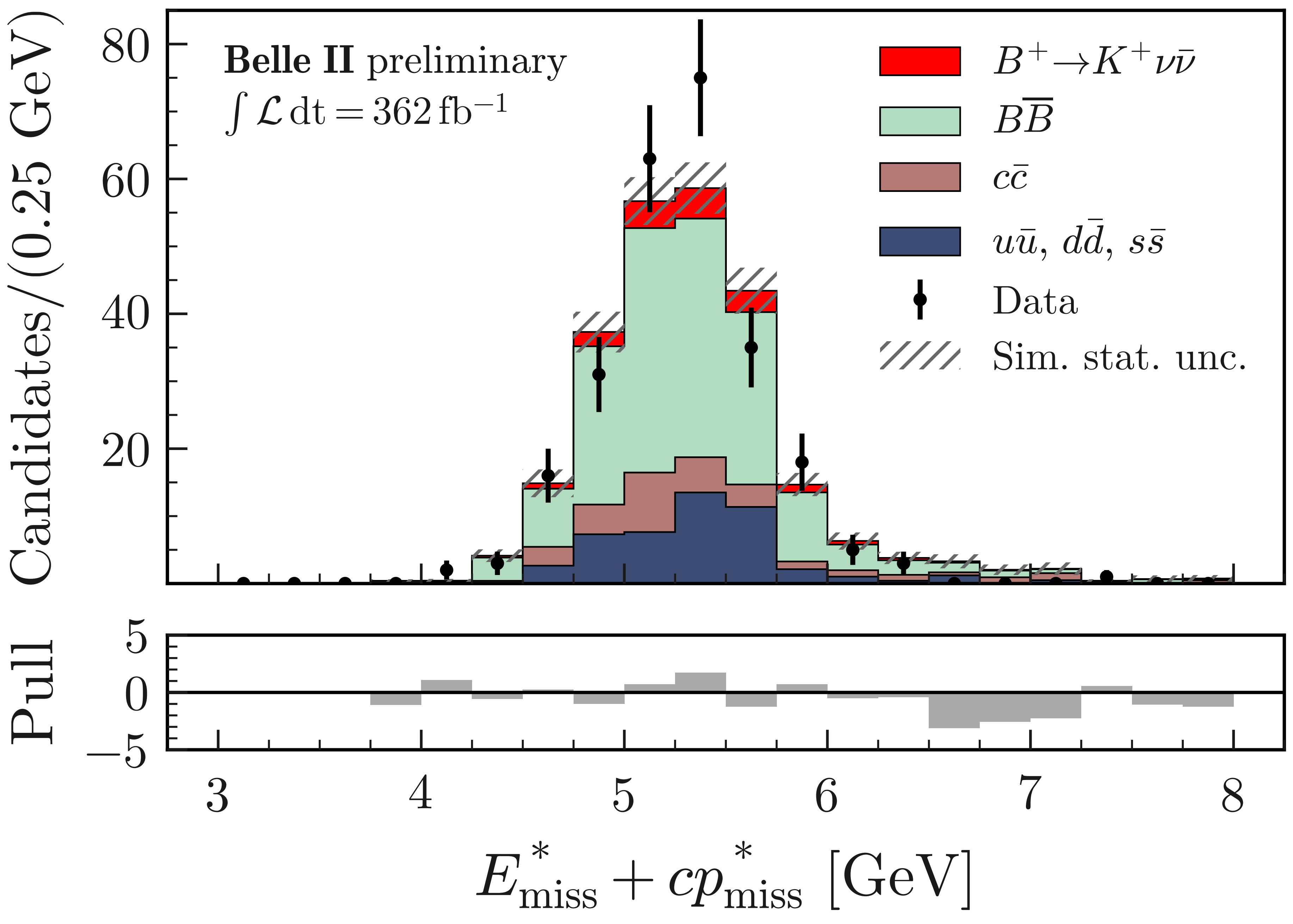

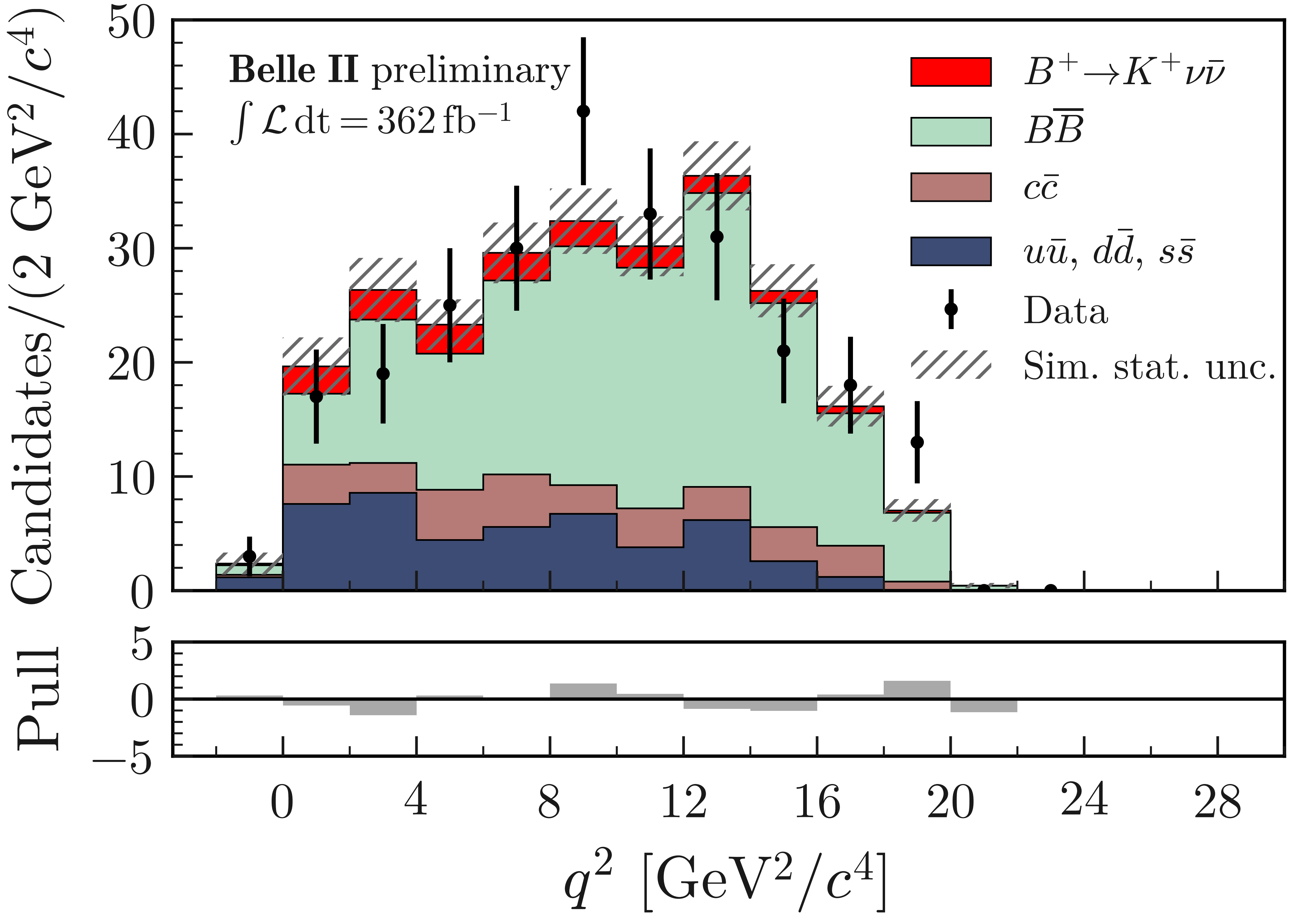

Uncertainty on the Signal Strength μ

Belle II Snowmass paper : 2 scenarios baseline (improved*)

3σ (5σ) for SM $B^+ \to K^+\nu\bar{\nu}$ decays with 5 ab^{-1}

*The "improved" scenario assumes a 50% increase in signal efficiency for the same background level

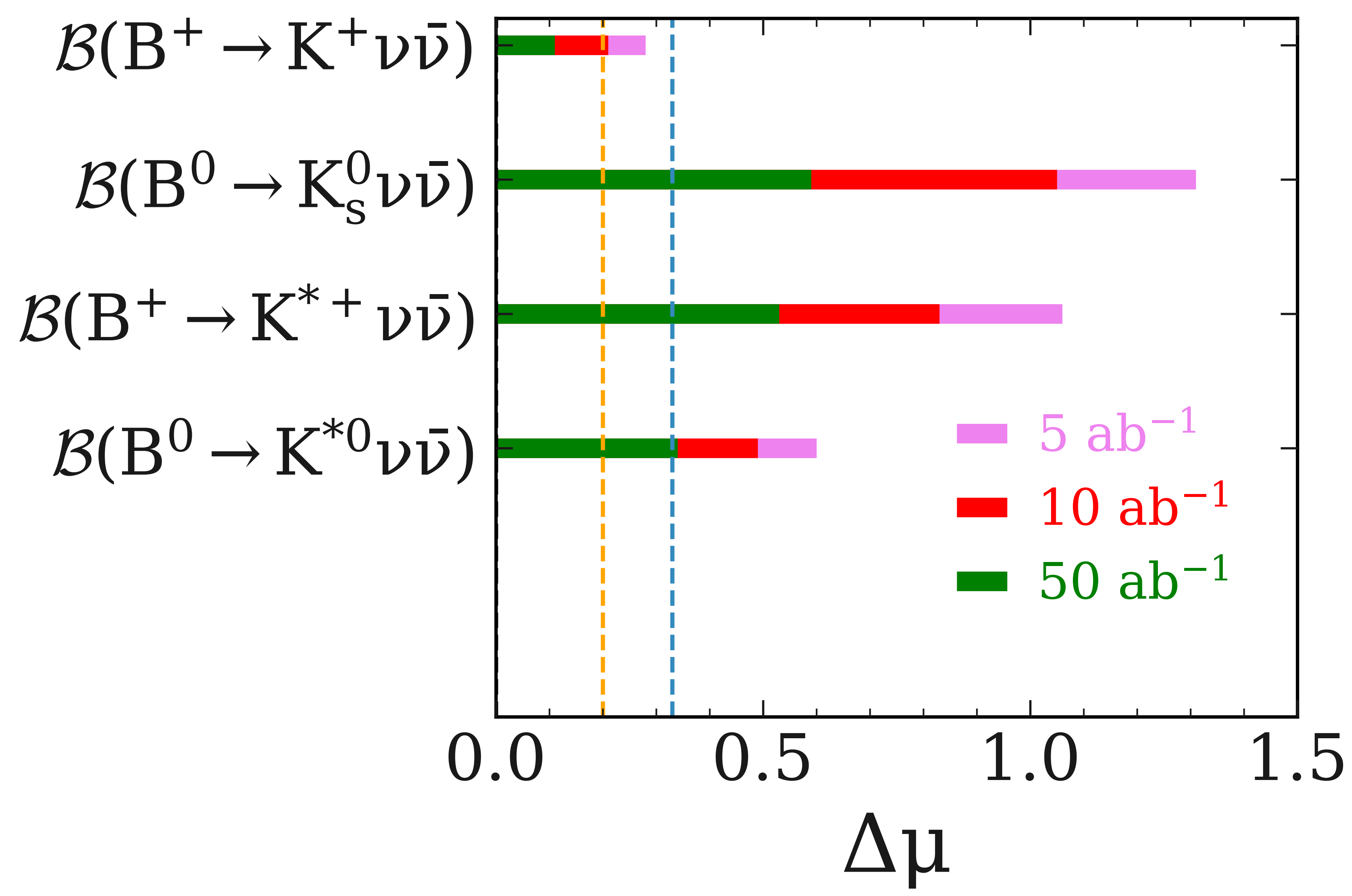

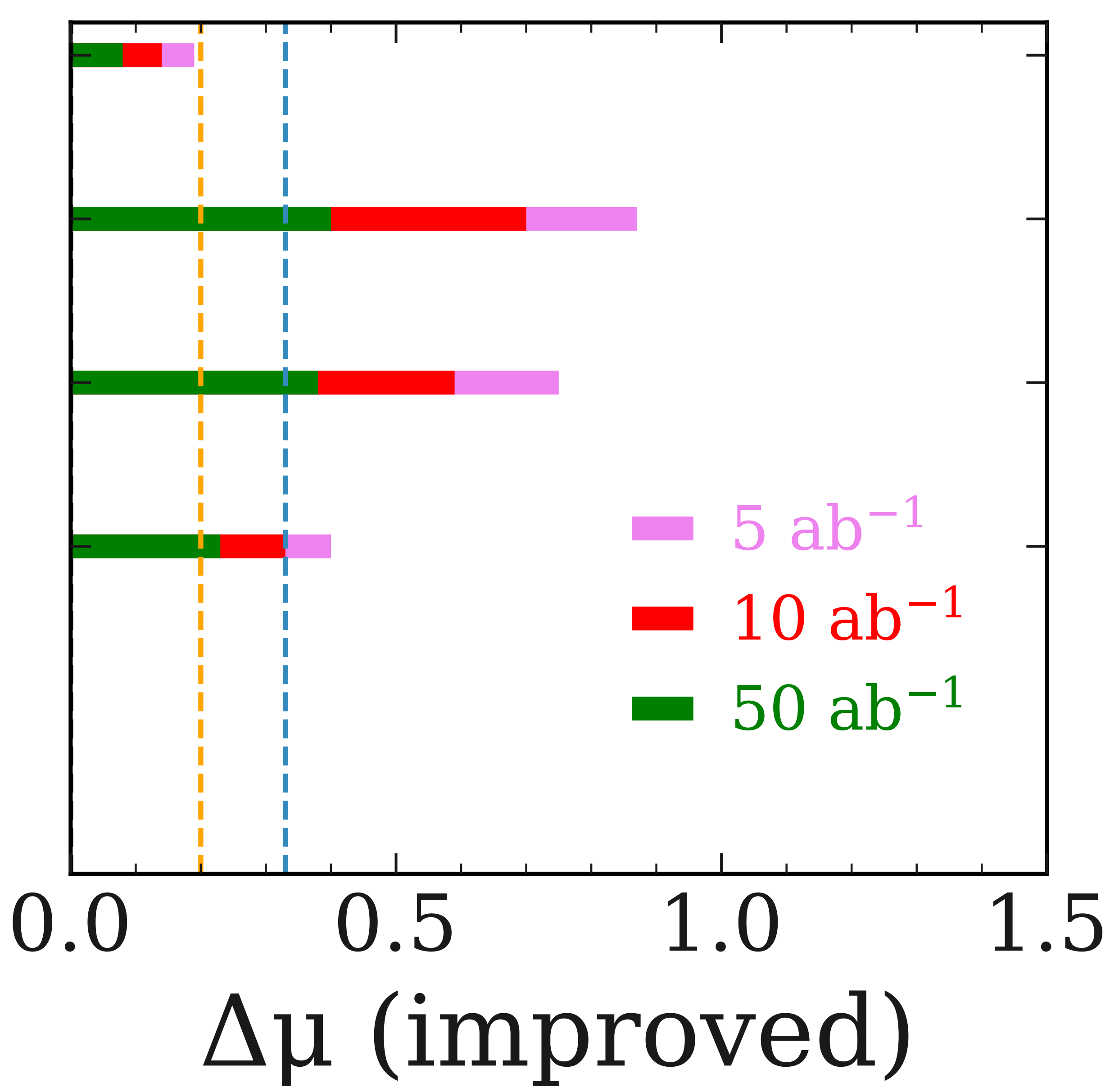

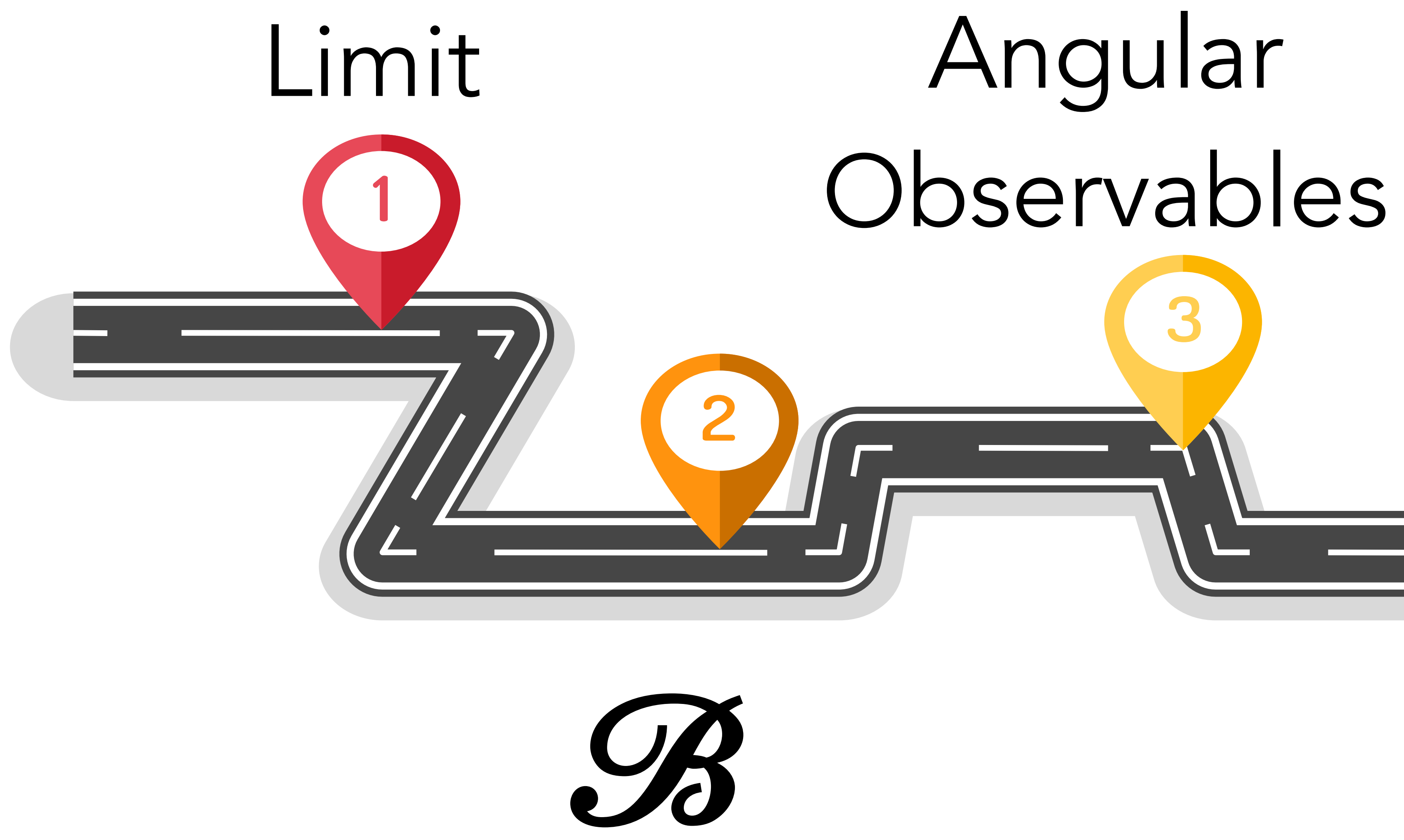

Other Avenues with Invisibles

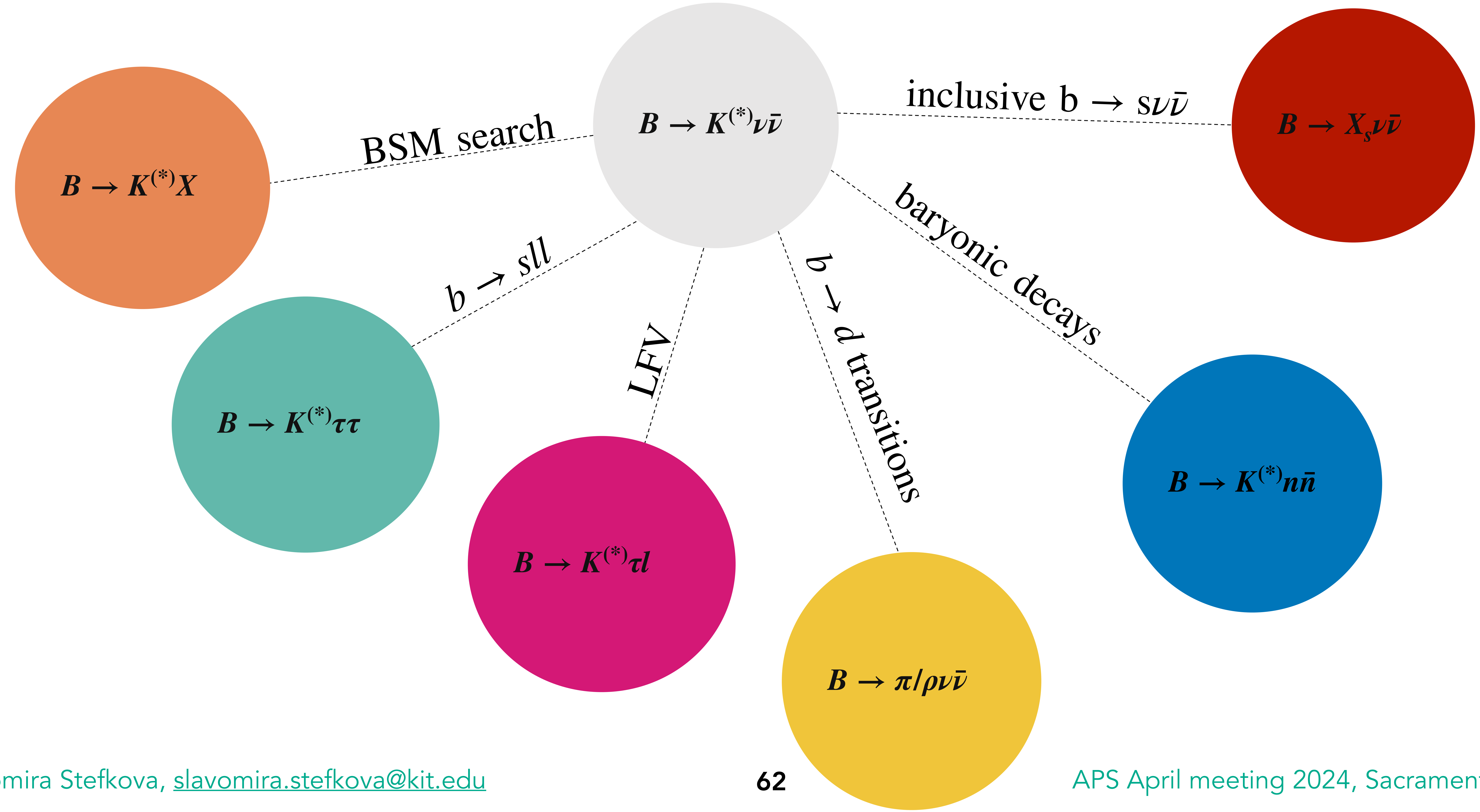

Flavour Anomalies

Anomalies observed in exclusive $b \to s\mu^+\mu^-$ and $b \to c l \nu$ transitions

[PRL 125 (2020) 011802]

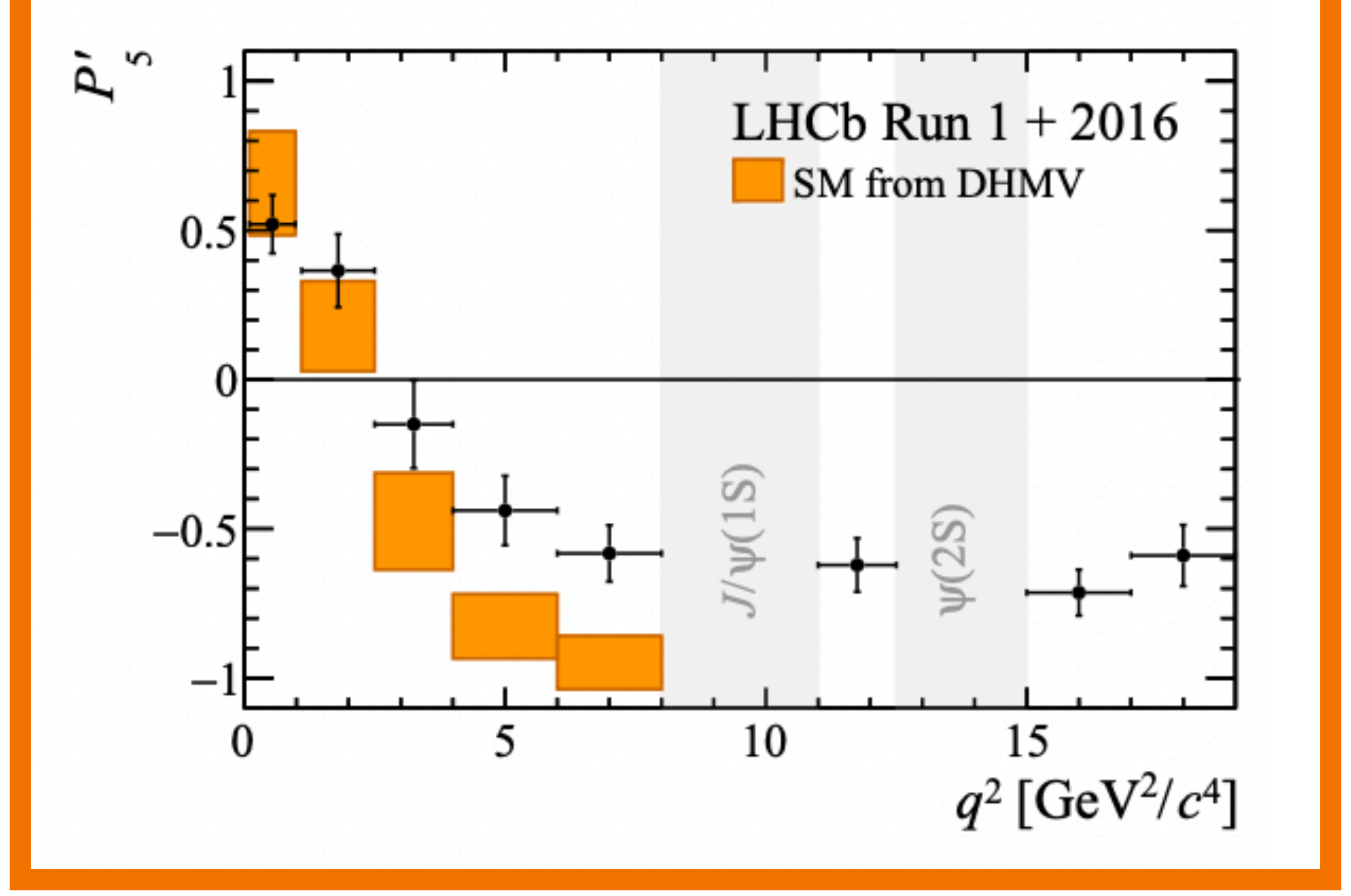

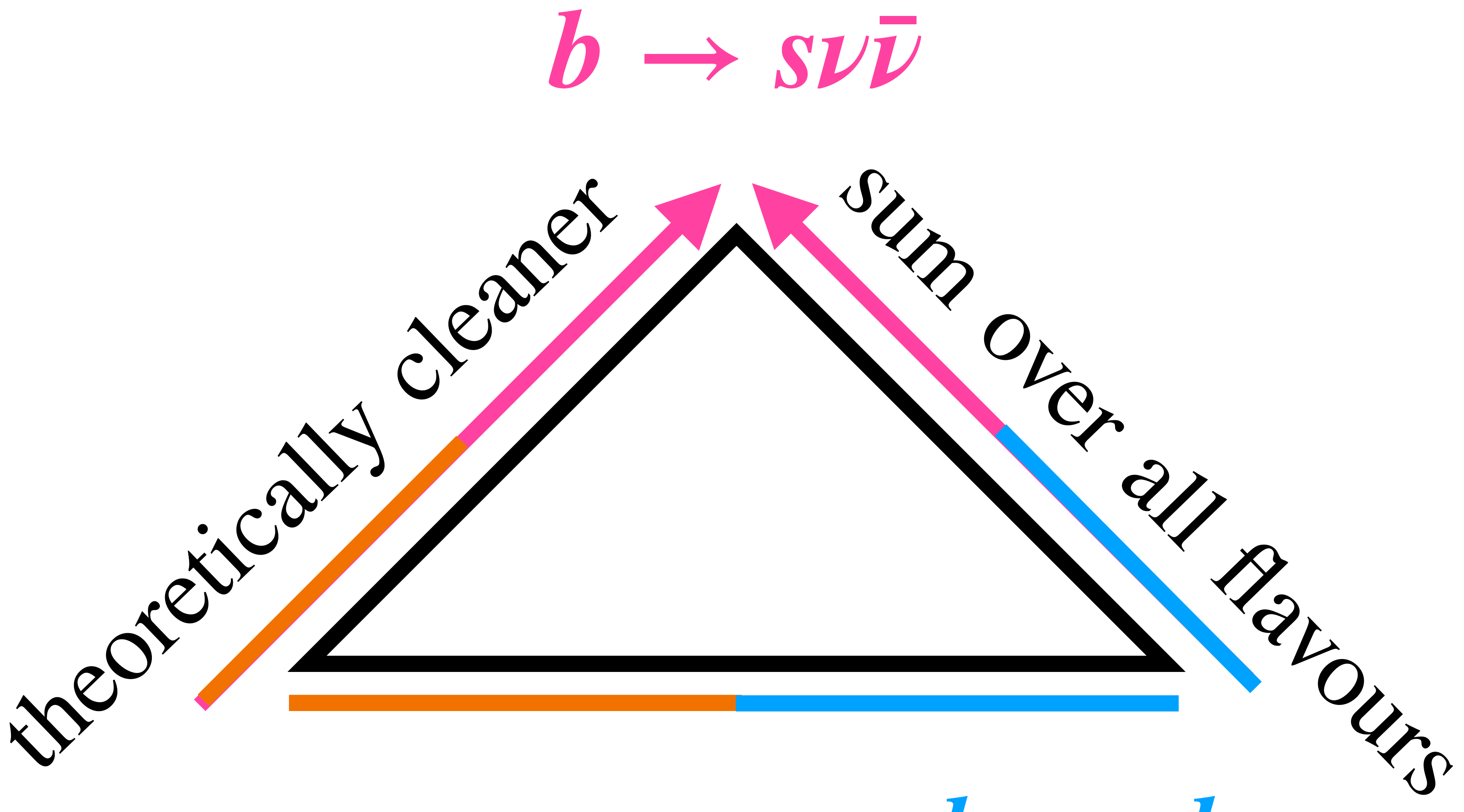

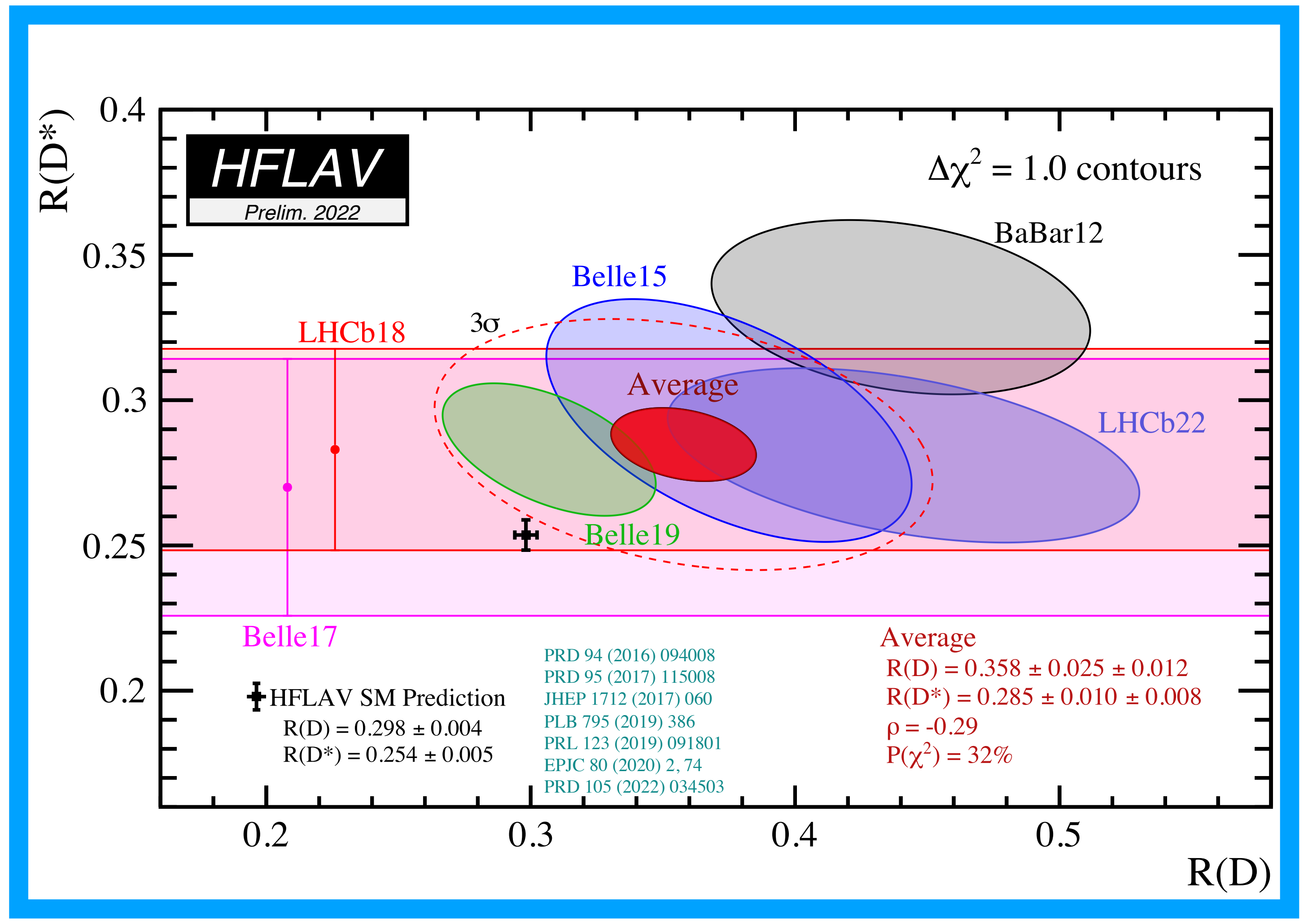

	$b \to s\mu^+\mu^-$	$b \to c l \nu$
Transition	$b \to s\mu^+\mu^-$	$b \to c l \nu$
Observable	P'_5 , $\mathscr{B}$	$R(D^{(*)}) = \dfrac{\mathscr{B}(B \to D^{(*)}\tau\nu)}{\mathscr{B}(B \to D^{(*)} l \nu)\ (l = e, \mu)}$
Significance	Above 2.5 σ	Around 3.0 σ

$b \to s\nu\bar{\nu}$ transitions are correlated to flavour anomalies

Related to $B^0 \to K^{*0}\mu^+\mu^-$

LHCb-PAPER-2024-011

BRAND NEW

Presented for the first time @ Moriond QCD on 2.4.2024

$B^0 \to K^{*0}\mu^+\mu^-$ Measurements

$B^0 \to K^{*0}\mu^+\mu^-$ has caused lots of interest in the community

$b \to s\mu^+\mu^-$ Weak Effective Theory

$$\mathscr{L} \propto \sum_i C_i \mathcal{O}_i$$

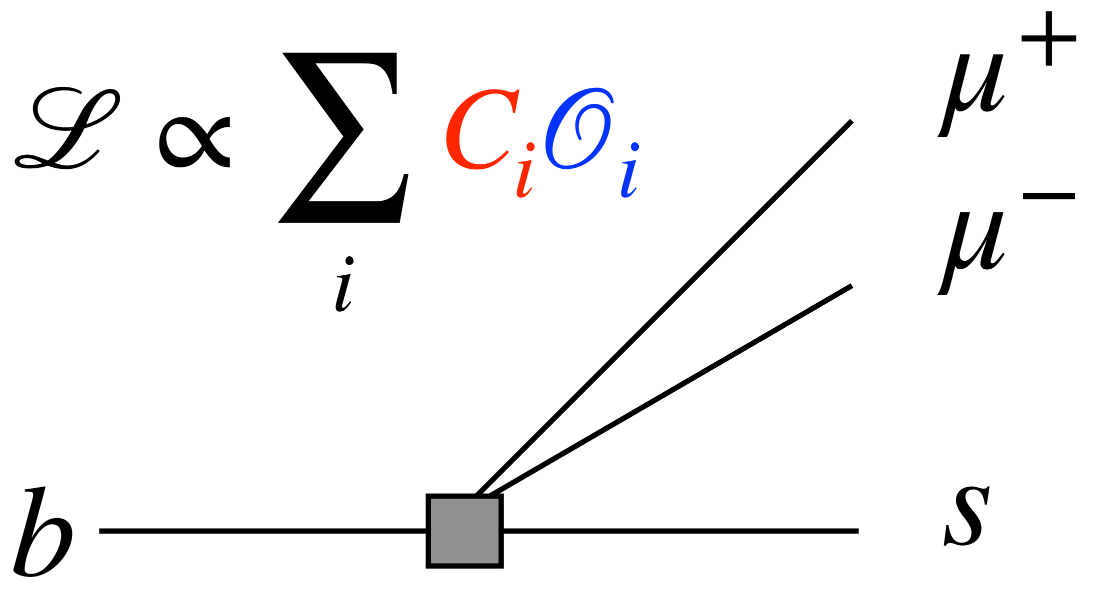

Electromagnetic $C_7^{(\prime)}$

Vector $C_9^{(\prime)}$

Axial vector $C_{10}^{(\prime)}$

Tensions have remained for ~10 years

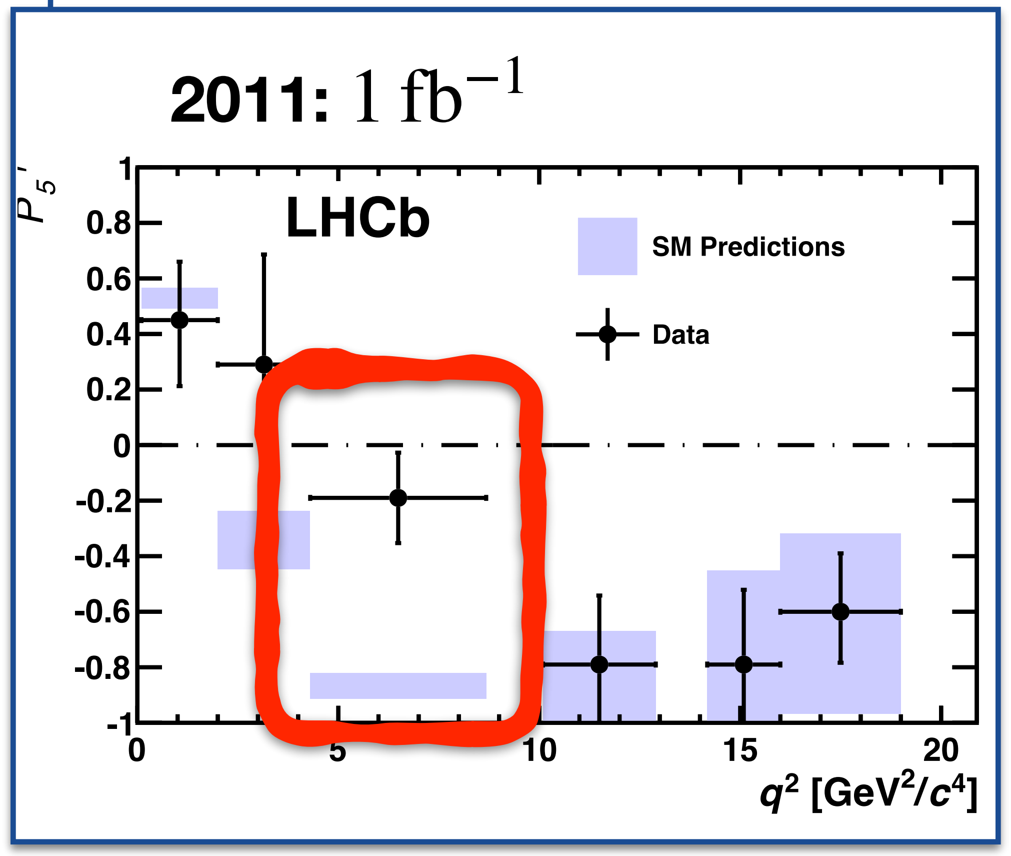

[LHCb-PAPER-2013-037]

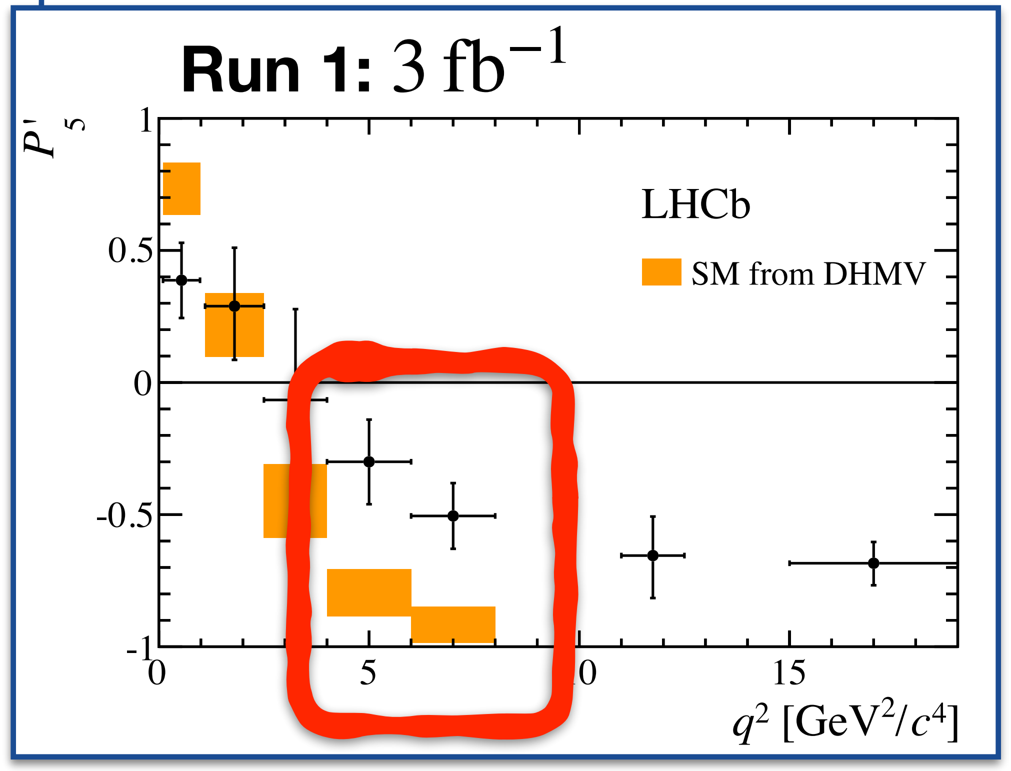

[LHCb-PAPER-2015-051]

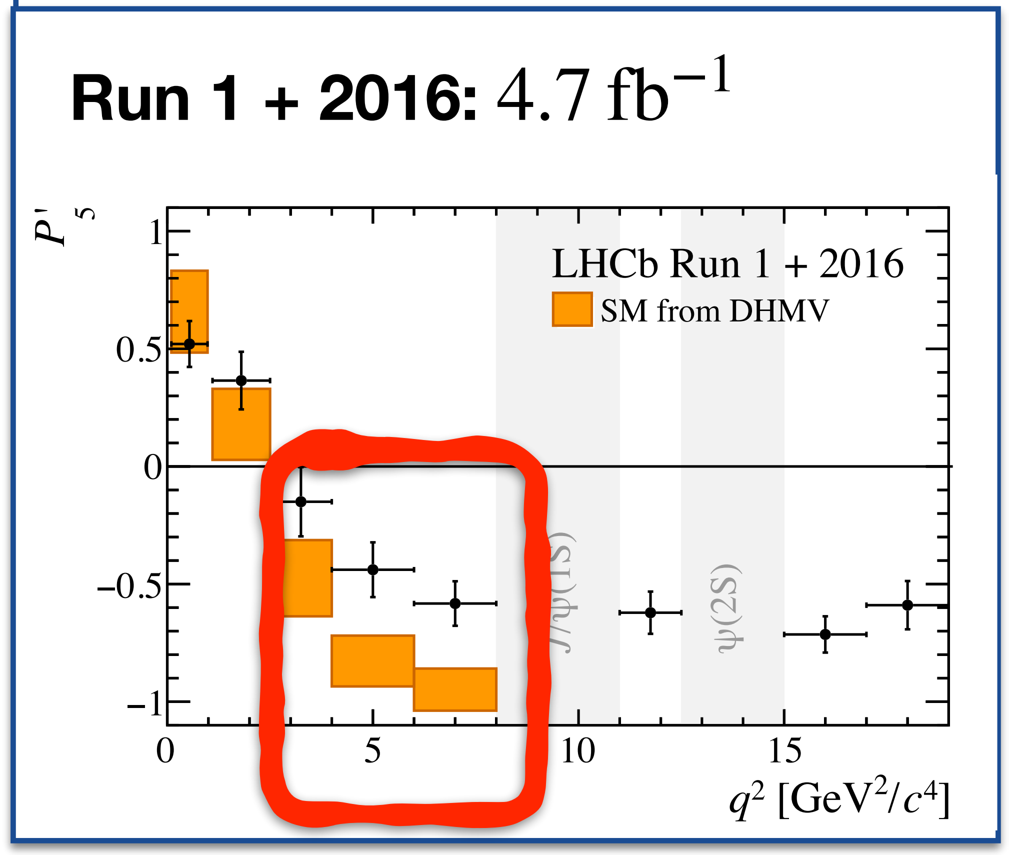

[LHCb-PAPER-2020-002]

Discrepancies are present in multiple observables and the differential decay rate

Charm Loops in $B^0 \to K^{*0}\mu^+\mu^-$

The $B^0 \to K^{*0}\mu^+\mu^-$ decay doesn't live in isolation…

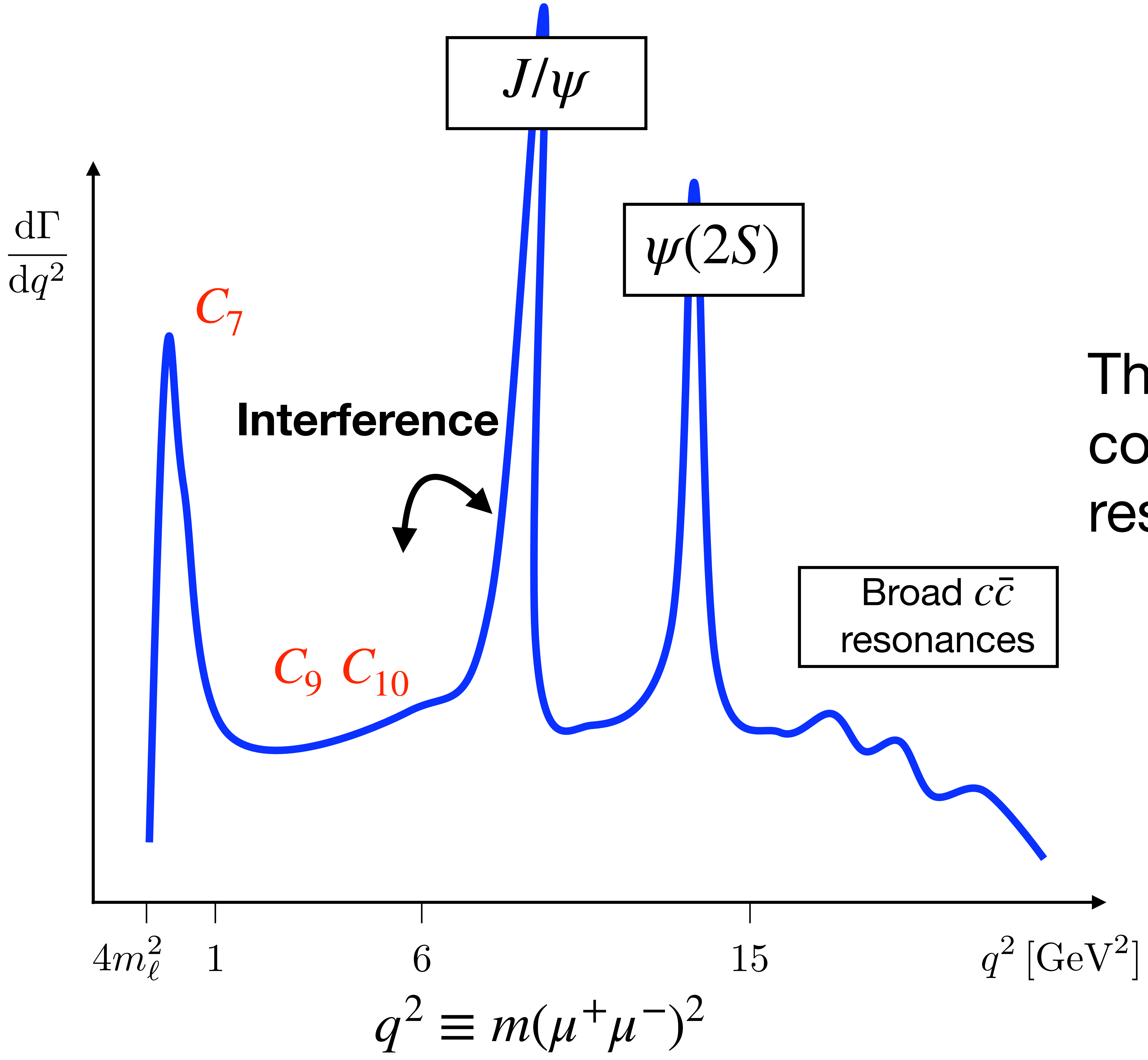

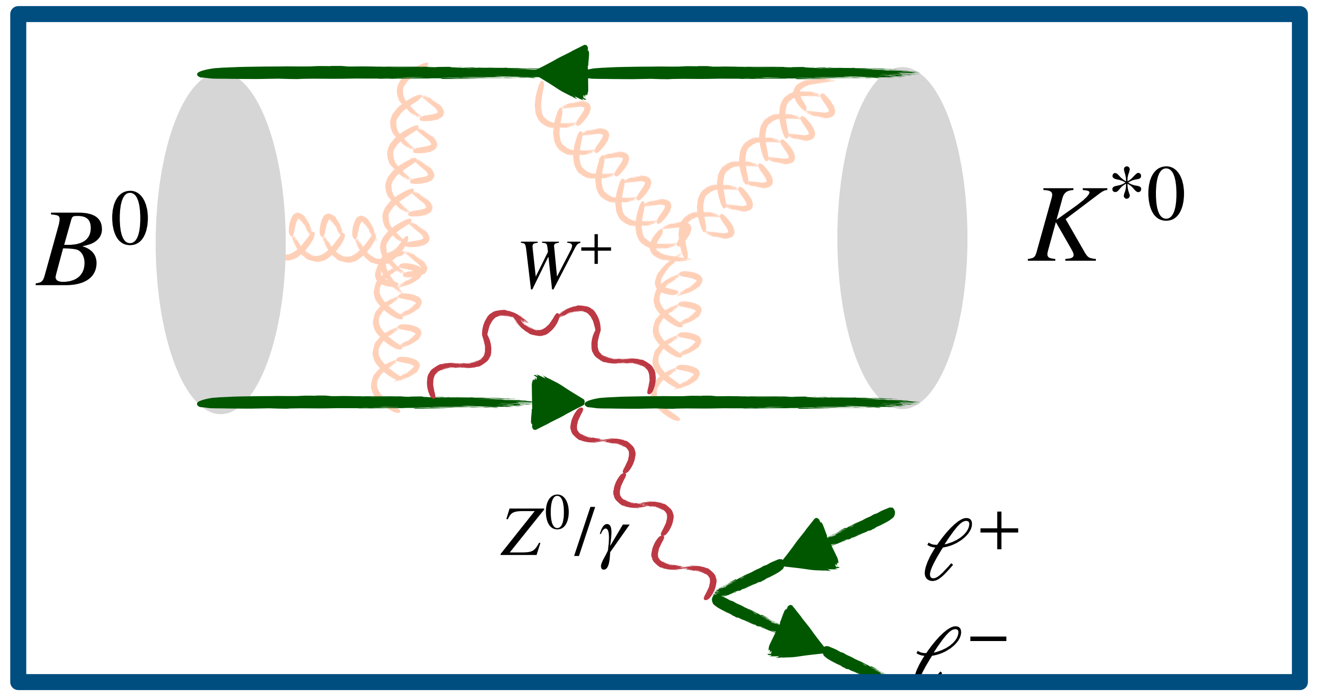

The final state receives large contributions from **'charm-loop'** resonances

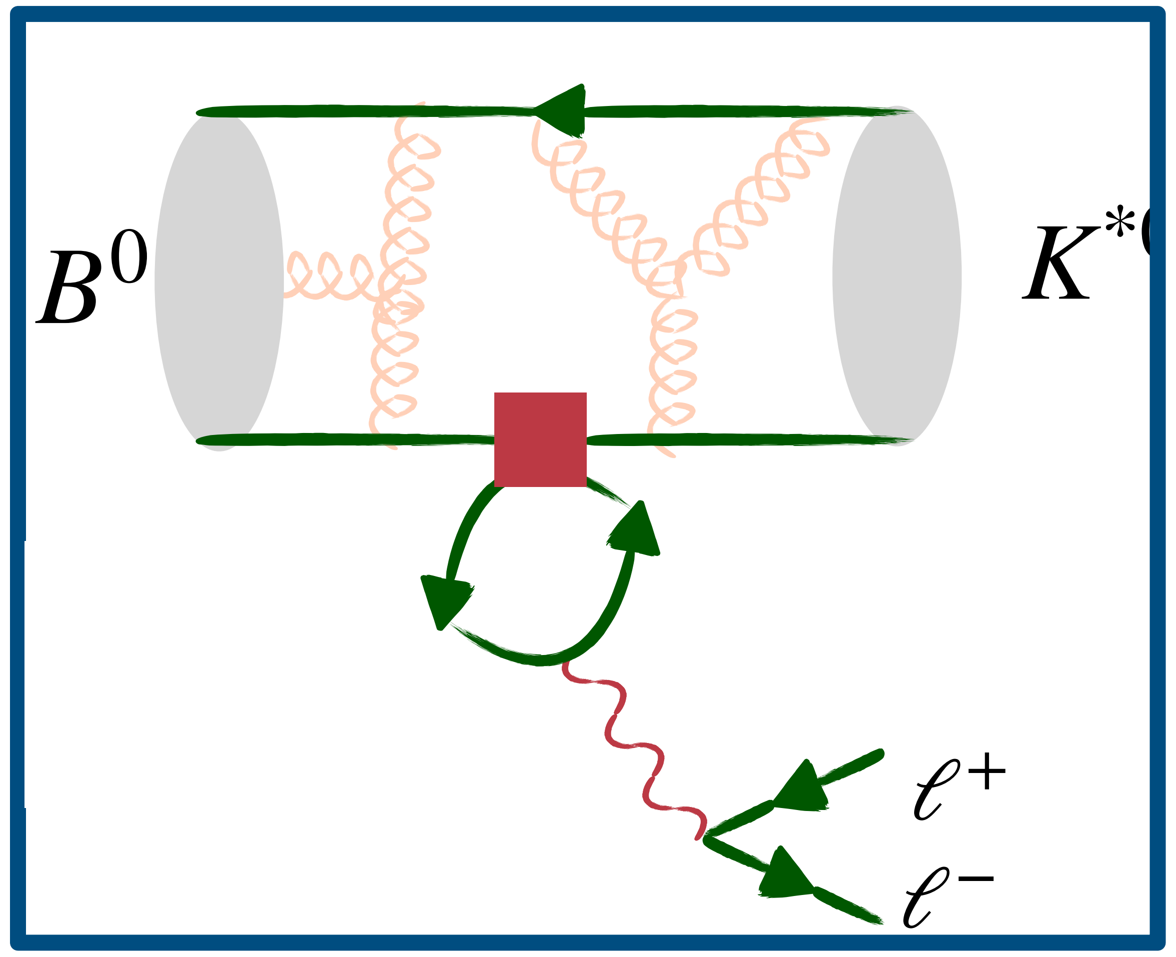

Many of the contributions are vector-like

→ This mimics the C_9 contribution

Can we model them?

New Unbinned $B^0 \to K^{*0}\mu^+\mu^-$

- ✓ **Unbinned** amplitude analysis to the whole $q^2 \equiv m^2(\mu^+\mu^-)$ region
- ✓ **First measurement** using the full Run1 [2011-2012] and Run2 [2016-2018] data

Dispersion Relation

Local | Non-local contributions

$$C_9^{\text{eff},\lambda}(q^2) = C_9^{\mu} + Y_{c\bar{c}}^{(0),\lambda} + Y_{c\bar{c}}^{1P,\lambda}(q^2) + Y_{\text{light}}^{1P,\lambda}(q^2) + Y_{c\bar{c}}^{2P,\lambda}(q^2) + Y_{\tau\bar{\tau}}(q^2)$$

$$C_7^{\text{eff},\lambda}(q^2) = C_7^{\mu} + \epsilon^{\lambda} e^{i\omega^0}$$

ΔC_7^{λ}

Polarisation dependent shift to C_7

This is determined theoretically at negative q^2 values

Subtraction term

Asatrian, Greub, Virto [JHEP 04 (2020) 012]

Negligible impact from light quarks

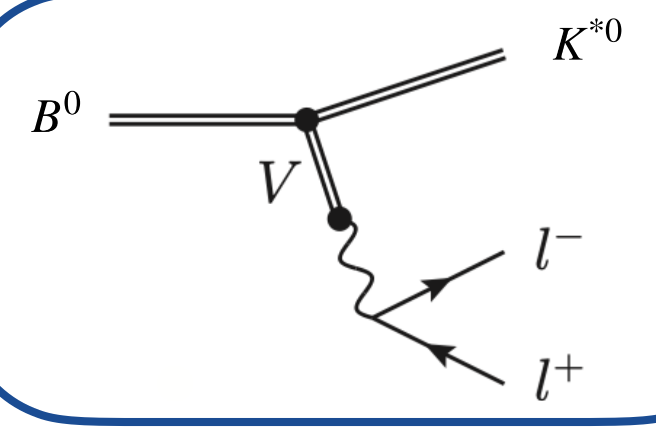

1-particle contributions

Includes:
$\omega(782)$, $\rho(770)$, $\phi(1020)$, J/ψ, $\psi(2S)$, $\psi(3770)$, $\psi(4040)$, $\psi(4160)$

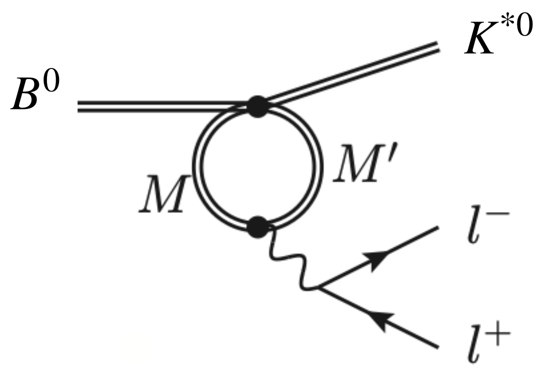

2-particle contributions

Includes:
$D\overline{D}$, $D^*\overline{D}$, $D^*\overline{D}^*$

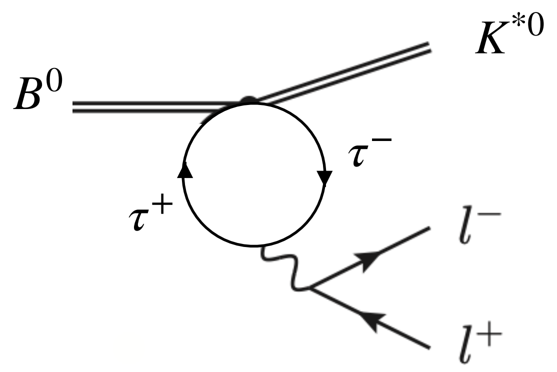

Tau loop contribution

Sensitive to C_9^{τ}

C. Cornella, G. Isidori, M. König, S. Liechti, P. Owen, N. Serra [Eur.Phys.J.C 80 (2020) 12, 1095]

Analysis Strategy

Angular analysis preformed in the three decay angles and q^2

From Simulation

- Acceptance model

From Data

- Resolution
- S-wave parameters
- Background model

From Theory

- Local $B \to K^*$ Form factors

Gaussian constrained GRvDV [JHEP 09, 133 (2022)]

Fit determines 150 parameters:

- $\mathfrak{R}(C_9), \mathfrak{R}(C_{10}). \mathfrak{R}(C'_9), \mathfrak{R}(C'_{10}), \mathfrak{R}(C_9^\tau)$
- Mag. and Phase of 1-particle resonances
- Real+Imag $D^{(*)}\overline{D}^{(*)}$ per helicity
- ΔC_7 per helicity
- Form factors

Results I

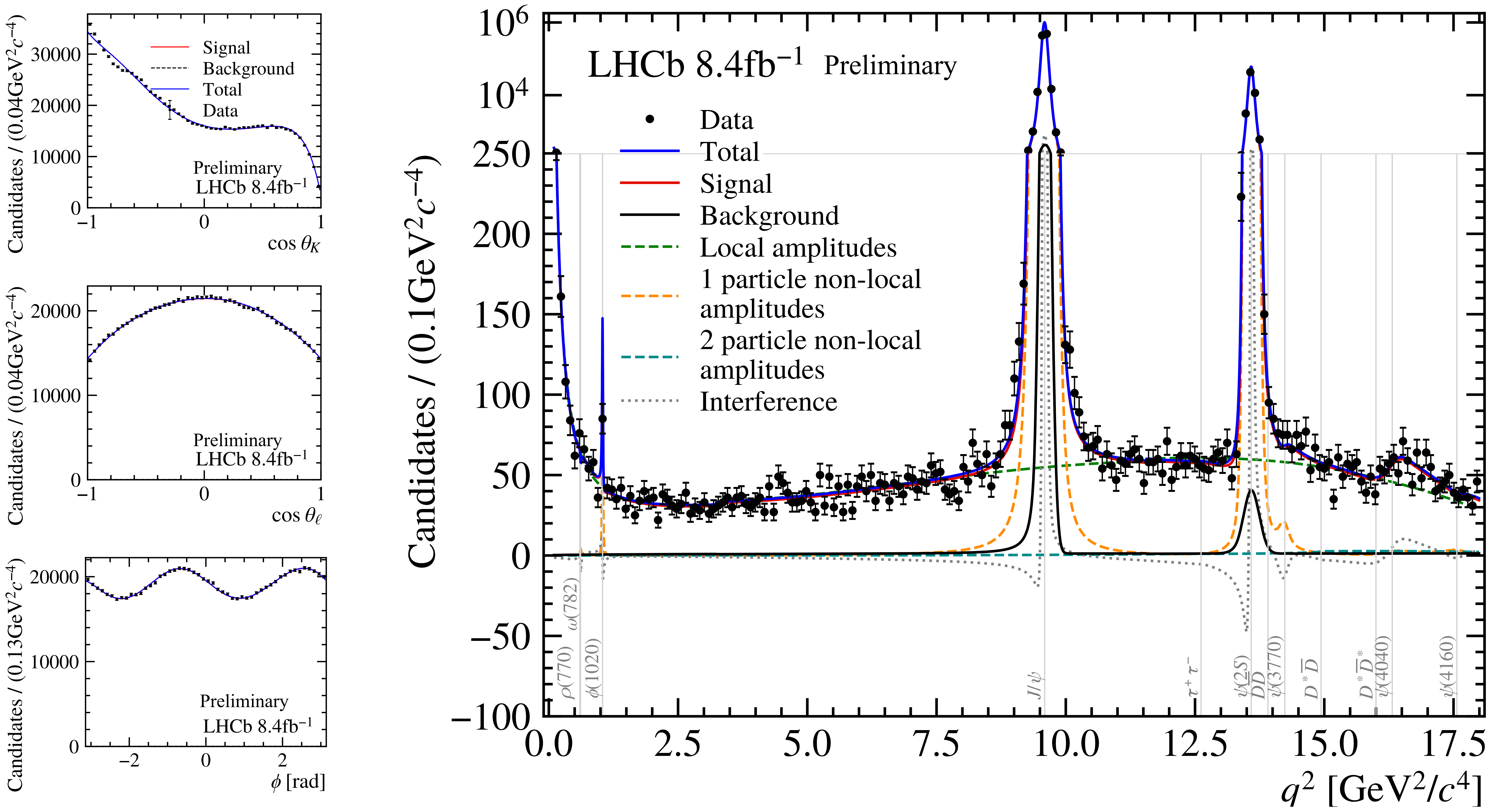

Signal
Background
Total
Data
Preliminary
LHCb 8.4fb−1
cos θK
cos θℓ
ϕ [rad]
Candidates / (0.04GeV2c−4)
Candidates / (0.13GeV2c−4)
LHCb 8.4fb−1 Preliminary
Data
Total
Signal
Background
Local amplitudes
1 particle non-local amplitudes
2 particle non-local amplitudes
Interference
Candidates / (0.1GeV2c−4)
q2 [GeV2/c4]
ρ(770)
ω(782)
ϕ(1020)
J/ψ
τ+τ−
ψ(2S)
ψ(3770)
ψ(4040)
ψ(4160)

Results II

Biggest deviation is C_9 with
$\Delta C_9^{NP} = -0.71$ at 2.1σ from SM

$\mathcal{C}_9$	$3.56 \pm 0.28 \pm 0.18$	2.1σ
$\mathcal{C}_{10}$	$-4.02 \pm 0.18 \pm 0.16$	0.6σ
$\mathcal{C}_9'$	$0.28 \pm 0.41 \pm 0.12$	0.7σ
$\mathcal{C}_{10}'$	$-0.09 \pm 0.21 \pm 0.06$	0.4σ
$\mathcal{C}_9^{\tau}$	$-116 \pm 264 \pm 98$	0.4σ

Global significance $\sim 1.5\sigma$ from SM

In agreement with previous unbinned analysis

$\mathscr{B}(B^0 \to J/\psi K^{*0})$ **dominates systematic uncertainty**

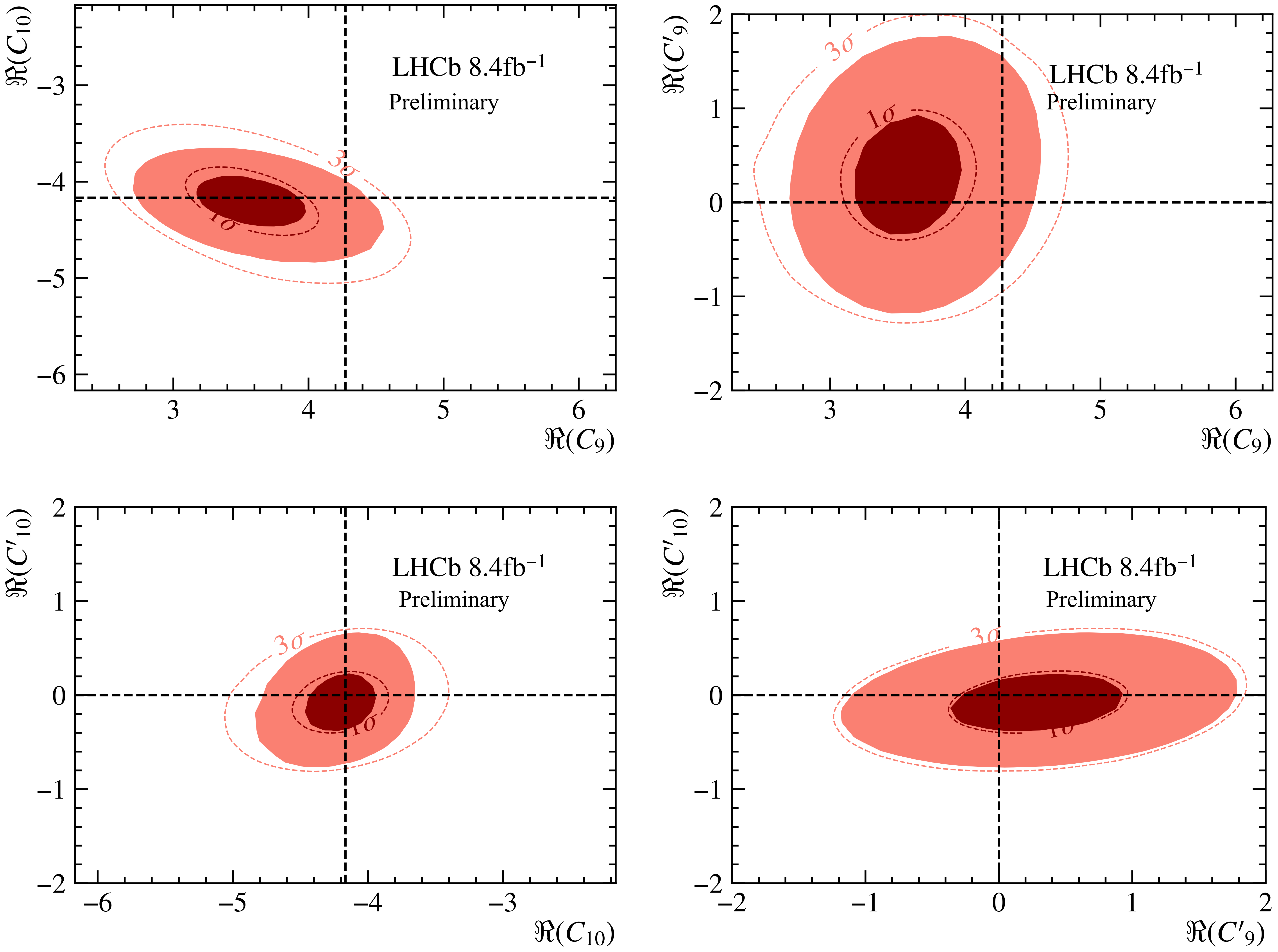

Results III

Nonlocal contributions *do* influence angular observables

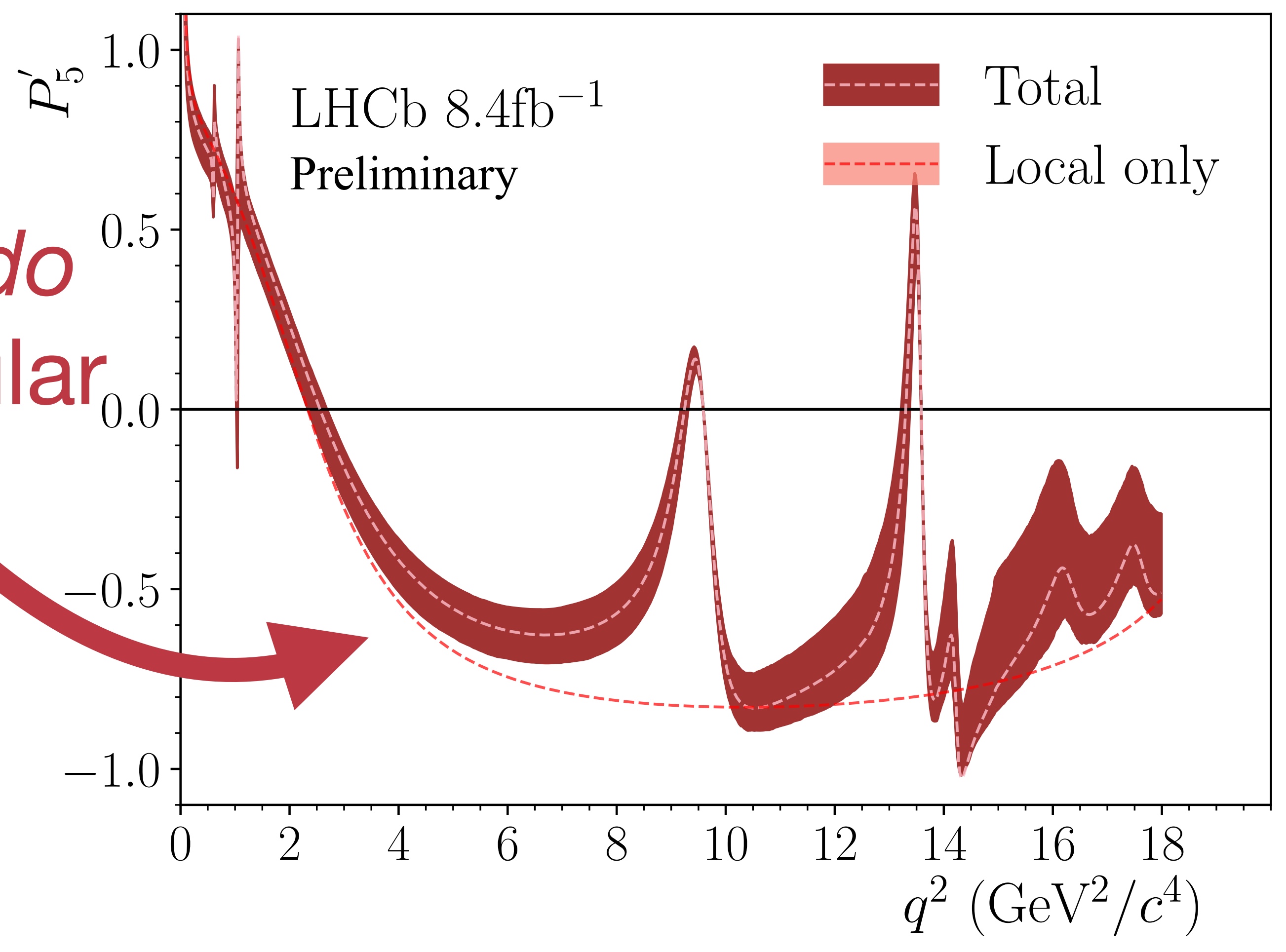

Integrate in bins

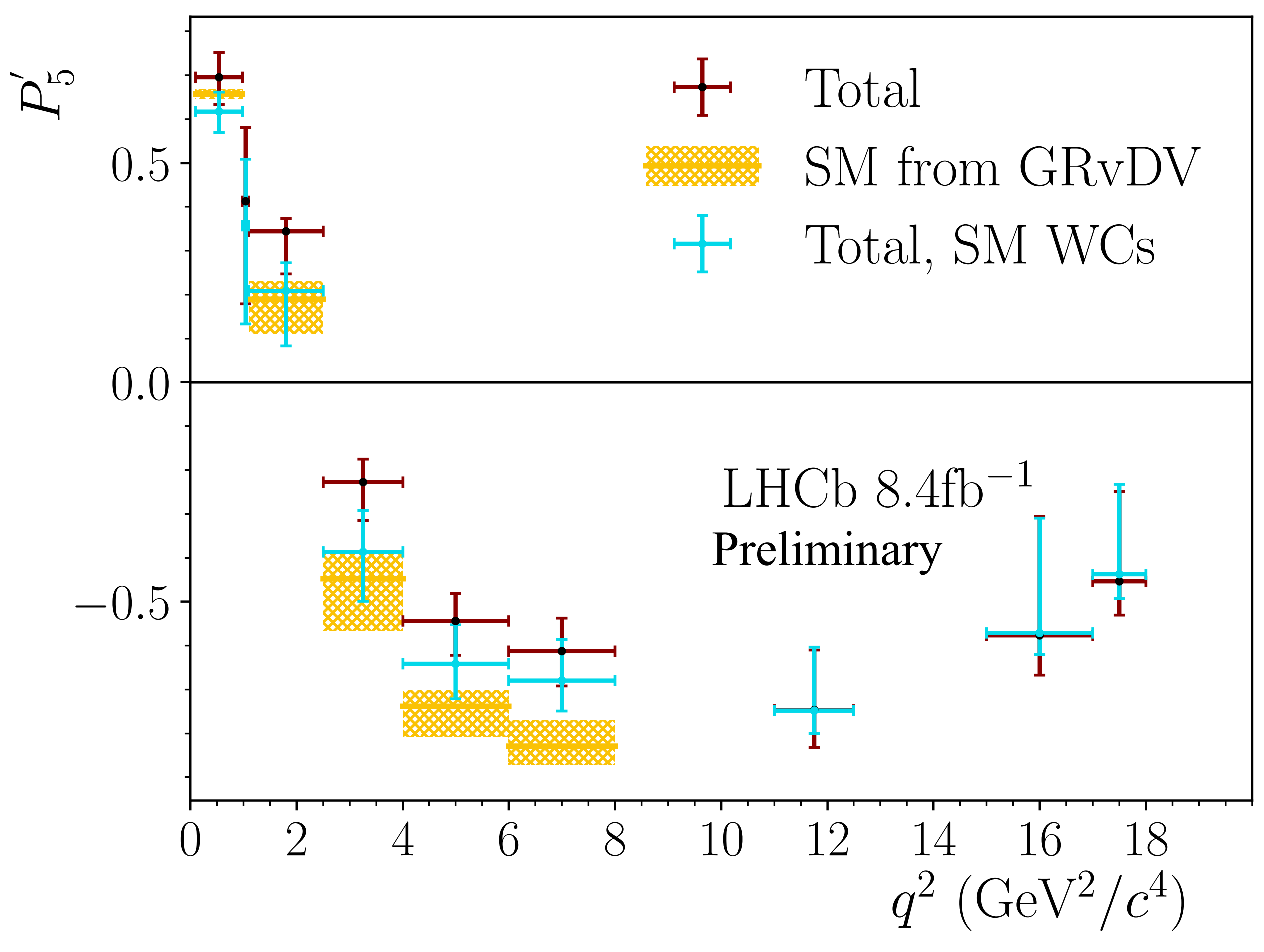

Red vs. Cyan
Impact of allowing NP

Cyan vs. Yellow
Impact of nonlocal modelling

Note: bins are correlated